HAZARD ASSESSMENT OF HIGH-NITROGEN EXPLOSIVE COMPOUNDS:

A NOVEL *IN VITRO* MULTI-CELLULAR APPROACH

by

Captain Tony Maurais

Bioscience Officer

Canadian Armed Forces

Thesis submitted to the Faculty of the
Preventive Medicine and Biometrics Graduate Program
Uniformed Services University of the Health Sciences
In partial fulfillment of the requirements for the degree of
Master of Science in Public Health 2016

DISSERTATION APPROVAL FOR THE MASTER IN SCIENCE IN PUBLIC HEALTH DISSERTATION
IN THE DEPARTMENT OF PREVENTIVE MEDICINE AND BIOSTATISTICS

Title of Thesis: "Hazard Assessment of High-Nitrogen Explosive Compounds: A Novel *In Vitro* Multi-Cellular Approach"

Name of Candidate: Capt Tony Maurais
                       Master of Science in Public Health Degree
                       March 21, 2016

THESIS AND ABSTRACT APPROVED:

                                    DATE:

                                    21 Mar 2016

Mary T. Brueggemeyer, MD, MPH
DEPARTMENT OF PREVENTIVE MEDICINE & BIOSTATISTICS
Committee Chairperson

                                    8 APR 2016

Christopher A. Gellasch, PhD
DEPARTMENT OF PREVENTIVE MEDICINE & BIOSTATISTICS
Thesis Advisor

                                    8 APR 2016

Keri B. Donohue, PhD
USACE ENGINEER RESEARCH & DEVELOPMENT CENTER
Committee Member

                                    8 APR 2016

Kurt A. Gust, PhD
USACE ENGINEER RESEARCH & DEVELOPMENT CENTER
Committee Member

ACKNOWLEDGMENTS

DEDICATION

En mémoire de ma cousine Vicky.

COPYRIGHT STATEMENT

The author hereby certifies that the use of any copyrighted material in the thesis manuscript entitled: Hazard Assessment of High-Nitrogen Explosive Compounds: A Novel *In Vitro* Multi-Cellular Approach is appropriately acknowledged and, beyond brief excerpts, is with the permission of the copyright owner.

Captain Tony Maurais

May 20th, 2016

ABSTRACT

Hazard Assessment of High-Nitrogen Explosive Compounds: A Novel *In Vitro* Multi-Cellular Approach

Tony Maurais, Master of Science in Public Health, 2016

Thesis directed by: LTC Christopher A. Gellasch, Ph.D., Assistant Professor and MSPH Program Director, Preventive Medicine and Biostatistics

The energetic properties of high-nitrogen (high-N) content materials have increased the interest towards their development for use in insensitive munitions. However, the use of such compounds in the production of explosives is known to lead to an increased risk of adverse health effects in munition factory workers and the general population through various occupational and environmental exposure pathways. While chemical hazard assessment with live animals has many advantages, the high cost of *in vivo* testing, in terms of resource consumption, animal usage, and time, only allows for the testing of a limited number of compounds. Current *in vitro* systems are limited by screening cells in isolation, thereby potentially underestimating the cytotoxicity of metabolites. In order to address these limitations, the objective of this research is to use a rapid and efficient *in vitro* model capable of assessing the toxicological impact of an insensitive munition of emerging importance, 2,4-dinitroanisole (DNAN), a high-N candidate for the replacement of the legacy munition 2,6-trinitrotoluene (TNT).

The Integrated discrete Multiple Organ Co-Culture (IdMOC) system allows for the co-culture of up to 6 discrete organ cell types; demonstrating cell-specific toxicity of parent compounds and of metabolites generated by other cells, such as the liver. In this research, five human cell lines were used: kidney, liver, lung, heart and vascular endothelium. TNT, with its well-documented toxicological research-base, served as a comparative model by which to assess the toxicity of the novel and lesser-described munition, DNAN. Cytotoxicity was assessed for each chemical using cell viability characterizations, biomarkers for each cell type, and metabolic/functional pathway enrichment analysis from microarray-based global transcript expression analysis. Protein - for all cell lines - and transcript expression - for kidney cells - profiles between cell mono- and co-cultures were compared in order to assess the influence of TNT metabolites and of the parent compound, thus contributing to the validation of the IdMOC system.

Enriched pathways within kidney cells exposed in co-culture to TNT included pathways related to p53 signaling, cytochrome P450, biological oxidative stress mitigation, and glutathione metabolism, which are all reflective of the known toxicity of TNT metabolites, such as TNT hydroxylamino metabolites. Following viability assays with the cell lines used in the IdMOC system, the toxicity of DNAN based on the lethal concentrations 50 (LC_{50}s) was significantly lower for three cell lines (liver: 145 µM (TNT) vs 1,503 µM (DNAN); vascular endothelium: 261 µM vs 5,875 µM; heart: 176 µM vs 7,015 µM). Two-way ANOVA and principal component analysis showed very few differently expressed transcripts between mono- and co-cultures of kidney cells, which can be attributed to the detoxification capability of the latter. Kidney cells exposed to 100 µM of DNAN in co-cultures led to a significantly lower number of

differently expressed transcripts (180) than the same concentration of TNT (3,074). Both TNT and DNAN exposures resulted in enhanced p53 signaling pathway in kidney cells, but the mechanism of toxicity for DNAN is related to uncoupling of oxidative phosphorylation while TNT toxicity is related to DNA damage. DNAN also led to the enrichment of pathways related to metabolism of amino acids, nitrogen metabolism and glutamine-glutamate metabolism. This pathway enrichment reflects the known toxicity of DNAN metabolites, including dinitrophenol, and associated to proteinuria. The increased expression of specific transcripts such as KCNJ2, coding for a potassium channel, is also in accordance with dinitrophenol metabolism and observed hyperkalaemia in workers exposed to this DNAN metabolite.

Pathway enrichment within kidney cells exposed to TNT through the IdMOC system reflects the literature based *in vivo* toxicity of active toxicants generated from the metabolism of the model chemical, thus contributing to the validation of chemical hazard assessment in co-culture setting. The same conclusion can be stated from co-cultures exposed to DNAN, which led to differences in enriched pathways reflecting dissimilarities in toxicity compared to TNT. Based on the small proportion of differently expressed transcripts within kidney cells exposed to DNAN in co-cultures, the latter showed a lower potency than TNT, which is also supported by higher LC_{50}s. The IdMOC system has the potential to play an increasing role in the hazard assessment of high-N compounds in order to facilitate the safe development and use in insensitive munitions. Future work necessary to further validate the IdMOC system includes microarray analysis with non-detoxifying cells exposed to TNT in co-cultures as well as the dosing of TNT metabolites within the culture media.

TABLE OF CONTENTS

LIST OF TABLES

LIST OF FIGURES

LIST OF ABBREVIATIONS

Ab .... Antibody

ACGIH .... American Conference of Governmental Industrial Hygienists

ADNT .... Aminodinitrotoluene

Ah .... Axyl hydrocarbons

ANOVA .... Analysis of variance

BEGM .... Bronchial epithelial cell growth medium

BMD_{10} .... Benchmark dose, 10%

BPE .... Bovine pituitary extract

BSA .... Bovine serum albumin

cRNA .... Complimentary ribonucleic acid

CPK1 .... Phosphoenolpyruvate carboxykinase 1

CYP 1A1 .... Cytochrome-P450 1A1

DAAN 2,4-diaminoanisole

DAVID .... Database for annotation, visualization and integrated discovery

DEG .... Differentially expressed genes

D.G. .... Dangerous goods

DMSO .... Dimethyl sulfoxide

DNA .... Deoxyribonucleic acid

DNAN 2,4-dinitroanisole

DNase .... Deoxyribonuclease

DNP .... Dinitrophenol

DNT .... Dinitrotoluene

DT .... Doubling time

EDTA .... Ethylenediaminetetraacetic acid

EGF .... Epithelial growth factor

ELISA .... Enzyme-linked immunosorbent assay

EPA .... Environmental Protection Agency

ERDC .... Engineer Research and Development Center

CHAPTER 1: INTRODUCTION

BACKGROUND

The approaches that have been used in the past 50 to 80 years to quantitatively assess the health risks of chemical exposure have mainly focused on high-dose studies measuring the adverse outcomes in homogeneous animal populations. This process represents a low-throughput approach relying on conservative extrapolations relating animal studies to human exposure to common low doses (18). The high cost of *in vivo* testing, in terms of resource consumption, animal usage, and time, only allows for the testing of a limited number of compounds. Depending on the chemical and its purpose, it has been estimated that up to 7,000 animals can be used for *in vivo* chemical assessment at a cost often reaching tens of millions of dollars during several years (170). In order to overcome these limitations, government agencies are increasingly looking at new approaches to evaluate the safety of the relatively large number of chemicals in commerce and in the environment (86; 177). In 2006, the European Union (EU) launched the Registration, Evaluation, Authorization and Restriction of Chemical substances (REACH) legislation that dramatically reorganized chemical safety regulations for the EU (193). By embracing the precautionary principle, REACH shifts the burden of compliance from regulators to industry, requiring companies wishing to sell chemicals in the EU to demonstrate their safety through imbedded registration process (193). Furthermore, the EU has enacted the Seventh Amendment to the Cosmetic Directive which promulgates the elimination of animal testing (158). In response to the same concerns, the United States (U.S.), through the U.S. National Research Council (NRC), published a report in 2007 named: *Toxicity Testing in the 21ˢᵗ Century: A Vision*

and a Strategy (132). In the report, NRC recommends the transformation of toxicity testing by reorienting the process towards the evaluation of the responses of toxicity pathways in well-designed *in vitro* assays using human cells (18; 132). The NRC report identifies a number of emerging fields and techniques that are contributing to a better understanding of the biologic responses to chemicals in human tissues. For instance, systems biology is a recent and powerful approach that uses computational models and laboratory data to describe and understand biologic systems as a whole and how they operate (132).

These new technologic developments, combined with the lack of rapid and accurate methods for predicting the health hazards of new chemicals, led the Engineer Research and Development Center (ERDC) of the U.S. Army Corps of Engineers to develop mammalian cell-based, fish embryo assays and computational tools to rapidly assess potential health hazard effects of new military chemicals to mammals and the environment. More specifically, the ERDC Rapid Hazard Assessment of Army Compounds (RHAAC) Project focuses on the assessment of high-Nitrogen (high-N) compounds as they are being developed for use as insensitive munitions (IM). One objective of the RHAAC Project consists of developing a mammalian cell-based assay based on the Integrated discrete Multiple Organ Co-culture (IdMOC) system.

The IdMOC system (Figure 1) represents a rapid screening system that allows for the co-culture of up to 6 discrete organ cell types that share the same media, offering the advantage of observing the effects due to compound metabolism. This model, developed in 2004 by Li, Bode and Sakai (104), allows for the incorporation of a metabolic component for *in vitro* toxicity screening. The system takes into account the following

properties of accurate *in vitro* experimental systems: xenobiotic metabolism by key

organs; target cells representative of key organs; multiple organ interactions; and

predictive endpoints (103). In this approach, cells are cultured independently in short

inner wells that are housed together in the same outer chamber. By doing so, the cell

types are connected by a shared medium that floods the outer chamber. Soluble

metabolites can then interact with all the different cell types.

Figure 1. The Integrated discrete Multiple Organ Co-culture (IdMOC) system (144).
By either testing the culture of selected cell lines individually in each well, or by
overflowing the six-well chambers with culture media, one can use the IdMOC
plate in a monoculture or co-culture setting.

For instance, the system allows for the culture of hepatocytes in the presence of

other organ-specific cell types, and, consequently, the effects of metabolism on cell-type

specific toxicity, as well as for hepatotoxicity, can be evaluated for a chemical of interest

(32). When using the IdMOC system for toxicity assessment, one needs to consider the

key organs affected by the chemical(s) of interest and choose the appropriate cell lines

accordingly. Once the key cell lines for the IdMOC system are selected, a validation is

required using a model chemical for which the toxicity properties are well known. In this

regard, 2,4,6-trinitrotoluene (TNT), an energetic compound that has been used for a

century and a half, appears to be the ideal candidate for the validation of an IdMOC system in the assessment of high-N compounds.

While the toxicity of TNT is well documented, there are several other high-N compounds used in insensitive munitions for which limited information about their potential harmful effects is available. Among those, 2,4-dinitroanisole (DNAN) is of particular interest. DNAN is an explosive nitroaromatic that is less shock sensitive than TNT and is therefore proposed as a TNT replacement for melt-cast formulations[1] (44). The peer-reviewed scientific literature is relatively scarce concerning DNAN as opposed to TNT (54 results vs 1581 on PubMed as of April 2016). From the 54 articles on DNAN, 46 articles were published in the last five years, which reflects the more recent synthesis and application for DNAN compared to the lengthy history for TNT. Consequently, the use of the IdMOC system represents a unique opportunity to learn more about the cytotoxicology of high-N compounds, such as DNAN, and on their potential adverse health effects.

INSENSITIVE MUNITIONS AND HIGH-N COMPOUNDS

Most of the explosive compounds used by the military, including IM, consist of elements of carbon, hydrogen, oxygen and nitrogen. Since the molecular nitrogen is at a lower state of internal energy than the oxides of nitrogen (NO, NO_2, NO_3, etc.), any nitrogen in the explosive composition will be given out as N_2 if the combustion is complete. The $-NO_2$ and $-ONO_2$ represent the major sources of oxygen in the energetic molecules, which are the main contributors to the detonation or combustion processes

---

[1] Melt-cast formulation: explosive mixture created from the melting of different proportions of insensitive compounds and used to fill explosive (e.g. artillery) shells.

(10; 185). This is the reason why most of high energetic materials are high-N compounds, mainly under the form of nitro-aromatic groups. The high nitrogen content in the molecules increases the density and leads to the generation of large quantities of gas per gram. The search for the promising high-energy materials during recent years has led to the discovery of numerous energetic compounds. The exploitation of structure property relationships, combined to the use of computer models to predict the energetic properties, has led to the development of new materials with increased performance, reduced sensitivity to external stimuli and/or enhanced chemical and thermal stability (185).

As part of this effort to minimize accidental detonations of munitions during military firing range training, the U.S. military is developing IM compounds that detonate only when intended. However, the manufacturing, loading, assembling and packing of explosives into munitions for use in testing on training sites or the battlefield has been shown to contaminate terrestrial and aquatic sites, leading to an increased risk of adverse health effect of sensitive populations and species (113; 168).

While there is a recognized lack of information on the possible toxicity effects and mechanisms of explosive compounds, the toxicity of nitro-aromatics is more documented than for other explosives. The exposure of humans to nitro-aromatic explosives is accompanied by multiple toxic effects, which depend on the genetic or individual susceptibility, and by the workplace standards (43; 99; 127). For instance, methemoglobinemia, reproductive toxicity, skin lesions and dermatitis have all been observed following exposure to nitro-aromatic compounds such as TNT (28; 43; 106). Cytotoxicity of several nitro-aromatic explosives is often accompanied by lipid

peroxidation, which suggests the involvement of oxidative stress resulting from the enzymatic redox cycling of anion-radicals of these explosive compounds (23; 127; 155; 157). Other cytotoxic mechanisms of nitro-aromatic explosives have been suggested as being involved in parallel to the oxidative stress. For example, redox cycling of hydroxylamines, their binding to macromolecules, and the possibility of the generation of toxic hydroxylamines from amines (127; 198). Despite numerous clinical and ecotoxicological reports, the exact biochemical mechanisms triggered by several nitro-aromatic explosives are not well understood and further investigation is required. An example of such high-N compounds with an incomplete toxicological profile is DNAN.

2,4-DINITROANISOLE (DNAN)

The first recorded use of DNAN in an explosive military device was as a main charge ingredient in the warhead of some V-1 flying bombs during World War II. Interestingly, the main reason for the use of DNAN was not particularly because of any performance gains, but because of its availability when other materials such as TNT became increasingly scarce (50). Indeed, TNT appears to have a higher performance than DNAN (by approximatively 10%). However, the recent renewed interest for DNAN comes from two characteristics of this energetic compound. First, it is less shock and temperature sensitive than TNT (Table 1). Secondly, based on the United Nations classification system of dangerous goods (DG), DNAN is categorized in the class 4.1 "Flammable Solid" and is subject to less stringent transportation requirements than TNT, classified as DG 1.1. material "Explosive with a mass explosion hazard" (35). Consequently, DNAN is proposed as a TNT replacement for melt-cast formulations (44).

Table 1. Physical properties of TNT and DNAN.

Compound	TNT	DNAN
DG Classification[1]	1.1 Explosive with a mass explosion hazard	4.1 Flammable solid
Detonation velocity (D)[1]	6.94 km/s	5.6 km/s
Density (p)[1]	1.64 g/cm3	1.34 g/cm^3
Detonation pressure (P)[1]	29 GPa	7.02 GPa
Melting Point[1]	80.8ºC	94.5ºC
Friction sensitivity[2,1 respectively]	353 N	170 N
Impact sensitivity[3,1 respectively]	88 cm	220 cm

1. Values extracted from (148).
2. Value extracted from (97).
3. Value extracted from (154).

While several standards organizations, such as the American Society for Testing and Materials (ASTM) International, provide guidance on how to progressively assess the environmental and human health impacts of new energetic compounds according to their respective stage of development, this process seems to have been considerably shortened for DNAN (83). Undeniably, it is already widely used in several insensitive explosive formulations, such as IMX 101 (105 mm & 155mm Artillery HE), IMX 104 (60/81/120mm Mortar), PAX 21 (60mm M720A1/M768 Mortars), PAX-41 (Spider Grenade), and PAX-48 (120mm HE-T), while little evidence has been gathered concerning DNAN toxicity (44; 154). However, with DNAN being proposed as a TNT replacement for melt-cast formulations, research has been conducted to compare the performance and toxicity of both compounds (44). For such comparison, one can expect DNAN to have similar acute and chronic toxic effects in human and ecological receptors than TNT since both chemicals are structurally similar. Indeed, DNAN has been found to transform as easily as TNT under abiotic and biotic conditions to initially produce amino-

reduced products (44; 133; 142; 143; 147). Figure 2 shows the structure of both

molecules.
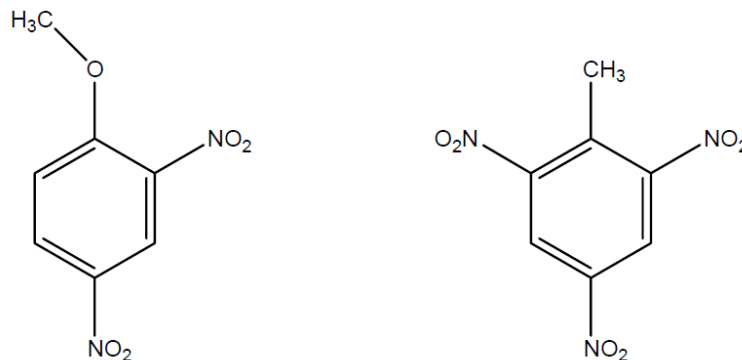
Figure 2. Chemical structures of the explosive compounds 2,4-Dinitroanisole (left) and
2,4,6-Trinitrotoluene (right).

The absorption of DNAN is low, with values as small as 0.002% from ingestion

(77). Like TNT, DNAN has a high elimination rate in living organisms, and therefore it

is believed that an individual can experience harmful effects only if under constant

exposure (113). A recent study by Dodard et al. (44) suggests that DNAN is equally or

less deleterious to organism health than TNT, depending on the species and toxicity test.

Similar results have been obtained with *Rana pipiens* tadpoles which were found to be

very sensitive to TNT, with a lowest-observed-effect-concentration (LOEC) three orders

of magnitude lower than for DNAN (168).   However, one study showed that, for a single

dose exposure, DNAN is more acutely toxic than TNT in an experiment with rats (45).

Nonetheless, the same study also showed that the skin absorbance of DNAN is smaller

than TNT (0.74 vs 1.14 $\mu g/cm^2$-hr, respectively) and that no sign of toxic effects were

observed at necropsy for an exposure to a DNAN aerosol at a concentration of 2900

mg/m^3.

In mammals, DNAN is hydrolyzed into dinitrophenol (DNP), which is known to uncouple oxidative phosphorylation at high dose leading to acute toxicity and mortality (77). Consequently, DNP is therefore believed to be the main cause of the toxicity of DNAN. Even though the toxicity of DNP was identified in the 1930s, this compound has regained interest since its resurgence in the last decade as an unregulated diet aid or weight loss drug (77; 200). Deadly results have been reported after self-administered high doses of DNP (67). The compound can be found in urine of DNAN exposed mammals at much lower levels than blood, where it is found at a very high concentration (20-fold) compared to the original compound (77). It is suggested that the metabolism of DNAN begins in the intestinal lumen or villi, where DNP - highly soluble - is then rapidly transported to the blood (77). It is also suggested that DNP undergoes nitroreductase metabolism to 2-amino-4-nitrophenol or 4-amino-2-nitrophenol, and finally to 2,4-diaminophenol (77). Studies with rats and monkeys showed widely different metabolic rates at similar doses depending on individual animals and species. Differences in metabolizing enzymes could explain these observations (77).

Recently, it was found in a rodent study that DNAN causes a dose-dependent increase in extramedullary hematopoiesis in female rats (98). A preliminary occupational exposure level (OEL) of 0.09 mg/m^3 has been suggested, although it is undergoing an external peer review (182). As a comparison, the threshold limit value for TNT is set at 0.1 mg/m^3 (skin designation) by the American Conference of Governmental Industrial Hygienists (ACGIH). The small amount of evidence about DNAN toxicity as well as the application of uncertainty factors contributed in establishing a conservative OEL (45).

Kennedy and his colleagues (87) studied the lethal concentration, 50% (LC_{50}) in *Pimephales promelas* (fish) and 2 cladocerans (water fleas) (*Ceriodaphnia dubia*, *Daphnia pulex*). The results showed a LC_{50} that ranged from 14.2 mg/L to 42 mg/L for acute (48h) exposure and depending on species. Chronic exposure to DNAN resulted in LC_{50}s of 10.0 mg/L (fish) and 13.7 to 24.2 mg/L (cladocerans). A similar study by Liang et al. (107) investigated the inhibitory effects of DNAN and two of its metabolites (2-methoxy-5-nitroaniline (MENA) and 2,4-diaminoanisole (DAAN)) toward various microbial targets. The resulting LC_{50}s ranged from 8-11 mg/L (*A. fischeri*) to 77 mg/L (aerobic heterotrophs). Reduction of DNAN to MENA and DAAN resulted in partial detoxification. It also has been shown that DNAN has an oral lethal dose, 50% (LD_{50}) of 200 mg/kg with rodents (77). A study comparing DNAN and TNT toxicity towards *Rana pipiens* (leopard frog) tadpoles during a 96h exposure found a LC_{50} of 33 μM for TNT and 123 μM for DNAN (168).

It is interesting to note that 2,4,6-trinitroanisole (TNAN), which only has one more nitro group than DNAN, has a low melting point of 68ºC, which represents a practical limitation. Furthermore, TNAN produces skin eczemas and is considered physiologically unsafe (148). Overall, while several studies on DNAN have focused on its ecotoxicological effects, little information is available concerning the cytotoxicological mechanisms of DNAN and its reduction products, underlying a need for further research.

As demonstrated in the current section, TNT has been used as a model chemical in several studies assessing DNAN toxicity. Indeed, with toxic effects observed as early as 1919, TNT now has a well-understood toxicological profile (186). Consequently,

TNT represents an excellent model chemical to validate the IdMOC system before it can be used to assess DNAN cytotoxicity.

2,4,6-TRINITROTOLUENE (TNT)

TNT: A Long-Known Toxicant

TNT is a yellow, odorless, solid compound that is made by combining toluene with a mixture of nitric acid and sulfuric acid. TNT has been widely used in the military for several reasons related to its characteristics: low melting point (80.1-81.6 °C); stability; low sensitivity to impact, friction, and high temperature; and its safe methods of production and manufacture (184). Consequently, TNT is found as an explosive in military shells, bombs, and grenades, in industrial uses, and in underwater blasting. As such, TNT enters the environment in wastewater and solid wastes resulting from the manufacturing, processing and destruction of munitions. Even though it is rapidly broken down into other chemical compounds in water and sediment, TNT has been found to accumulate in fish and plants (150). During World War I alone, 117,000 cases of TNT poisoning and 475 deaths have been reported in U.S. munitions plants (176).

TNT Toxicological Profile

TNT Absorption

Munition factory workers can be exposed to TNT via inhalation of dust and vapors, and through dermal absorption of dust. Exposure to TNT vapors can occur when the compound is melted and poured into shells. Exposure to TNT dusts can take place in several settings such as during tilling operations using TNT powder or during the loading of melt kettles. The uptake of TNT through inhalation provides a low estimate of TNT

metabolites found in urine of exposed individuals and therefore dermal absorption contributes significantly to the total uptake in a munition factory environment (150). Oral absorption can also be significant if TNT is ingested, with approximately 60% of the initial dose being detected through metabolites in urine 24 hours after ingestion (the rest being mainly detected in feces) based on an *in vivo* study with rats, mice and dogs (150; 181).

TNT Distribution

The small proportion of TNT metabolites remaining in tissues has been found to distribute among the blood, liver, kidney, spleen, lungs, brain, and skeletal muscle of dogs after a single oral dose (5 mg/Kg) (181). A higher distribution of TNT metabolites was also found in the liver, skeletal muscle, and blood of rats, mice and rabbits. Rats that received a 50 mg/kg of TNT by intratracheal administration showed the highest tissue concentration in body fat and the gastrointestinal tract (181). Therefore, it is now known that TNT and its metabolites are lipid soluble (150).

TNT Metabolism

The TNT molecule may undergo various biotransformations, mainly occurring in the liver, and include oxidation of the methyl group, conjugation, oxidation of the benzene ring and reduction of the nitro groups (150). However, the toxic action of nitro-aromatic compounds, including TNT, that is the most frequently observed is the enzymatic reduction of the nitro groups via a flavoenzyme-catalyzed redox cycling (127; 156). This single-electron reduction is induced by flavoenzymes dehydrogenases-electron-transferases and results in the formation of nitro-radicals (156). The reaction initiates the redox cycling of nitro-aromatics and, subsequently, oxidative stress (156).

The phase I enzymes involved in this reduction include the NADPH-cytochrome P450

reductase (P-450R), which greatly contributes to the release of nitrite (162). When the

reduction occurs under hypoxic conditions, amines can be formed. Hydroxylamine

products can also be formed from the two-electron reduction of nitro-aromatics by DT-

diaphorase, and as side-products under aerobiosis (156). TNT mono- and diamino

metabolites have a lower cytotoxicity as compared to TNT and its hydroxylamine

metabolites (156). Figure 3 shows TNT and resulting metabolites from enzymatic

reduction.
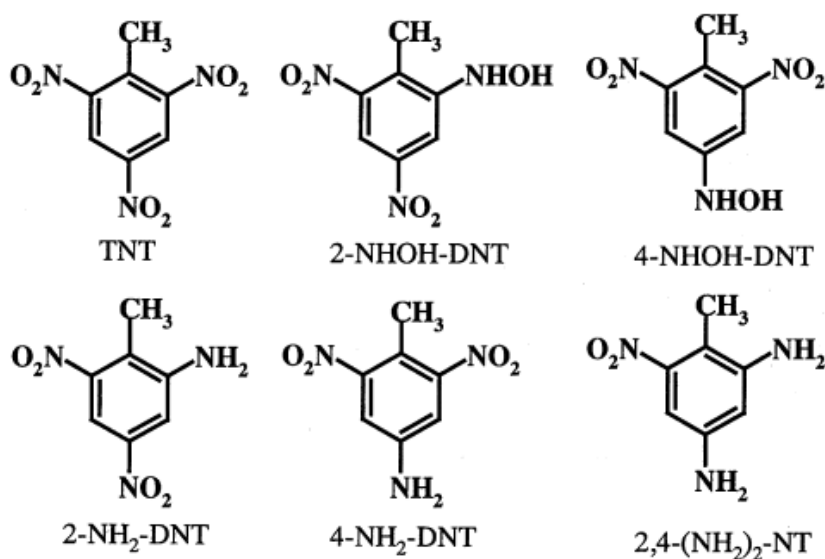
Figure 3. TNT and metabolites derived from TNT enzymatic reduction.
From left to right starting with the upper row: 2-hydroxylamino-4,6-
dinitrotoluene (2-NHOH-DNT), 4-hydroxylamino-2,6-dinitrotoluene (4-
NHOH-DNT), 2-amino-4,6-dinitrotoluene (2-NH$_2$-DNT), 4-amino-2,6-
dinitrotoluene (4-NH$_2$-DNT), and 2,4-diamino-6-nitrotoluene (2,4-(NH$_2$)$_2$-NT).
Extracted from (156).

The two most observed phase II enzymes involved in TNT biotransformation are

uridine-diphosphate glucuronosyltransferase-1 (UDPGT-1) and glutathione-S-transferase

(36). The former catalyzes the glucuronidation of TNT metabolites by transferring

glucuronic acid from UDP-glucuronic acid leading to water-soluble glucuronides that have an increase rate of excretion from cells (159). As for GST, it is responsible for the conjugation of electrophilic metabolites, playing an important role in protecting tissues from oxidative stress by decreasing the amount of reactive TNT intermediates (52). An increase of both enzymes have been reported in TNT-exposed rainbow trout *Oncorhynchus mykiss* (46), European ell *Anguilla anguilla* (37), and rats (56; 206).

The most accepted cytotoxic mechanism of TNT metabolites is the covalent binding of hydroxylamino-dinitrotoluenes and/or their nitroso reoxidation products to sulfhydryl proteins via an acid labile sulfonamide linkage (101; 111). Bioactivation of hydroxylamines in the liver involves oxidation by nicotinamide adenine dinucleotide phosphate (NADPH)-dependent hepatic microsomal enzymes and in blood with oxyhemoglobin. The covalent binding of hydroxylamines to sulfhydryl proteins is dose dependent and has been observed with globin, plasma proteins and proteins in the liver and kidney, resulting in a faster degradation and turn-over of the protein adducts (111). Interestingly, the binding of TNT metabolites is not observed as much in *in vitro* monocultures as *in vivo* since plasma proteins (mainly albumin) in systemic circulation are in close contact with liver cells, trapping active electrophilic metabolites produced in the liver more effectively. In *in vitro* studies, not every liver cell line used is able to produce albumin (111).

Hydroxylamino-dinitrotoluenes can also cause deoxyribonucleic acid (DNA) damage by undergoing the transition metal-catalyzed oxidative redox cycling, inducing direct damage to spermatozoa in sperm of Fisher rats (76; 156). The same study demonstrated that the TNT metabolite 2-NHOH-DNT induced Cu(II)-mediated damage

to DNA fragments *in vitro*. On the other hand, TNT itself did not alter DNA *in vitro*. The study also demonstrated that DNA damage is enhanced by NADH-mediated redox reactions leading to TNT metabolites, while catalase and bathocuproine inhibited DNA damage, suggesting the involvement of H_2O_2 and Cu(I). The later suggests the formation of DNA-Cu(I)-hydroperoxo complex, which can act as a crypto hydroxyl radical leading to DNA damage (76). Notwithstanding these results, the mechanism related to the dynamics between TNT induced reproductive toxicity and gene expression still remains unclear and needs to be further investigated (63).

It is believed, as for most of the nitro-aromatic compounds, that TNT generates reactive oxygen that causes lipid peroxidation in the liver (127; 150). One study has reported the formation of malondialdehyde (MDA) in lamb kidney fibroblast cells exposed for 24 hours to TNT and other nitrocompounds, a product of lipid peroxidation resulting from oxidative stress (23). Molecules that are of particular susceptibility to peroxidation are polyunsaturated fatty acids since they possess multiple double bonds. As a product of lipid peroxidation, MDA is known for its interactions with nucleic acids and induction of mutations (194).

With regard to TNT immunotoxicity, studies show that TNT induces splenomegaly in rats and mice and inhibits splenic macrophage phagocytosis (42; 102; 123). TNT and its metabolites have also been found to impair the immune functions of earthworms *Eisenia fetida* and to inhibit the growth and cytokine production of human peripheral blood mononuclear cells (16; 64). It has been advanced that the net immunotoxicity of TNT and its metabolites to mammalian species increases with an increase in their electron-accepting potency according to the following order: TNT >

hydroxylamino metabolites of TNT > amino and diamino metabolites of TNT. Consequently, the suggested mechanism of action for TNT immunotoxicity is related to oxidative-stress (123).

TNT Elimination

Studies showed that TNT and its metabolites – the major one being aminodinitrotoluene (ADNT) – are primarily eliminated in the urine of Sprague-Dawley rats after administration of a single oral dose (181). Hassman and Hassmanova (73) demonstrated that the levels of ADNT in 88 TNT factory workers increased rapidly during the workday and then declined within 24 hours to close to the levels at the beginning of the workday, suggesting rapid absorption and elimination. The authors also demonstrated that TNT is metabolized completely and that no detectable amounts of unchanged compound are present in the urine.

TNT LC$_{50}$

Several LC$_{50}$s for TNT exposure of mammalian cells in *in vitro* conditions have been reported: 25 µM for fatal liver kinase (FLK) cells (24h exposure); 106 µM for Chinese hamster ovary KI cells (24h exposure); 17.6 µM for rat hepatoma H4IIE cells (24h exposure); 197 µM for Chinese hamster lung V79 cells (24h exposure); and 22 µM for human lymphoblast TK-6 cells (48h exposure) (128).

TNT Induced Genetic Dysregulation

TNT exposure leads to the dysregulation of several genes involved in many biological functions. Deng et al. (2010) found more than 4500 transcripts significantly dysregulated by TNT *in vivo* and 300 TNT-dysregulated transcripts *in vitro*. From the genes dysregulated by TNT both *in vivo* and *in vitro*, the biological functions affected by

this nitrotoluene included: cell cycle; carbohydrate metabolism; molecular transport; cellular growth and proliferation; cell death; DNA replication, recombination and repair; lipid metabolism; cellular assembly and organization; immune cell trafficking; and humoral immune response. A similar study (63) conducted with earthworms exposed to TNT found more than 300 dysregulated genes involved in oxygen transport and iron homeostasis; blood coagulation and fibrinolysis; muscle contraction and cell motility; immune response; antioxidant response; calcium signaling; and protein degradation. A study by Tchounwou et al. (176) investigated the cytotoxicity and the molecular mechanisms of TNT and DNTs via a mammalian gene profile (CAT-Tox) assay with human hepatic cells (HepG2). CAT-Tox allows for the assessment of 13 specific stress gene promoters or response elements. Their results indicated that HepG2 cells exposed to TNT lead to the activation of genes involved in phase I and phase II biotransformation, sequestration of heavy metals, cell cycle regulation, protein repair/sequestration and DNA repair (176). The activation of stress genes by 2,4 and 2,6-DNTs, TNT byproducts, was significantly lower. Table 2 summarizes the results of this study.

Table 2. Activated stress genes promoter/response element by TNT (extracted from (176)).

Promotor	Name/Endogenous Gene Product	Biologic Function
CYP 1A1	Cytochrome-P450 1A1	Phase I biotransformation enzyme
GST Ya	Glutathion-S-transferase Ya subunit	Phase II biotransformation enzyme
HMTIIA	Metallothionein$_{IIA}$	Sequestration of heavy metals
FOS	*c-fos*	Member of AP-1 transcription factor complex
HSP70	70-kDa heat shock protein	Protein chaperone – helps to refold or sequester damaged protein
GADD153	153-kDa growth arrest and DNA damage protein	Involves in cell cycle regulation and response to genotoxic agents
GADD45	45-kDa growth arrest and DNA damage protein	Involves in cell cycle regulation and response to genotoxic agents
XRE	Xenobiotic response element	Binding site for Ah-receptor-planar aromatic hydrocarbon complexes

The same study also suggests that TNT and/or its metabolites bind to the cytoplasmic aryl hydrocarbons (ah) receptor, which is present not only in the liver but also in different tissues such as lung, skin, and kidney. The ah receptor ligand complex then translocates to the nucleus and binds to XRE in the CYP1A1 gene, inducing its transcription. The activation of cytochrome-P450 A1A (CYP 1A1) and of glutathione-S-transferase Ya subunit (GST Ya) by TNT correlates with the capacity of the liver to detoxify active compounds. The promoters *c-fos* and HMTIIA were also responsive to TNT. The *c-fos* is an integral part of several nuclear proto-oncogenes including *c-jun* and is also known to be involved in DNA damage response. The stimulation of *c-fos* and HMTIIA is similar to the response induced by several toxic metals such as cadmium, zinc, copper, silver and arsenic. The activation of HSP70 is thought to be the result of alterations in protein structure from decreased nonprotein thiol groups and formation of disulfide linkages between proteins. Finally, the activation of GADD153 and GADD45 promoters following exposure of HepG2 cells to TNT indicates potential damage at the genomic level. Such damage can be associated to alterations in DNA sequence or to conformational changes in its helical structure. A different study also demonstrated the carcinogenic effects of TNT where the expression of p53 tumor suppressor was observed in MCF-7 human breast cancer cells under the action of the TNT metabolite 2-NH_2-DNT (12).

TNT Impact on Energy Metabolism

TNT and its metabolites, and more specifically their nitro groups, are also known to cause the oxidation of the hemoglobin heme iron, leading to the formation of

methemoglobin (i.e. methemoglobinemia[2]), decreasing oxygen delivery, and resulting in cyanosis (93; 119; 192). The latter can impact energy metabolism by reducing oxidative phosphorylation (192).

A recent study also suggests that 2,6-DNT impacts energy metabolism via dysregulation of glycolysis/gluconeogenesis (149). More specifically, the decreased expression of phosphoenolpyruvate carboxykinase 1 (PCK1), aspartate aminotransferase (GOT1), and malate dehydrogenase 1(MDH1), in several tissues of avian species Northern bobwhite exposed to 2,6-DNT was consistent with a shift in equilibrium away from gluconeogenesis.

Other studies indicate that the impacted energy metabolism by TNT and its metabolites, such as 2,4-DNT, is also caused by the dysregulation of peroxisome proliferator-activated receptor α (PPARα) dependent lipid metabolism (39; 149; 192; 195; 197). PPARα is a ligand-activated transcriptional regulator involved in cellular fatty acid uptake, fatty acid activation, intracellular fatty acid transport, triglyceride storage, lipolysis, ketogenesis, and gluconeogenesis. The decreased expression of PPARα by 2,4-DNT has been functionally-connected to impaired energy metabolism, weight loss, and decreased exercise performance in mice (192).

Human Exposure to TNT and Health Effects

TNT exposure can be assessed through the detection of several metabolites in the urine and blood. Such metabolites include hemoglobin adducts, derived from the covalent binding of TNT metabolites to blood and tissue proteins. For instance, 2ADNT

---

[2] The presence of a higher than normal level of ferric [Fe^{3+}] rather than ferrous [Fe^{2+}] haemoglobin, decreasing its ability to bind oxygen.

and 4ADNT have been isolated from hydrolyzed hemoglobin of Chinese workers in a

munition factory (153). TNT metabolites 2- and 4ADNT have also been detected in the

urine of munition factory workers in Czech Republic and China (152; 188). In some

cases, the assessed level of exposure to TNT can then be used to estimate the risk of

developing particular health outcomes, though the dose-response relationship of TNT in

terms of health effects is still under investigation. Such relationship between dose and

exposure includes an increased prevalence of cataract and increased degree of lenticular

damage in workers with an elevated blood level of hemoglobin adducts (112). The

biomarker hemoglobin adduct 4ADNT has also been associated with an increased risk of

hepatomegaly and splenomegaly (152). Yan et al. (199) have shown a 2.3 fold increased

risk of death from cancer in workers of Chinese TNT factories compared with workers

employed elsewhere, demonstrating the importance of hazard controls.

The route (oral, respiratory or dermal) of exposure combined to the level of

exposure to TNT determine the series of adverse health effects that exposed people can

experience. A first exposure to TNT and/or its byproducts can result in mild irritation on

respiratory passages leading to nasal discomfort, sneezing, epistaxis, and rhinitis, as well

as irritation of the skin (201). The latter can develop into erythema and papular eruptions

and eventually into desquamation and exfoliation (201). Other symptoms of initial TNT

intoxication are gastrointestinal disorders, including nausea, anorexia, and constipation

(176; 183). When absorbed in sufficient amounts through the skin or lungs, TNT and

DNTs can lead to toxic jaundice, hepatitis, aplastic anemia (consequence of damages to

the erythropoietic system), cataracts, menstrual disorders, neurological manifestations,

and kidney damage (176). As mentioned above, methemoglobinemia, reproductive

toxicity (decrease volume of semen and of percentage of motile spermatozoa), skin lesions and dermatitis have been observed in exposed workers or in laboratory from TNT exposure (28; 43; 106). Furthermore, TNT is a known carcinogen and urinary tract, kidney, and liver tumors have been reported (21; 72; 99; 106; 127; 199).

Consequently, TNT, with is known toxicological profile, to include the numerous activated genes by exposed human cells, represents an excellent candidate for a model chemical capable of validating a system, such as the IdMOC system, expected to be used for the toxicity testing of high-N compounds.

INTEGRATED DISCRETE MULTIPLE ORGAN CO-CULTURE (IdMOC) SYSTEM

As mentioned earlier, there has been for the last decade a strong international interest from governmental agencies towards *in vitro* testing for chemical assessment in comparison to the low-throughput *in vivo* testing. However, the complex physiology that influences toxicity *in vivo* is difficult to replicate *in vitro*, and research is required to develop models that will reduce the dependence on animal testing (14). In this regard, recent microarray studies have shown that the gene expression profile from *in vitro* testing in liver slices treated with various compounds could accurately predict the toxicity and pathology observed *in vivo* (32; 38; 47). Furthermore, this system is expected to replicate the binding of TNT electrophilic metabolites (and possibly of high-N metabolites) to plasma proteins by the incorporation of an albumin-producing liver cell line in the co-culture (111).

While considering *in vitro* testing, an investigator needs to choose between primary cultures or established cell lines. Human primary cultures are certainly the most

21

relevant system for *in vitro* screening with regards to species specificity and maintenance of the optimal genetic profiles and signaling pathways. However, a major inconvenience of human primary cultures is the poor availability of human samples, leading to little control over the phenotypes selected for screening. An alternative to primary cultures is immortalized human cell lines. While the latter have the advantage of being easy to culture and the ability to increase screening throughput, there is a risk that they present altered signaling pathways, and in some cases their metabolism is changed (14).

Several *in vitro* models have been developed to replicate as accurately as possible *in vivo* testing. One of the most promising approaches is the IdMOC system. As mentioned earlier, this model allows for the incorporation of a metabolic component for *in vitro* toxicity screening.   It can play a crucial role in both the improvement of our understanding of many biological processes, such as tissue repair, tissue regeneration and malignant spreading, and chemical assessment. The system parameters, such as proliferation rates, can be estimated by calibrating a mathematical or computational model to the observed experimental data. However, parameter estimates can be highly sensitive to the modeling framework and great care needs to be exercised when estimating the parameters of the IdMOC system (117).

A recent study presented earlier investigating TNT with a monocultures system of hepatocytes found 341 transcripts differentially expressed in common among *in vitro* and *in vivo* assays (38). The authors of the study analyzed the changes in gene expression using commercially available genome microarrays after total RNA extraction from samples of both *in vitro* and *in vivo* assays. Consequently, it can be expected that the use of microarray analysis following the co-culture of cell lines from different organs using

the IdMOC system would allow, with the appropriate controls, for the assessment of the changes in gene-transcript expression caused by an exposure to TNT and DNAN.

PUBLIC HEALTH SIGNIFICANCE

High-N molecules give the military the opportunity of improving the performance and the intrinsic characteristics of IM compounds. However, the latter have been found to be very soluble in water, raising environmental concerns about their fate and transport (175). Recently, analysis following the use of the insensitive high explosive PAX-21, found in mortar rounds used by the U.S. and Canadian military, have shown traces of perchlorate residues capable of contaminating billions of liters of groundwater (189). This resulted in the prohibition of these rounds in order to avoid expensive future groundwater cleanup liabilities and reinforced the necessity of risk assessment of chemicals before their production and use. In 1997, it was estimated that more than 21,000 contaminated U.S. military sites existed in many countries; a considerable proportion of those sites being contaminated by explosives (173). The U.S. Army estimated that 1.2 million tons of soil have been contaminated with explosives in the U.S. alone (74). Considering the water solubility of many explosives, both civilian and military populations can be exposed to these compounds following manufacturing, loading, assembling and packing of explosives into munition items (140). It is therefore of the utmost importance that the new high-N compounds being developed have their toxicity assessed and the safer candidates be selected.

Furthermore, while the toxicity of traditional explosives such as TNT is well known, little evidence has been gathered with regards to the effects on human health of high-N compounds in general, including information on their cytotoxicity. While

methemoglobinemia, reproductive toxicity, skin lesions and dermatitis have all been observed in humans exposed to different high-N compounds, the health effects vary in function of the nature of the compound (28; 43; 106). Hence, a system capable of efficiently assessing the cytotoxicity of high-N compounds, when combined with pharmacodynamics, would allow for the estimation of the associated health effects to humans. Among the toxicity components to be determined are the effects of high-N compounds on the level of production of biomarkers and on the level of expression of genes regulating biological functions; two aspects that the present Master of Science in Public Health (MSPH) project seeks to assess with regards to human cells exposed to DNAN.

Previous work by ERDC and partners assessed the relevance of interspecies uncertainty factors in ecological risk assessment (190). A 10-fold uncertainty factor is often applied to account for the fact that humans may be differently sensitive than the test animals from *in vivo* studies. The authors compared the responses of zebrafish and fathead minnow to the high-N compound 1,3,5-trinitroperhydro-1,3,5-triazine (RDX). The results of the study showed a significant difference in responses to RDX between zebrafish and fathead minnows, indicating potential concerns concerning the use of pre-established uncertainty factors based on results from a specific species. A similar study also involving ERDC investigated the neurotoxic effects of RDX among multiple species and found that as evolutionary distance increases, common responses decrease with impacts on energy and metabolism dominating effects in the species that are the most basal in phylogenetic origin (59). Therefore, a system using human cells in a co-culture setting would eliminate the need of using the interspecies uncertainty factor.

The above conclusions support developing a tool that would allow for the efficient assessment of chemical toxicity based on a model representative of human metabolism. The IdMOC system offers the possibility of improving our understanding of chemical perturbations of pathways, including activation or inactivation of specific receptors, enzymes, or transport proteins (141). In the current project, the collection of both media and cells from the co-culture allowed for the assessment of the level of production of biomarkers from high-N exposed human cells, and the evaluation of the gene expression profiles, respectively. The results of such analysis, when processed by pharmacodynamics methods, will lead to a better understanding of the potential human health effects from an exposure to high-N compounds. The IdMOC system can also serve as a cost-effective screening process of high-N chemicals prior to undertaking *in vivo* studies. Ultimately, the system has the potential of improving efficiencies in hazard assessments and preventing exposures not only to high-N compounds, but potentially also to other natural and industrial contaminants.

HYPOTHESIS

Human cell types representative of multiple organs exposed to TNT and DNAN in co-culture: (1) have unique responses relative to cell types exposed separately in monoculture and (2) have unique chemical-exposure specific gene-transcript expression profiles and resultant functional responses indicative of systemic toxicity and of the lower relative toxicity of DNAN compared to TNT.

RESEARCH OBJECTIVES

1) Assess the IdMOC system by comparing results against monoculture assays using TNT as model chemical where cell viability, novel assays measuring functional

biomarker proteins; and molecular pathway enrichment derived from global-

transcript expression assays are used as the primary data for hypothesis testing.

2) Once validated, use the IdMOC system to characterize the toxicity, molecular

   pathway-level impacts and resultant functional impacts of DNAN.

CHAPTER 2: MATERIAL AND METHODS

EXPERIMENTAL DESIGN

All the experiments of this MSPH project were conducted in the cellular biology laboratory of ERDC in Vicksburg, MS, and as such the project was funded by ERDC as part of the RHAAC Project. This project was composed of 6 preliminary experiments and of the final IdMOC experiment. In this final experiment, the efficacy of the IdMOC system as a rapid hazard assessment tool was assessed using TNT as model chemical, while DNAN was also used to collect information about its cytotoxicity.

Five cell lines were selected for the project: kidney: HK-2; liver: THLE-3; lung: NuLi-1; vascular endothelial cells: TeloHAEC; and cardiac muscle cells: AC10; all from ATCC®, Manassas, VA, USA. The cell lines have all been created from normal tissues and express the related cell-type markers. They also have preserved functions from their organ of origin. The cell lines were chosen in order to allow for broad representation of organ systems to maximize coverage of toxicity screening. As seen earlier, the literature indicates that TNT metabolites distribute in the liver, lungs and kidney while no TNT toxicity has been reported on vascular endothelial cells. Consequently, a difference in the toxicity for these cell lines is expected, which would contribute to the validation of the IdMOC system for high-nitrogen compounds.

Figure 4 represents the conceptual model of the IdMOC validation experiment. The details of the experiment are further presented at the end of this chapter. Briefly, the experiment comprised a monocultures setting serving as control, and a co-culture setting using the IdMOC plates (*In vitro* ADMET Laboratories®, Columbia, MD, USA, Catalogue # 71035). For each of these settings and for each cell line, the cells were

plated in the 96-well plates and incubated for 24 or 48 hours (depending on the cell line) at 37ºC until they reached confluence in their respective optimal media (each cell line growing in a specific medium). Once confluence was reached, the cell media was replaced by the co-culture media and for each setting (mono and co-culture), cells were exposed to four concentrations of TNT. Since TNT was first dissolved in dimethyl sulfoxide (DMSO, Sigma-Aldrich®, St-Louis, MO, USA, Catalogue # D2650), the experiment included two controls: co-culture media with and without DMSO. For the co-culture setting, the media covered a set of 6 wells within a chamber, allowing for paracrine interactions. The experiment included four replicates per condition.
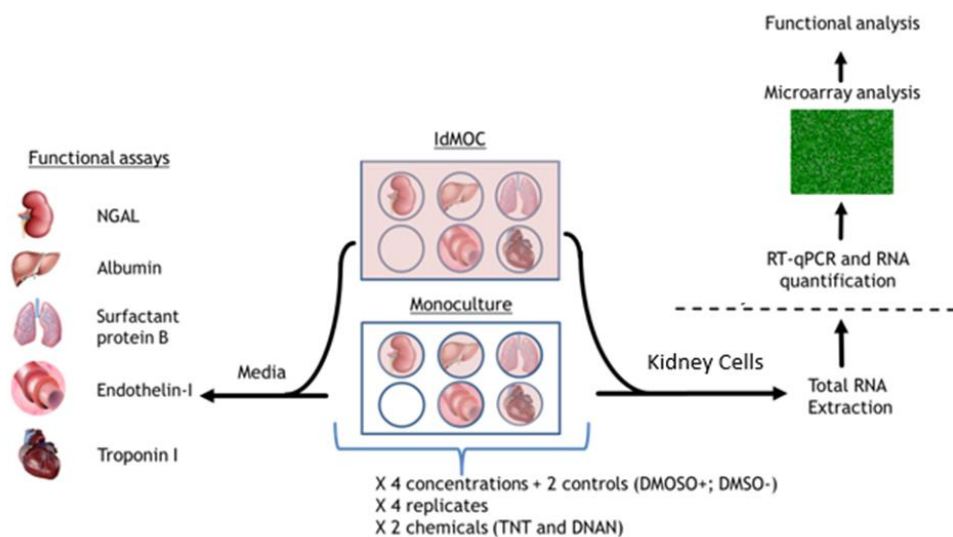
Figure 4. Conceptual model for the validation of the IdMOC system. The cells lines used are from the kidney, liver, lung, vascular endothelium and heart muscle.

Following the 24 hour exposure, cytotoxicity was assessed by two different means: 1) by determining the concentration in cell media of five pre-selected biomarkers, each protein being expected to be produced by one of the cell lines and for which the production is expected to be affected by toxicity; and 2) by collecting the cells for functional analysis using microarray-based global transcript expression analysis.

Following the validation of the IdMOC system using the model chemical TNT, the same system was used to assess the toxicity of DNAN. Additionally, a comparative transcript expression analysis among TNT and DNAN was conducted using a two-way analysis of variance (ANOVA) including Benjamini-Hochberg multiple-test corrections for the statistical analysis.

Before proceeding to the IdMOC experiment, several variables needed to be assessed:

- the growth curve of the cell lines needed to be determined in order to ensure that the cells are used in the same stage of growth during the different exposures. Furthermore, the information obtained from the growth curves is useful for the regular culture of the cells.
- the normal production of the biomarkers by the cells;
- the number of cells to plate in a 96-well plate;
- for each cell line, the quantity and quality of ribonucleic acid (RNA) obtained from a confluent 96-well plate well;
- the effect of reference compounds on the production of the biomarkers;
- TNT (and subsequently DNAN) solubility in the IdMOC system;
- TNT (and DNAN) concentrations to use with the IdMOC system.

The following sections describe in details the related material and methods used to assess these variables (through 6 preliminary experiments) and to accomplish the final IdMOC experiment.

PRELIMINARY EXPERIMENTS

Cell Growth Analysis and Initial Assessment of Biomarkers

Upon reception, the vials were thawed and the cells cultured according to the supplier's protocols specific to each cell line (see Appendix A for the information on the related protocols). Briefly, for each cell line, a 75 cm^2 culture flask containing the recommended culture medium was placed in the incubator. For the culture of the lung cells, flasks were pre-coated with a solution of human placental collagen IV (Sigma Aldrich, Catalogue # C7521); and for the culture of the liver cells, flasks were pre-coated with a solution of fibronectin/bovine collagen/bovine serum albumin (all components from Sigma Aldrich, Catalogue # F4759, C4243, and A2153 respectively). Once thawed, the content of each vial was transferred to a centrifuge tube containing 9.0 mL of culture medium and centrifuged at approximately 1560 relative centrifugal force (RCF) for 5 to 7 minutes. The supernatant was then discarded and the cells were resuspended in fresh growth medium. The vials were centrifuged again and the cell pellets were resuspended in 10 mL of culture medium. The suspension was then added to the prepared culture vessel before being incubated at 37 ºC, 5% CO$_2$, and 90% humidity in the incubator.

In order to estimate the growth rates of each cell line, the cells were then subcultured in 10 x 25 cm^2 flasks. The subculture of the cells was performed according to the manufacturer's protocol. Based on the same protocols, an inoculum from 1.0 x 10^4 to 2.5 x 10^5 cells/cm^2, depending on the cell line, was then cultured. Each day for the next 10 days, the cells from one of the flasks were counted. In order to do so, and unless indicated otherwise by the manufacturer's protocols, 2.0 mL of 0.25% (w/v) trypsin - 0.53 mM ethylenediaminetetraacetic acid (EDTA) solution (Life Technologies®, Grand

Island, NY, USA) was added to the flask. This allowed the cells to detach from the surface of the flasks. To stop trypsinization, 2.0 mL of 1% fetal bovine serum (FBS from Life Technologies®, Catalogue # 1600-044) in Dulbecco's phosphate buffered saline were added and the cells were transferred to a 15 mL tube. From the dilution, two quantities of 10 µL each were deposited on a hemocytometer and the cells were counted under an inverted microscope. The averaged count was than multiplied by a factor of 10^4 in order to have an estimate of the concentration of cells per mL of dilution.

From the curves obtained by plotting the number of cells per cm^2 (Y axis) over the days after subculture (X axis), the population doubling time (PT) was calculated for each cell line. The following equation was used:

DT = T ln 2 / ln (Xe/Xb)

Where: T is the incubation time in any units;

Xb is the cell number at the beginning of the incubation time;

Xe is the cell number at the end of the incubation time.

It can be noted that cells grow at different rates in each of the different phases of growth cycle. However, the growth during the exponential phase (log phase) is relatively constant and reproducible for a given set of conditions. Therefore, the plotting of the growth curves allowed for the determination of the ideal number of cells per cm^2 to inoculate at each passage (i.e. the number of cells corresponding to the middle of the exponential growth phase) as well as the related DT.

In order to determine the initial production of biomarkers by the cell lines, the supernatants of the cells from the flasks of the growth curve experiment were collected

during the first four days. For each cell line, one protein that is expected to be particularly produced by the cell line (readily or once under stress) was selected:

Kidney: neutrophil gelatinase-associated lipocalin (NGAL);

Liver: albumin;

Lung: surfactant-associated protein B-1 (SP-B);

Vascular endothelial cells: endothelin I;

Heart: cardiac troponin I.

The description of these proteins is provided in the section concerning their response to reference compounds. The detection of four of these proteins (NGAL (R&D Systems®, Minneapolis, MN, USA, Catalogue # DLCN20), SP-B (Biomatik USA®, LLC, Wilmington, DE, USA, Catalogue # EKU07525), endothelin I (Boster Biological Technology®, Pleasanton, CA, USA, Catalogue # EK0945), and cardiac troponin I (RayBiotech®, Atlanta, GA, USA, Catalogue # ELH-CTNI)) was conducted through sandwich enzyme-linked immunosorbent assay (ELISA). The technique is relatively similar from one protein to another and an example is presented in Figure 5.
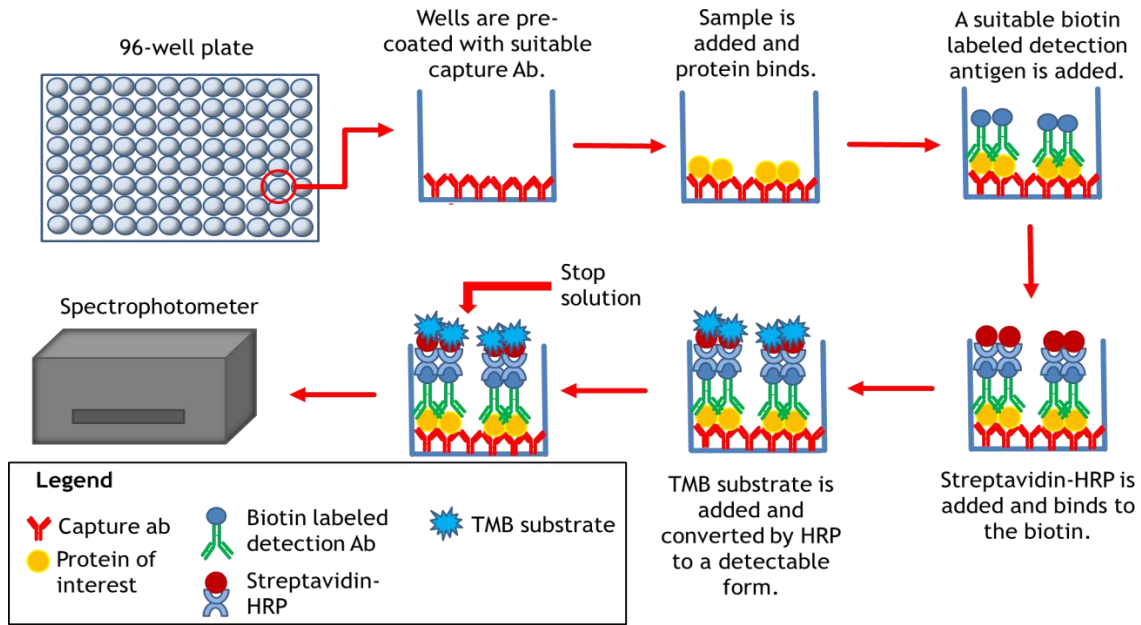
Figure 5. General principle of the sandwich enzyme-linked immunosorbent assay
(ELISA). ELISA assay was used for the assessment of NGAL, SP-B, endothelin
I and cardiac troponin I.

For a protein of interest, the sample was added to a 96-well plate containing pre-

coated wells with a suitable capture antibody (Ab). Depending on the concentration of

the protein in the sample, the capture antibody bound to the protein. A suitable biotin-

labeled detection antibody was then added, followed by a solution of streptavidin

covalently conjugated to horseradish peroxidase (HRP) enzyme. While the streptavidin

binds to the biotin of the detection antibody, the HRP is readily available for its

chromogenic substrate, tetramethylbenzidine (TMB), which is subsequently added.

Between the adding of the different binding agents and substrate, the 96-well plate was

rinsed 4 times with the wash solution recommended by each assay. Finally, a stop

solution (sulfuric acid) was added, changing the samples from blue to yellow, stabilizing

the color development to enable accurate measurement of the intensity at, usually, 450

nm using a spectrophotometer or plate reader. The obtained results of absorbance are

proportional to the concentration of the protein of interest in the samples. The use of standards allowed for the correlation of the absorbance values with the known concentrations of the standards.

With regards to the determination of the concentrations of albumin, the Active Motif Albumin Blue Fluorescent Assay Kit (Active Motif®, Carlsbad, CA, USA, Catalogue # 15002) was used. This assay uses a dye that directly reacts with albumin, leading to a fluorescence signal for which the intensity is proportional to the concentration of albumin. First, 25 µl of the diluted samples was loaded on a standard 96-well plate along a suitable range of standard dilutions. Then, 150 µl of dye reagent working solution was added to each well, followed by a 5 minute incubation at room temperature with gentle shaking. The fluorescence was then measured with the Tecan Safire® plate reader (MTX Lab Systems®, Vienna, VA, USA) at an excitation of 560 nm and an emission of 620 nm. As per the ELISA assays, a standard curve was produced in order to determinate the albumin concentration of the samples.

Determination of the Number of Cells Required per Well

In order to determine how many cells to plate to obtain a confluent monolayer after 24 hours in culture, different numbers of cells were incubated for 24 hours on a 96-well plate. For each cell line, 8 different quantities of cells were assessed: from 10,000 to 80,000 with 10,000 increments. For each quantity of cells, 6 replicates were prepared. Cell confluence was then assessed after the period of incubation by examination of the wells under inverted microscope. Based on the results obtained, the number of cells required to reach confluence was further defined by repeating the same experiment with 1,000 increments. For each cell line, the initial number of cells that led to 100%

confluence after a 24 hour incubation period, or if necessary after a 48 h incubation period, was then used for the final IdMOC experiment.

Co-culture Testing and RNA Quantification

A media capable of supporting the co-culture of the selected cell lines for a maximum of 48 hours (at 37°C with 5% CO_2) was pre-determined: Universal Primary Cell (UPC) Plating Media (*In vitro* ADMET Laboratories®, Catalogue # 81017). In order to ensure that all cell lines were viable in this medium and that enough RNA would be provided for microarray analysis, the cells were plated in the co-culture medium in a 96-well plate and incubated for 8, 24, 32 and 48 hours, with four replicates for each condition. The different incubation times allowed to visually assess, under the inverted microscope, any cell impairment directly noticeable, and to test if the planned 24 hour incubation for the final IdMOC experiment would be sufficient to provide enough RNA. After the period of incubation, the cells were collected by removing the media, washing the cells with a solution of phosphate-buffered saline (PBS), and adding 100 ul of trypsin in order to detach the cells from the surface of the wells. A solution of PBS with 1% FBS was then added to stop the activity of the trypsin and the cells were centrifuged at 1560 RCF for 7 minutes. The supernatant was then discarded and the cells were either flash frozen in liquid nitrogen before being stored at -80°C, or directly processed for RNA extraction.

RNA from the cell samples was then extracted using the RNeasy Plus Universal kit from Qiagen® (Germantown, MD, USA, Catalogue # 73404) and quantified. RNA extraction started by the addition of 300 µl of lysis buffer (RLT buffer). The samples were vortexed before being centrifuged for a few seconds to bring the material down.

The lysis of the cells was completed using a pellet pestle. Three hundred microliters of a

solution of 70% ethanol was then added to the samples, before each sample being

transferred to a filter tube with collector, the filter being selective to retaining RNA. The

tubes were then centrifuged at 9,000 RCF for 40 seconds and the liquid from the collector

was discarded. Three hundred and fifty microliters of wash buffer (RW1 buffer) was

added to the samples before a centrifugation at 9,000 RCF for 40 seconds. The liquid

from the collecting tubes was discarded and 40 μl of a prepared deoxyribonuclease

(DNase) buffer was added on top of the filters. The samples were then incubated at room

temperature for 15 minutes. Three hundred and fifty microliters of RW1 buffer was

added to the samples and the tubes were centrifuged at 9,000 RCF for 40 seconds. The

liquid from the collecting tubes was discarded before the samples undergoing two other

rounds of rinsing with 500 μl of wash buffer (RPE buffer) with a centrifugation at 9,000

RCF for 40 seconds and finally 2 minutes. The filters were transferred to new collecting

tubes before being centrifuged at 16,500 RCF for 1 minute. The filters were transferred

to 1.5 mL Eppendorf tubes and 25 μl of RNase free water was added on top of the filters

to collect RNA. The samples were then centrifuged at 9,000 RCF for 1 minute before

being put on ice. RNA quantification was then undertaken using 1 μl of the samples with

the NanoDrop-1000 spectrophotometer (Thermo Fisher Scientific Inc.) and the ND-1000

v.3.7.1 software.

Several variants of the above RNA extraction protocol have been tested in order

to find the optimal conditions. The use of the RNeasy Micro Kit from Qiagen®

(Catalogue # 74004) allowed for the best yield of RNA. While the protocol is similar, the

kit includes micro-columns and an RNA carrier allowing the further concentration of the

RNA samples.   RNA carriers are molecules mimicking nucleic acid and increasing the concentration necessary to form aggregates that can be precipitated.

Evaluation of Biomarkers Response to Stress

Functional assays were conducted with each cell line in order to assess the response to reference compounds known to have an effect on the selected biomarkers (Table 3). Cells of each cell lines were first incubated in their optimal medium for a 24 hour period in order to reach confluence. Each cell line was then exposed for 24 hours, in the UPC co-culture medium, to each of the five reference compounds for a total of six conditions including the appropriate control, with three replicates per condition (4). The medium from each condition was then collected in order to proceed to the respective functional assay. One-way ANOVA and pairwise comparisons were conducted on the results from the functional assays in order to determine significant changes among treatments. The following paragraphs describe the compounds selected and the biomarker specific to each cell line.

Table 3. Selected reference compounds and related biomarkers.

Cell line	Reference compound	Biomarker	Expected impairment	References
HK-2 (kidney)	Cyclosporin A	NGAL	Increase	(69; 80; 139; 160; 163)
THLE-1 (liver)	Troglitazone	Albumin	Decrease	(33; 57; 100; 118; 207)
NuLi-1 (lung)	All-trans retinoic acid	SP-B	Increase	(15; 22; 61)
TeloHAEC (vasc. endo.)	VEGF-121	Endothelin I	Decrease	(51; 75; 169)
AC10 (heart)	Daunorubicin	Cardiac troponin I	Increase	(2; 122; 129; 138; 161; 165)

HK-2 (Kidney): Cyclosporin A and Neutrophil Gelatinase-Associated Lipocalin Production

Cyclosporin A (Sigma Life Science®, Catalogue # C3662) was selected as reference compound for HK-2 kidney cells. Cyclosporin A is a nephrotoxic agent leading to vasoconstriction involving several mediators (prostaglandins, renal sympathetic nerves, dopamine, nitrogen monoxide, endothelin I) (163). Primary kidney cells exposed *in vitro* to cyclosporin A have shown elevated levels of the nephrotoxicity biomarkers neutrophil gelatinase-associated lipocalin (NGAL) (80). NGAL is produced and secreted by kidney tubule cells at low levels. However, following an ischemic, septic, or nephrotoxic injury of the kidneys, the amount of NGAL produced and secreted into the urine and serum increases dramatically (139). Consequently, NGAL has been suggested as a biomarker of acute kidney injury (69; 160).

THLE-1 (Liver): Troglitazone and Albumin Production

For the THLE-3 liver cells, troglitazone (Sigma-Aldrich®, Catalogue # T2573) was selected has reference compound. Troglitazone is known to cause serious idiosyncratic hepatotoxicity. The reactive metabolites of troglitazone covalently bind to cellular macromolecules but the role of these metabolites on troglitazone toxicity is controversial. Nevertheless, mitochondrial dysfunctions, especially mitochondrial permeability transition, apoptosis and PPARγ-dependant steatosis have all been observed (118). Furthermore, primary human hepatocytes exposed to troglitazone resulted in a decreased production of albumin. Albumin constitutes up to 70% of the total plasma proteins and is produced by the liver. Its main function is the regulation of the colloid osmotic pressure of the blood (53). Hepatocyte cytotoxicity has been found to lead to

decreased levels of albumin, making it a potential biomarker of high-nitrogen induced toxicity (33; 57; 100; 207).

NuLi-1 (Lung): All-Trans Retinoic Acid and Alveolar Surfactant-Associated Protein B Production

For the NuLi lung cells, all-trans retinoic acid (Sigma Life Science®, Catalogue # R2625) was selected as reference compound. All-trans retinoic acid (RA) is a metabolite of retinol (vitamin A), both playing a role in growth and differentiation of epithelial cells in several organ systems (61). However, at high concentration, RA dramatically alters the developmental pattern of the lung, leading to growth structures similar to proximal airways and suppressing distal epithelial buds (22). It has been shown that at high concentration, all-trans-RA decreases the accumulation of surfactant-associated protein (SP)-A and SP-C mRNA while it has an opposite dose-dependent stimulatory effect on SP-B mRNA in human lung adenocarcinoma cells (61). Pulmonary surfactant, which role is to reduce alveolar surface tension, is a lipoprotein produced by alveolar type II epithelial cells and composed of approximately 90% lipid and 10% protein by weight. From the protein portion, four SPs have been identified to date: SP-A, SP-B, SP-C and SP-D (61). The levels of SP-B, along with SP-A, have been shown to provide a non-invasive tool to evaluate the integrity of the broncho-alveolar/blood barrier. Induced toxicity on human lung cells often leads to a decrease expression of SP-B (13; 71). Consequently, the observed increase of SP-B in human lung adenocarcinoma cells can be the result of a conferred protection to all-trans RA since it has been shown that SP-B is critical to survival during acute lung injury (15).

TeloHAEC (Vascular Endothelium): Vascular Endothelial Growth Factor (VEGF)-121

and Endothelin I Production

Vascular endothelial growth factor (VEGF)-121 (Peprotech®, Rocky Hill, NJ, USA, Catalogue # 100-20A) was selected as reference compound for the TeloHAEC vascular endothelial cells. VEGF is involved in endothelial homeostasis, controlling differentiation, mitogenicity and endothelial survival (51). Loss of VEGF signaling is known to result in endothelial apoptosis. VEGF is also implicated in pulmonary arterial hypertension, where increased levels of VEGF are observed (75). It is suggested that VEGF may promote vascular health by decreasing endothelin I production in human microvascular endothelial cells (169). The endothelium of blood vessels produces paracrine regulators, to include endothelin I, which directly promotes vasoconstriction, and bradykinin, which promotes vasodilatation. Consequently, these two proteins play an important role in the control of blood flow and blood flow pressure (53). Several studies have shown that exposure to pollutants and biologic agents (including ambient pollutant particles, interferon inducers and polycyclic aromatic hydrocarbons) enhances the release of endothelin I (29; 60; 81).

AC10 (Heart): Daunorubicin and Cardiac Troponin I Production

For the AC10 cells, daunorubicin (Sigma-Aldrich®, Catalogue # W 4013) was selected as reference compound. Daunorubicin is an anthracycline discovered in the early 1960s and still used today as a component of chemotherapy protocols for acute myelogenous leukemia. Nevertheless, at sufficient dose, daunorubicin is known for causing heart function impairments, to include a decrease in heart rate (165). As part of its metabolic effects, daunorubicin increases the levels of cardiac troponin I and T in

rabbits (2). Troponin is a complex of three proteins: troponin I (which inhibits the binding of the cross bridges to actin), troponin T (binding to tropomyosin), and troponin C (binding Ca^{2+}). Troponin, along with tropomyosin, regulates the attachment of cross bridges to actin, and so doing serves as a switch for muscle contraction and relaxation. Cardiac muscle, like skeletal muscle, contains the troponin complex. Damage to myocardial cells, such as during myocardial infarction, leads to the release of cardiac troponin into the blood (53; 122; 161). Therefore, cardiac troponin I is highly specific for myocardial necrosis and has been used as biomarker for the detection of drug- or biologic agent-induced cardiac toxicity (129; 138).

Assessment of TNT and DNAN Loss to the Experimental Apparatus

After a 24 hour incubation (37ºC, 5% CO_2 / 95% air atmosphere) in an IdMOC chamber (unit composed of six wells), the remaining concentration of soluble TNT and DNAN in co-culture media was determined for an initial concentration of approximately 500 nM. For each chemical, two replicates were collected at time 0 h and time 24 h and sent for chemical analysis by research chemists of the ERDC Environmental Chemistry Branch. The method of detection used was Environmental Protection Agency (EPA) method 8330 intended for trace analysis of explosives residues via a high performance liquid chromatography with a UV detector.

Following this first experiment, the resulting TNT degradation observed was further investigated by incubating a solution of 500 nM of TNT in co-culture media according to three conditions: 1) in amber glass tubes; 2) in clear class tubes; and 3) in IdMOC plates containing wells with a confluent layer of vascular endothelial cells. The incubation times were 0, 1, 2, 6 and 24 hours. The first and second conditions were set in

order to determine the influence of light on TNT degradation. The third condition aimed at reflecting the final IdMOC experiment where the wells are covered with a confluent cell layer, limiting the possible binding of TNT to the plate material. The vascular endothelial cells were selected since they are not expected to metabolize TNT. For each condition at a specific incubation time, two replicates were assessed. After each incubation period, the samples were transferred in amber glass tubes and stored at 4 °C until chemical analysis. The latter was undertaken by the chemical analysis section of ERDC. The EPA method 8330 was conducted to assess the concentration of TNT, but also of 2-Amino-4,6-DNT and of 4-Amino-2,6-DNT, two major degradation by-products of TNT. The latter have been showed to form in various conditions, both aerobic (4-amino-2,6-DNT only) and anaerobic, to include in serum bottles incubated in reduced conditions (82; 89). Other degradation by-products were also analyzed and are represented in table 4 along with the conditions (aerobic/anaerobic) where they are met.

Table 4. TNT degradation by-products analyzed.*

TNT by-product analyzed	Detected in aerobic conditions	Detected in anaerobic conditions
2-Amino-4,6-DNT		X
4-Amino-2,6-DNT	X	X
2-hydroxylamino-4,6-DNT		X
4-hydroxylamino-2,6-DNT	X	X
2,4-diamino-6-nitrotoluene	X	X
4-hydroxytoluene		X

*Extracted from (89).

Range Finding Experiment

For the range finding experiment, each cell line was individually exposed to nine concentrations of TNT and DNAN plus three controls. The exposure concentrations for the individual TNT and DNAN exposure assays were 1 nM, 10 nM, 100 nM, 1 μM, 10 μM, 100 μM, 1 mM, 10 mM, and 100 mM. The high-N compounds were first dissolved in DMSO, so that the TNT and DNAN dilutions in co-culture media included a concentration of 1% DMSO. The three controls included co-culture media with and without 1% DMSO, and co-culture media where 4% of polysorbate 20 (Tween 20 by Sigma-Aldrich®, Catalogue # P2287) was added 30 minutes prior to the end of the incubation period of 24 hours. The latter was added in order to have a control simulating close to 0% survivability. The orders of magnitude of the TNT concentrations were derived from previous studies showing a LD_{50} of approximately 450 μM for human neuroblastoma NG108 (7-h incubation) and 460 μM for human hepatocarcinoma HepG2 (48-h incubation) (12; 176). Test functional assays were then completed as per previous experiments (albumin, NGAL, SP-B, endothelin I and cardiac troponin I). For each test, the default benchmark response rate of 10% was selected as point of departure (BMD_{10} and its 95% lower confidence limit or $BMDL_{10}$). The lowest BMD_{10} was used as point of reference for dosing in the IdMOC system. Additionally to the BMD_{10} and control, the three TNT and DNAN concentrations assessed that were just below the BMD_{10} were also selected for the IdMOC experiment.

As a supplemental tool to determine the range of TNT and DNAN concentrations for the final IdMOC experiment, the survivability of the cells was assessed via Neutral Red Assay. First, a desorbing solution was prepared containing 1% acetic acid, 50% ethanol, and 49% of distilled water. Then 30 minutes before use, a co-culture medium

solution containing a concentration of 33 µg/mL of neutral red (Sigma-Aldrich®,

Catalogue # N2889) was prepared. The media was then sterilized using a 0.22µm

syringe filter (Sigma-Aldrich®). After the incubation period, the culture media was

collected and the cells were rinsed with a solution of PBS. Then, 250 µl of neutral red

medium was added to each well and the cells were incubated for a 2 hour period at 37°C.

The medium was then removed and the cells were rinsed with a solution of PBS before

adding 100 µl of neutral red desorbing solution to each well. The plates were then

covered with a foil and incubated at room temperature for 45 minutes with rapid shaking.

The absorbance of each well was then read on a plate reader at 540 nm emission. Three

replicates of blank wells containing no cells were used in order to control for neutral red

binding to the plastic of the plates.

LC$_{50}$s were calculated for each pair of toxicant and cell line using a nonlinear (S-shaped) regression model (164) with the following equation:

$$\text{viability (\%)} = \frac{100}{1+e^{b(c-\mu)}}$$

where:

- b = the estimated parameter representing the curve elongation;
- c = log of the molar concentration; and
- µ = the estimated LC$_{50}$.

For each LC$_{50}$, a 95% confidence interval was generated from the regression. All LC$_{50}$s

and 95% confidence intervals were calculated in SPSS Statistics Software (Version 22,

IBM®).

IdMOC EXPERIMENT

Once the RNA yield obtained from cells in co-culture media was sufficient and the TNT dosing range determined, each cell line was placed in different wells on a 96-well IdMOC plate in its respective media as per manufacturer instructions and for 24 hours at 37°C with 5% CO_2. For cells requiring a collagen coated surface, individual wells had previously been coated with collagen/fibrinogen as needed. After having confirmed that each cell line forms a confluent (80-95%) layer, individual media was replaced by the pre-determined co-culture media, covering the entire set of wells. Plates were then incubated for an additional 24 hours while exposed to the five pre-determined TNT concentrations (including control). Each treatment included four biological replicates.

Following the incubation period, the media was harvested and functional assays specific to each selected biomarker were conducted. One-way ANOVA and pairwise comparisons were conducted on the results from the functional assays in order to determine significant changes among treatments. Cells were also harvested and stored at -80°C. The samples from the kidney cells exposed to the two highest concentrations of toxicants were selected for further investigation via transcript expression analysis. Once the RNA extracted was quantified, RNA quality was further analyzed using the Agilent RNA 6000 Nano Kit. The kit comprises RNA 6000 Nano LabChips (Agilent Technologies) with an interconnected set of microchannels allowing for the separation of nucleic acid fragments based on their size as they progress through the chip electrophoretically. First, the RNA from the ladder and samples was denatured for 2 minutes at 70ºC and the vial was immediately cooled on ice. The gel was then prepared

by pipetting 500 µl of RNA gel matrix into a spin filter. The filter was centrifuged at

1,500 RCF for 10 minutes and 65 µl of filtered gel was put in microcentrifuge tubes. The

gel-dye mix was then prepared by vortexing the RNA dye concentrate for 10 seconds and

adding 1 µl of dye into a 65 µl aliquot of filtered gel previously prepared. The solution

was vortexed and centrifuged at 13,000 RCF for 10 minutes. The gel-dye mix was

loaded on a RNA chip by putting a new RNA chip on the chip priming station. Nine

microliters of gel-dye mix was pipetted into the chip at the three indicated wells. Each

time, the chip priming station was closed and the plunger pressed until it was held by the

clip. The clip was then released 30 seconds later and the plunger was pulled back.

Following the loading of the gel-dye mix, 5 µl of RNA marker was loaded in all the

receiving wells. Finally, the ladder and samples were loaded by pipetting 1 µl of each in

the respective wells, while 1 µl of RNA marker was loaded in each unused well. The

chip was then vortexed for 1 minute at 2400 RPM before being run in the Agilent 2100

Bioanalyzer instrument (Agilent Technologies, Waldbronn, Germany) with RNA 6000

Nano LabChips. Only samples with RNA integrity numbers > 7 were used for the

microarray hybridizations.

MICROARRAY DATA ANALYSIS

Microarray analysis complemented the experimental design, allowing for the

assessment of changes in molecular and cell functionality. Microarrays provide a

snapshot of transcriptional activity in each biological sample. By going further than the

study of a single gene or small set of genes, microarrays facilitate the discovery of global

transcript expression providing higher-order functional associations of genes to metabolic

and genomic signaling networks. It is therefore a valuable tool to identify the underlying

mechanisms of xenobiotic agents. On the other hand, this technology produces a considerable amount of data which, in the past, were challenging to interpret. Fortunately, several computational tools have been developed in the last decade to greatly enhance the interpretation of microarray results. Figure 6 indicates the steps conducted within microarray experiment workflow (167).

Following the 24 hour incubation in co-culture and monocultures, the kidney cells were individually isolated and lysed for RNA extraction and analysis as described above. Total RNA was extracted from approximately 12 mg of cell pellet. The samples that underwent microarray analysis are the kidney cells exposed to the highest two TNT and DNAN concentrations as well as the related DMSO+ controls.
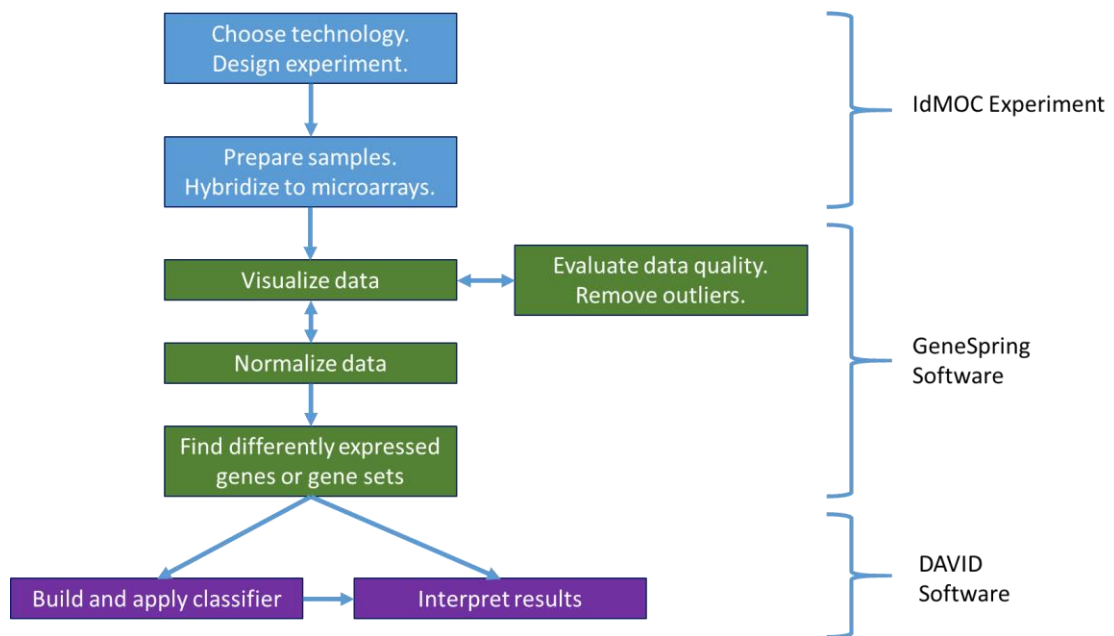
Figure 6. Overview of steps in a typical gene expression microarray experiment and application to the current project (modified from (167)).

The Agilent LowInput QuickAmp Labelling Kit protocol (Agilent Technologies) was utilized for cRNA synthesis with microarray hybridizations following manufacturer's recommendations. Fifteen ng of total RNA was utilized for starting

material and 600 ng of Cy3 labelled cRNA was used for hybridizations. An Agilent

Surescan Microarray Scanner (G2505 C, Agilent Technologies Inc.) was used to scan

microarrays at 3 μm resolution. Data were extracted from microarray images using

Agilent Feature Extraction software (Agilent Technologies). Analysis of internal control

spikes indicated that signal data was within the linear range of detection.

Microarray data analysis was performed using GeneSpring version GX11.5

(Agilent Technologies) where TNT and DNAN experiments were analyzed separately.

Microarray data were first normalized to the 75th percentile within each array followed

by median scaling among all exposures. For each chemical, the effects of the two main

experimental conditions, culture (mono- versus co-culture) and chemical exposure level

(control, dose 1 and dose 2), were tested for effects on global-transcript expression using

two-way ANOVA where $p = 0.01$, including Benjamini-Hochberg multiple test

corrections. Pairwise comparisons among experimental treatment levels were conducted

using Welch unpaired unequal variance t-tests including a 1.5 fold cutoff. Finally,

principal component analysis (PCA) was performed to visualize summary-level trends in

transcript expression among treatments.

FUNCTIONAL INTERPRETATION

To assist with the interpretation of the global transcript expression results, the

database for annotation, visualization and integrated discovery (DAVID, version 6) was

used to derive significant annotation clusters for gene-transcripts that had significant

differential expression within each exposure (78). DAVID is available for free online (1)

and allows for the functional interpretation of large lists of genes derived from genomic

studies. It uses agglomeration algorithm to condense a list of genes into organized

48

classes called biological modules. This bioinformatics resource helps in grouping functionally related genes into manageable biological modules facilitating the interpretation of genes in a network context. To this end, DAVID features the Gene Functional Classification Tool which analyses the list of differentially expressed genes (DEGs) by 1) measuring the functional relationship of gene pairs via the similarity of their global annotation profiles derived from different annotation categories such as National Institute of Health (NIH) Genetic Association DB and NCBI OMIM; 2) using an agglomeration method to partition genes into functional gene groups; and 3) displaying the results in text and graphic modes (79). DAVID is widely used and leads to the identification of genes playing important roles in the development of a disease or in a toxic response (196). The identified genes can then serve as potential biomarkers.

Additionally to identify significant differential expressions revealing toxicological pathways, microarray analysis results were compared with the results obtained from previous animal studies.

DETERMINATION OF CELL GROWTH RATE CHARACTERISTICS

Figure 7 indicates, for each cell line, the number of cells per square centimeter per number of days after inoculation. Consequently, the slope of each graphic is representative of how rapidly a specific cell line is growing. The doubling time, as described in the previous section, is indicated beside each cell line in the legend and fluctuates from 1.33 to 2.34 depending on the cell line. While these doubling times are favorable to cell growth, it is also important to look at when the cells reach the peak of their growth rate (the steepest area of each growth curve). For three of the cell lines (kidney, lung, vascular endothelial), this peak is reached one day after inoculation as indicated by the red markers. The liver cells are the slowest growing cell line, reaching their growth rate peak six days after inoculation, which represented a limiting factor for this project.
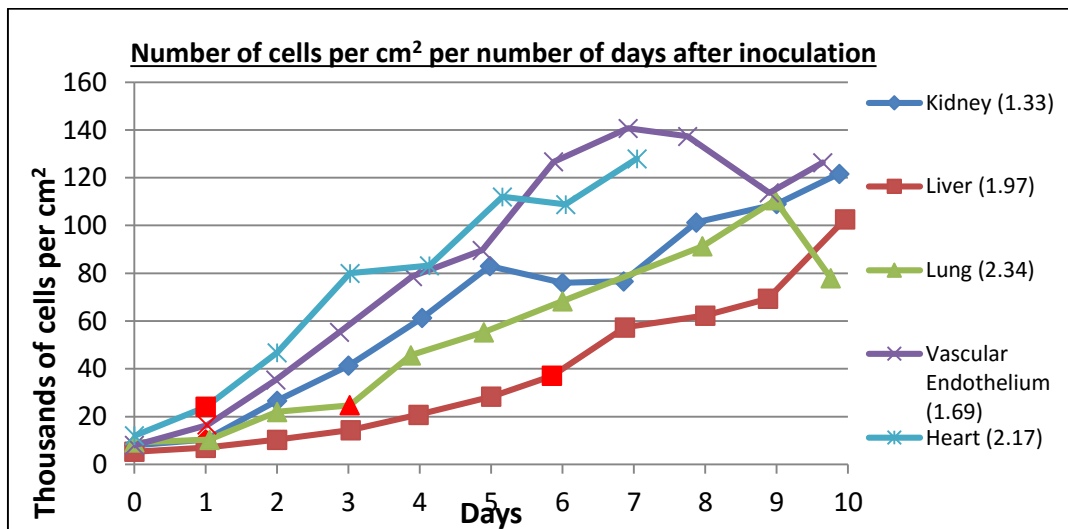
Figure 7. Number of cells per cm^2 per number of days after inoculation. The doubling times are indicated in the brackets beside each cell line in the legend. The red markers represent the day the cell lines reached the peak of their growth rate.

DETERMINATION OF CELL INITIAL BIOMARKER PRODUCTION

Figures 8 to 12 show the production of the selected biomarkers by each cell line. Cell lines that are expected to produce each biomarker are indicated by a red frame. The values were obtained from the media collected from the culture vessels of the growth curve experiment presented previously. Consequently, this preliminary experiment had one replicate only. While NGAL was expected to be produced mainly by the kidney cells, the lung cells were found to produce the protein at a higher level. The liver cells were producing the highest amount of albumin, but the kidney, lung and cardiac muscle cells were also producing albumin at a lower level. In all cases, the level of albumin decreased over time. SP-B was produced, as expected, by the lung cells. However, it was also produced by the liver cells, and at a higher level by the kidney cells. It is important to mention though that as per the instruction manual for the SP-B ELISA kit, cross-reactivity with SP-B analogues may be possible. Out of all the biomarker assays conducted, the endothelin I assay was the most conclusive. Figure 11 shows that endothelin I was mainly produced by the vascular endothelial cells as expected. Finally, cardiac troponin I production was observed with the cardiac muscle cells. However, it appears that the liver cells and lung cells were also producing significant levels of cardiac troponin I. Nonetheless, the level observed with the liver cells (on day 2) might be an outlier as no cardiac troponin I production was observed with the liver cells in subsequent assays.
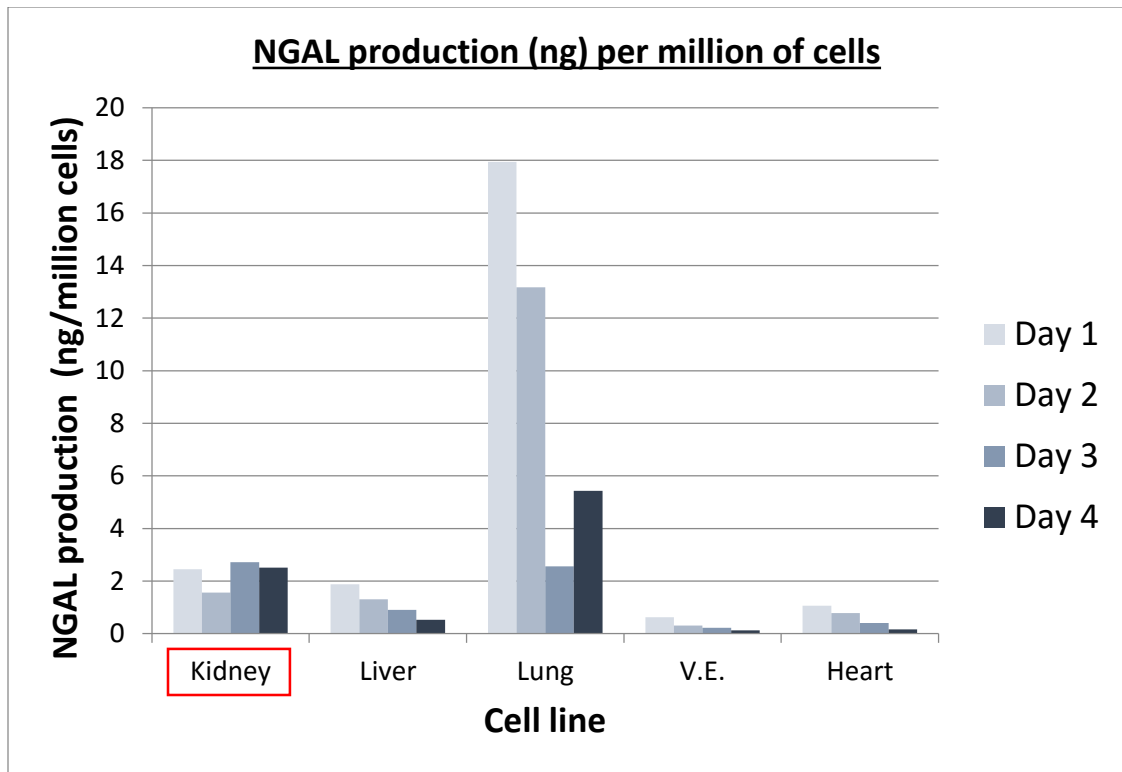
Figure 8. NGAL production (ng) per million of cells. Kidney cells were expected to produce the biomarker.
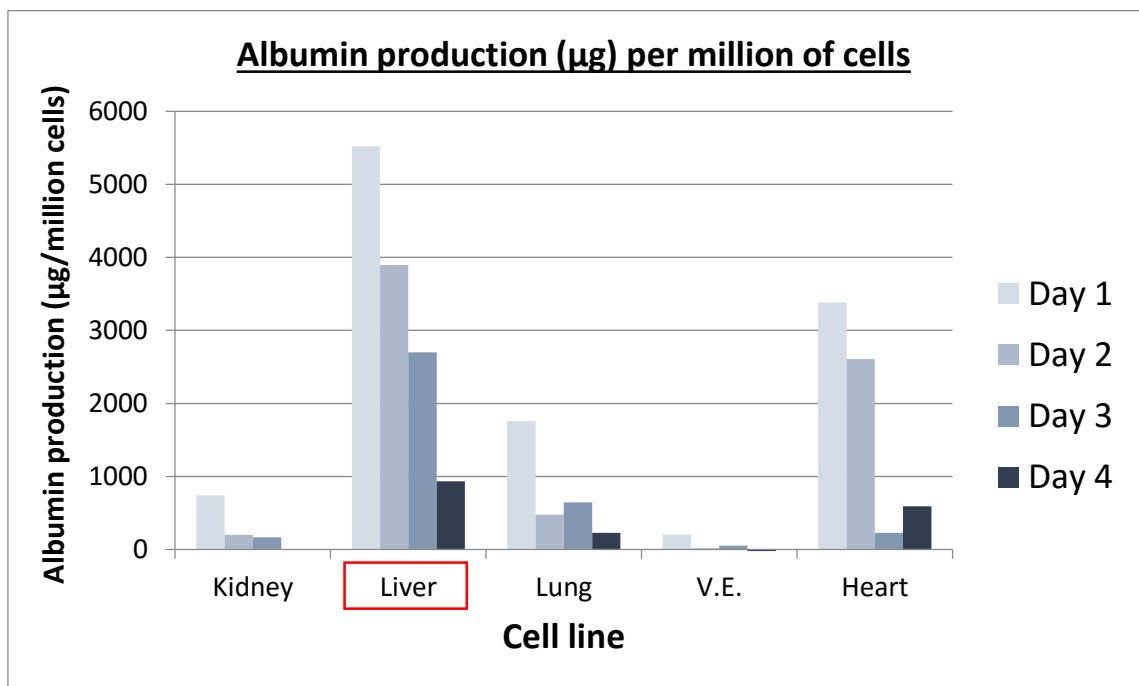
Figure 9. Albumin production (µg) per million of cells. Liver cells were expected to produce the biomarker.
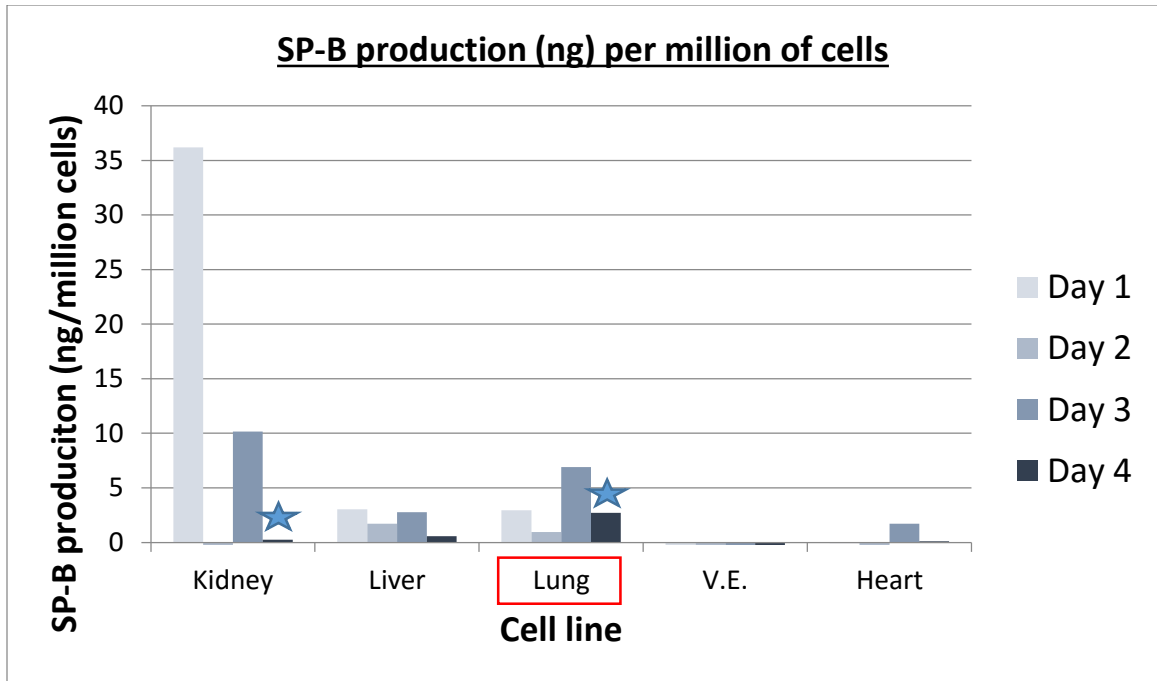
Figure 10. SP-B production (ng) per million of cells. The stars indicate where a change of media may have contributed to the observed decrease of protein production. Lung cells were expected to produce the biomarker.
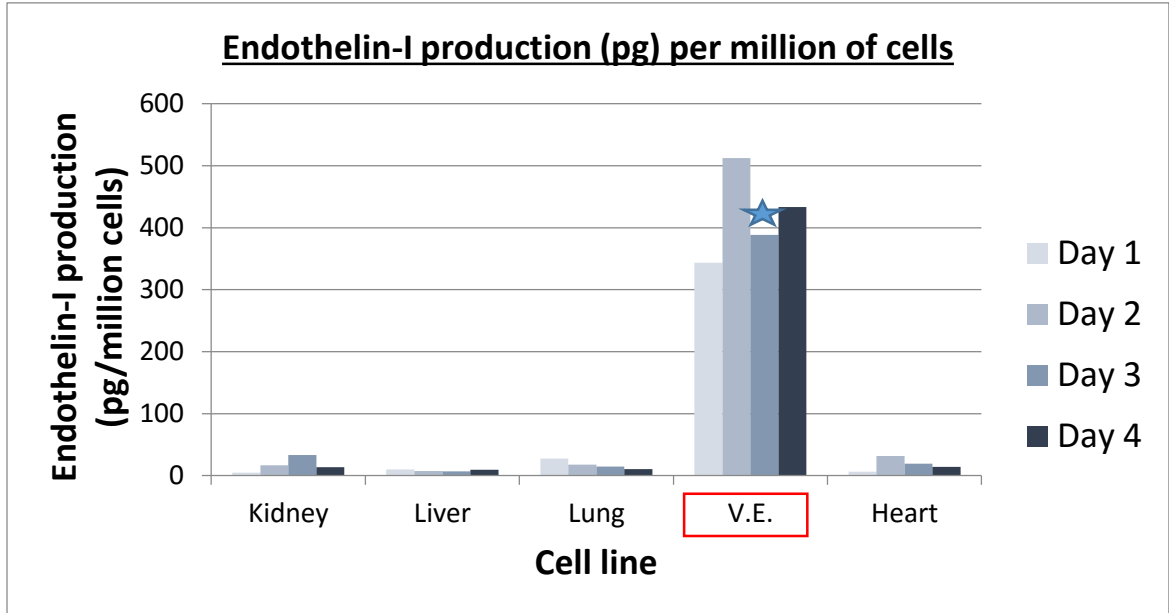
Figure 11. Endothelin I production (pg) per million of cells. The stars indicate where a change of media may have contributed to the observed decrease of protein production. Vascular endothelial cells were expected to produce the biomarker.
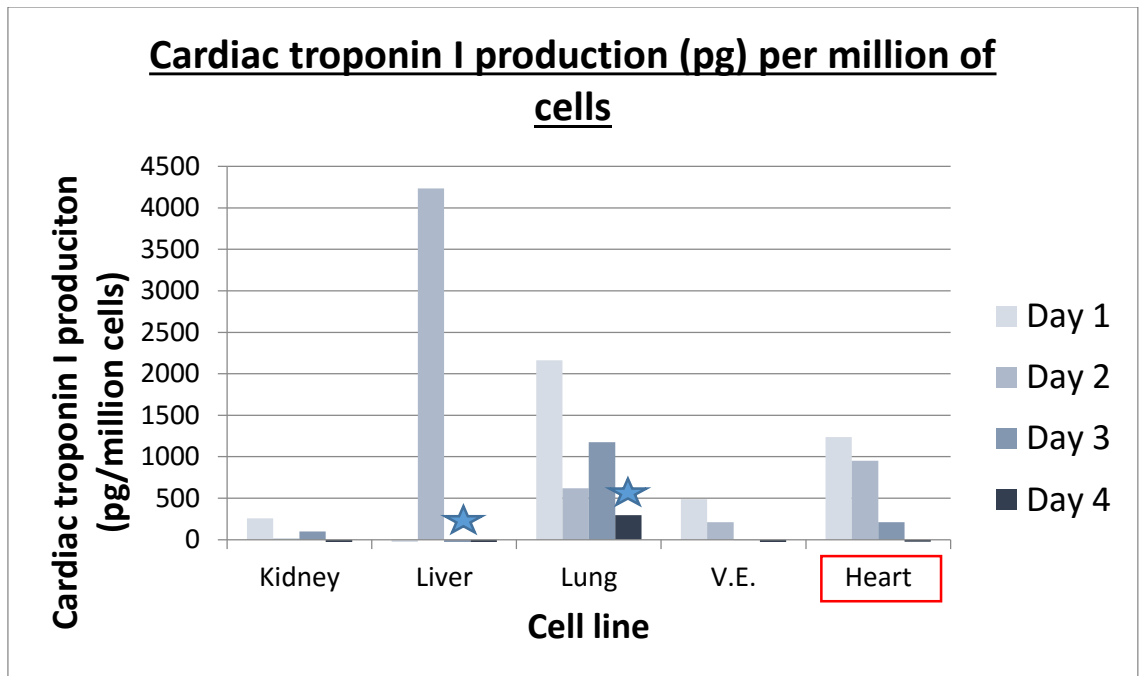
Figure 12. Cardiac troponin I production (pg) per million of cells. The stars indicate where a change of media may have contributed to the observed decrease of protein production. Heart cells were expected to produce the biomarker.

DETERMINATION OF NUMBER OF CELLS TO PLATE

Figure 13 shows, for each cell line, the number of cells required to reach confluence after a 24 hour (or 48 hour) incubation period in a well from a 96-well plate. While the number of cells is relatively similar for the kidney, liver, vascular endothelial cells, and cardiac muscle cells, only 24,000 lung cells are required due to their larger size. A 48 hour incubation was required for the cardiac muscle cells to reach confluence. While 24 hours were sufficient for 72,000 vascular endothelial cells to cover the surface of a well, a 48 hour incubation period was used in order to provide enough RNA to conduct potential future microarray analysis.
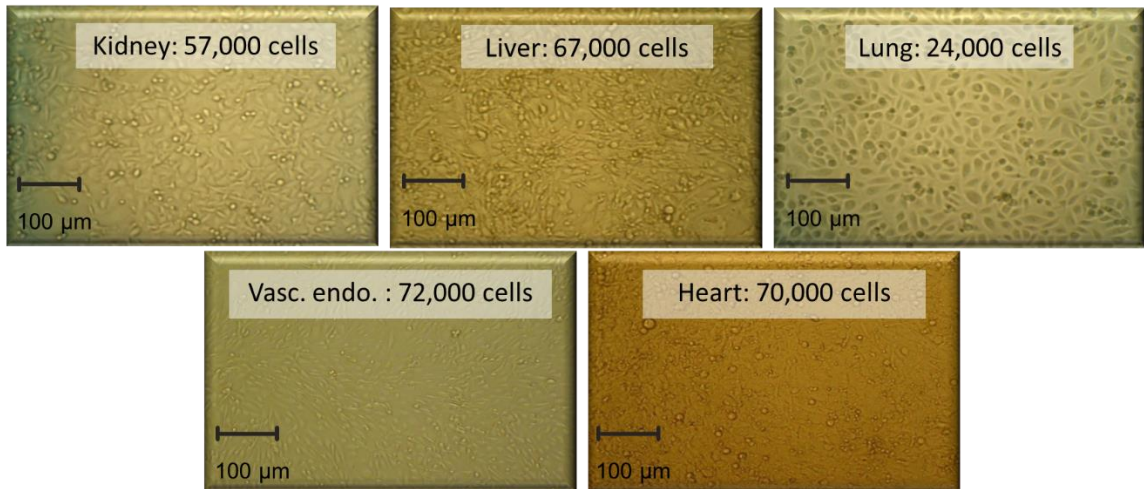
Figure 13. Number of cells to plate in order to reach confluence.

DETERMINATION OF RNA EXTRACTION CONDITIONS

Figure 14 shows the RNA yields obtained from three different RNA extractions with cells growth for 8, 24, and 48 hours in co-culture media. The red line indicates the minimum RNA yield (10 ng/μl) required to proceed to microarrays. The first RNA extraction was conducted using standard spin-columns and fresh cells from the 24 hour incubation in the co-culture media. These conditions provided a sufficient RNA yield for only two of the cell lines (liver and heart) when considering the standing error, with practically no RNA yield obtained for the vascular endothelial cells.

RNA yield (µg/ml) from cells plated in 96-well plates

Legend:
- 24h - Normal columns - Fresh cells
- 48h - Micro-columns - Fresh cells
- 8h - Micro-columns and RNA carrier - Frozen cells
- Required RNA concentration for microarrays
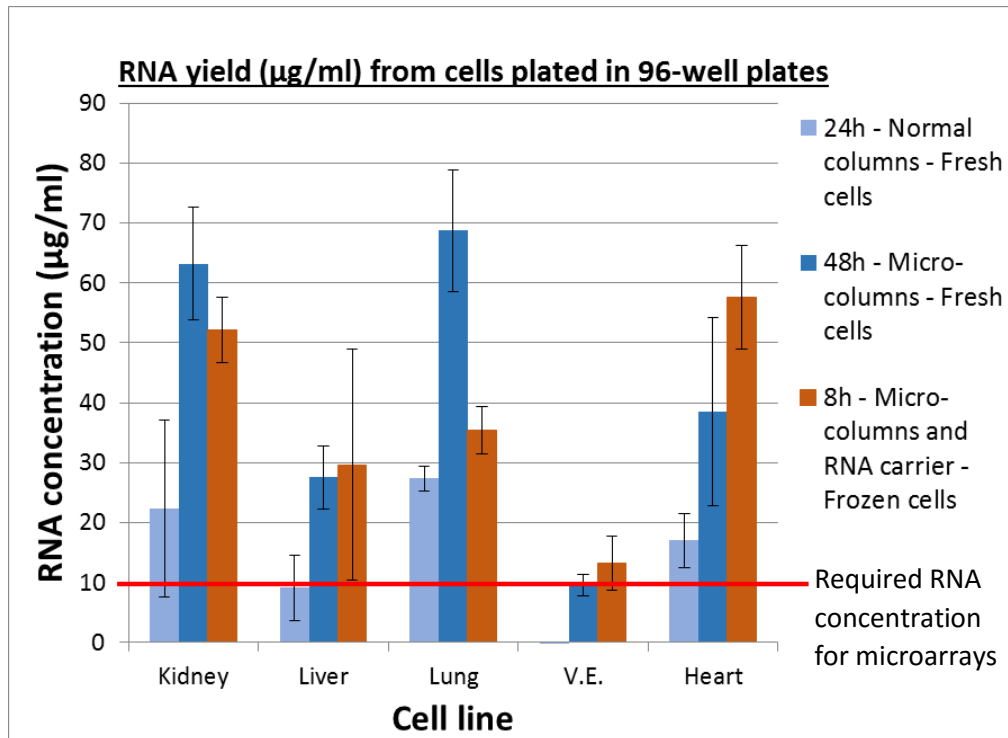
Figure 14. RNA extraction yield of cells exposed to co-culture media in a 96 well plate. The red line denotes the minimum total RNA requirement for microarray analysis.

The second extraction was conducted using micro-columns (RNeasy MinElute®

Spin Columns) and fresh cells from the 48 hour incubation in co-culture media. This

time, a satisfactory RNA yield was obtained for four of the cell lines, with the vascular

endothelial cells still providing too low a level of RNA. The third extraction was

conducted using cell samples that had been frozen in liquid nitrogen prior to being stored

at -80°C. The samples were obtained from cells incubated for 8 hours in co-culture

medium. The RNA yield was satisfactory for four of the cells lines while RNA yield was

slightly better for the vascular endothelial cells. The results of this third RNA extraction

are nevertheless positive since the number of cells collected was lower than for the

previous extraction considering the incubation time. Consequently, in order to improve

the RNA yield of the vascular endothelial cells, they were plated 48 hours before

exposure to TNT/DNAN. The method used for this third RNA extraction was selected

for future experiments.

Table 5 shows the absorbance 260/280 ratio, as indicator of RNA quality, of the

samples collected from the cell exposure to co-culture media. The values represent the

average of the absorbance ratios obtained for the four replicates of each condition using a

NanoDrop Spectrophotometer. A ratio of 2 or higher is considered as reflective of pure

RNA. A ratio lower than 2 is usually attributed to the presence of proteins, phenol or

other contaminants that absorb at or near 280 nm. A ratio equals to or higher than 2 was

obtained for all the conditions, except for the extraction performed with the vascular

endothelial cells from the 24 hour incubation and using the standard RNA extraction

columns. In this case, the poor value obtained can be attributed to the fact that almost no

RNA had been extracted with those samples.

Table 5. RNA quality of the samples collected from the cells exposed to co-culture media
in 96-well plates. The values were obtained from the Nanodrop measurements.

Absorbance 260/280 ratio			
Period of incubation	**24h**	**48h**	**8h**
RNA extraction conditions	**Fresh samples with standard columns**	**Fresh samples with micro-columns**	**Frozen samples with micro-columns and RNA carrier**
Kidney	2.34	2.20	2.14
Liver	2.00	2.28	2.50
Lung	2.19	2.14	2.31
Vasc. Endo.	1.17	2.50	2.20
Heart	2.15	2.31	2.31

EVALUATION OF BIOMARKER RESPONSE TO STRESS

In order to validate the selection of the cell lines for the IdMOC system, cells were exposed in monocultures to five different reference compounds (cyclosporin A, troglitazone, all-trans retinoic acid, VEGF-121, and daunorubicin) expected to significantly influence the production of the selected biomarkers (NGAL, albumin, SP-B, endothelin I, and cardiac troponin I). However, SP-B and cardiac troponin ELISAs were not conducted due to logistical complications.

Results from this experiment show no production of NGAL by liver, vascular endothelial cells and heart cells whether or not the cells were exposed to the reference compounds. Figure 15 shows the concentration of NGAL in culture media of kidney cells exposed to the five reference compounds. Pairwise comparison tests indicate that kidney cells exposed to VEGF-121, troglitazone and daunorubicin have a significant decreased production of NGAL. Furthermore, kidney cells exposed to cyclosporin A show no production of NGAL. Possible explanations about this unexpected result are provided in the discussion.

Lung cells show a significant initial production of NGAL. It can be noted that the NGAL ELISA kit used was tested by the manufacturer for human COX-2, human lipocalin-1 and human matrix metallopeptidase 9 (MMP-9), with negative results. Furthermore, lung cells have been shown to produce significant amount of NGAL in other studies (85). Figure 16 shows the production of NGAL by lung cells exposed to the reference compounds. Cyclosporin A is the only reference compound to significantly decrease the production of NGAL by lung cells.
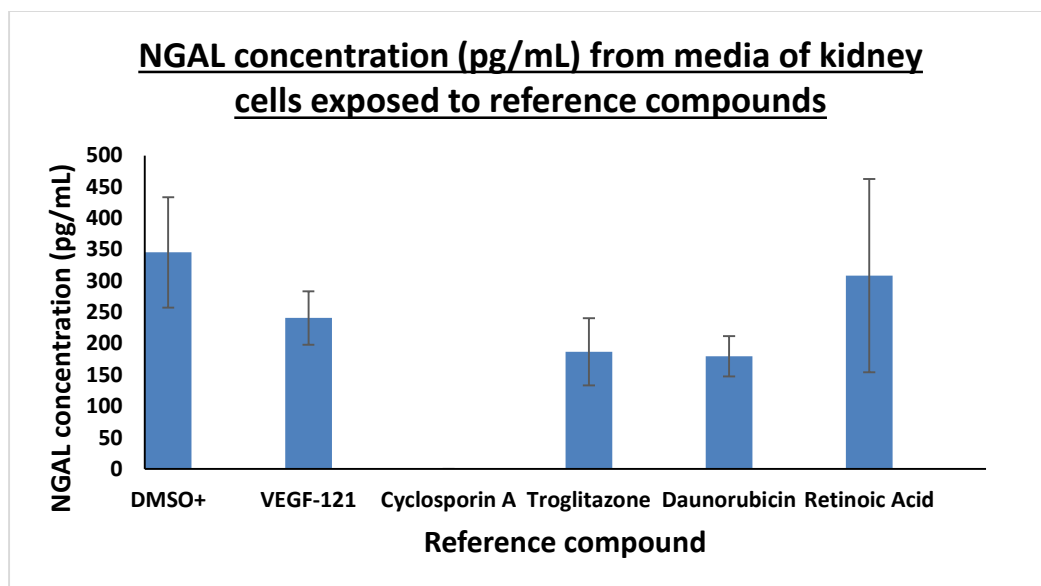
Figure 15. NGAL concentration (pg/mL) in culture media of kidney cells exposed to reference compounds in monocultures setting. Error bars represent 95% confidence interval.
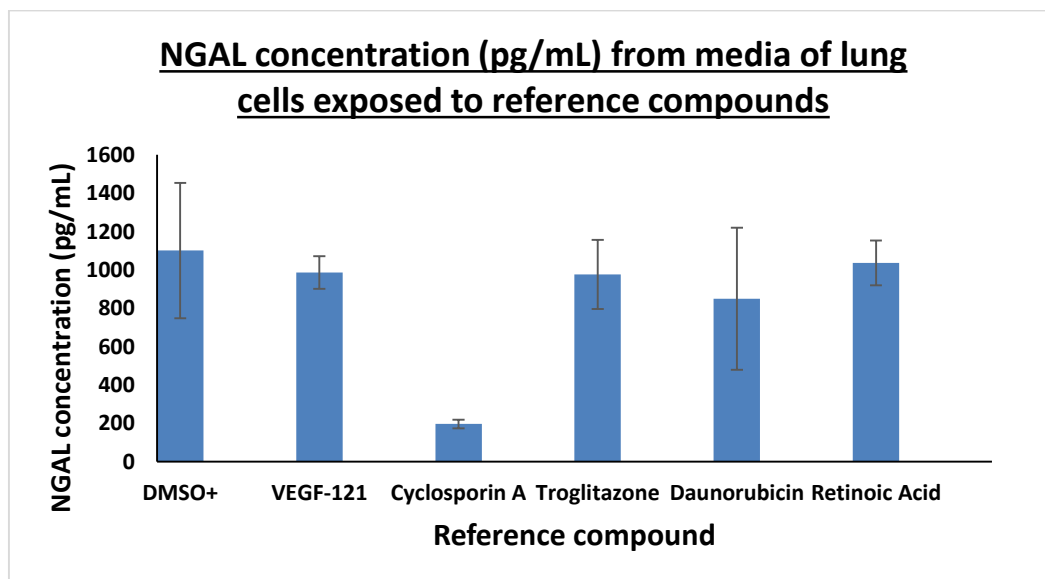
Figure 16. NGAL concentration (pg/mL) in culture media of lung cells exposed to reference compounds in monocultures setting. Error bars represent 95% confidence interval.

Figure 17 shows lung cells after a 24 hour exposure to the five reference compounds used in this project, and represents a simple observation more than a

monitored result. Cyclosporin A (a known nephrotoxicant) and daunorubicin (known to cause myocardial necrosis) both affected the morphology of the lung cells as observed under inverted microscope. These effects were also observed with the other cell lines, but were the most apparent with the lung cells. The observed morphologic changes (from elongated to rounded) are closely similar to those of necrotic or apoptotic cells.
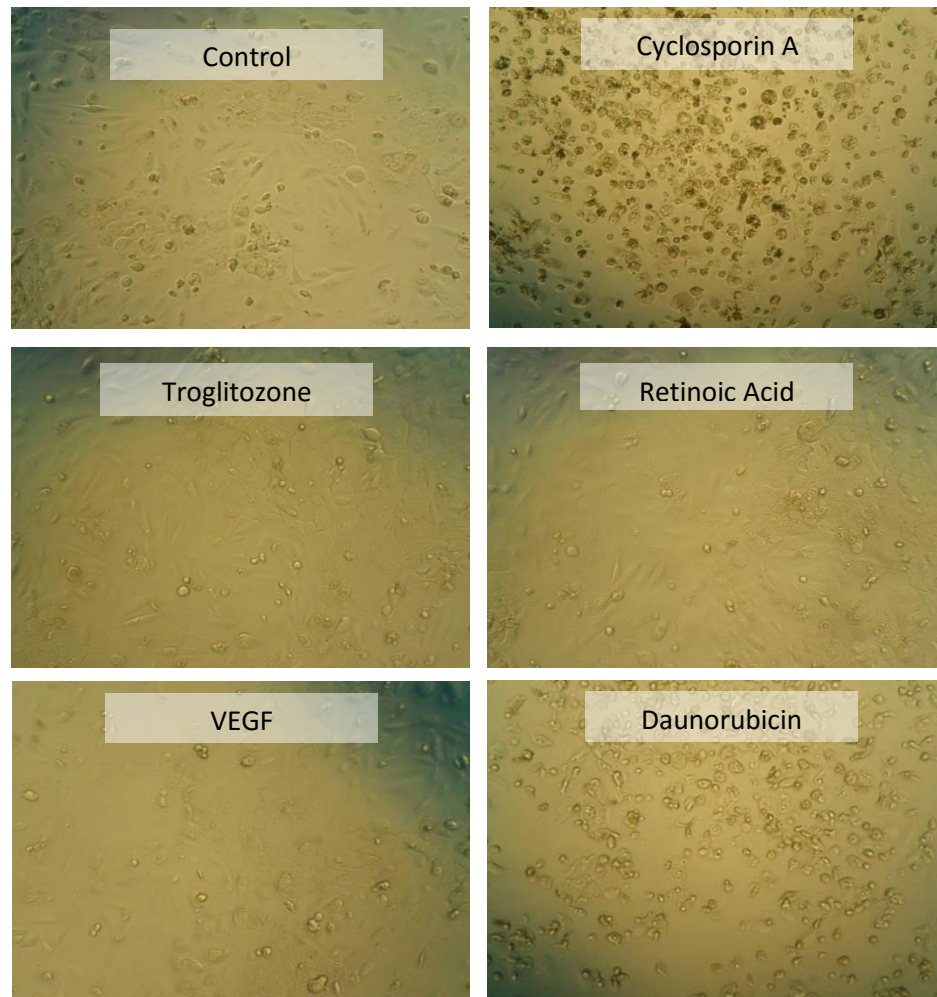
Figure 17. Effects of the reference compounds on the lung cell morphology.

While all cell lines show an initial average production of albumin varying from 15 to 20 mg/mL, no significant difference was observed in all cell lines exposed to the reference compounds.

The averaged initial level of production of endothelin I by the vascular endothelial cells was 493 pg/mL, which is significantly higher than the initial average of endothelin I production by the other cell lines which fluctuates between 65 and 100 pg/mL. Furthermore, the production of endothelin I by kidney, liver, lung, and heart cells exposed to the reference compounds did not significantly change. However, pairwise comparison tests show that vascular endothelial cells exposed to VEGF-121 have a significantly lower production of endothelin I (Figure 18). The decreased production of endothelin I is even more significant in vascular endothelial cells exposed to cyclosporin A and daunorubicin.
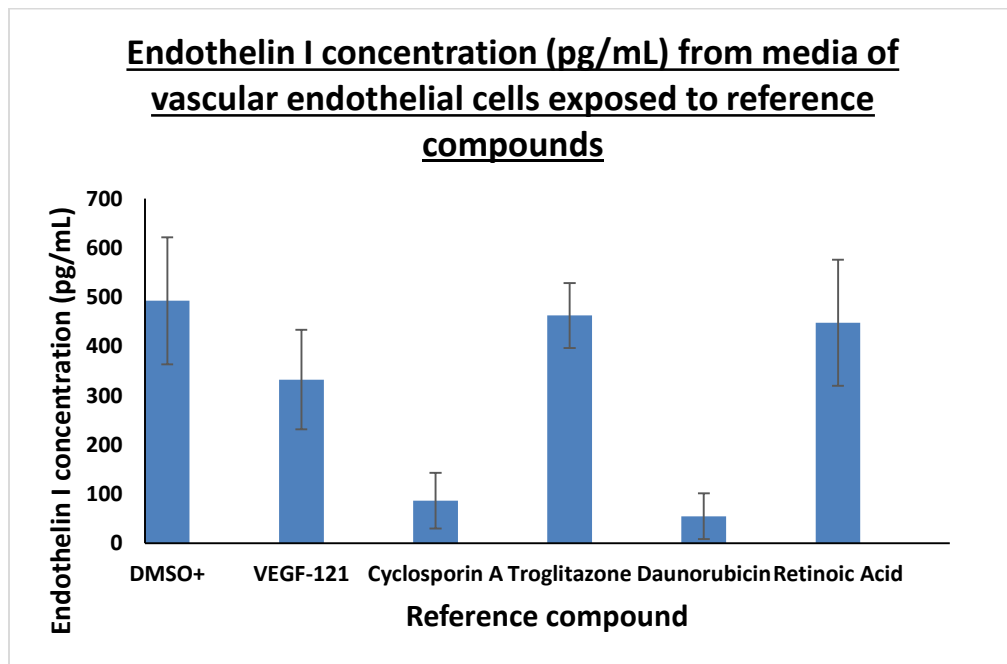
Figure 18. Endothelin I concentration (pg/mL) in culture media of vascular endothelial cells exposed to reference compounds in monocultures setting. Error bars represent 95% confidence interval.

DETERMINATION OF TNT AND DNAN LOSS TO THE EXPERIMENTAL APPARATUS DURING STANDARD INCUBATION METHODS IN CO-CULTURE MEDIUM

As seen in Figure 19, the concentration of TNT after 24 hours in co-culture medium in an IdMOC chamber significantly decreased ($p = 0.005$) from 539 nM to 467 nM (13.5 %), while DNAN concentration was not significantly affected (decrease of 1.8%, $p = 0.312$).
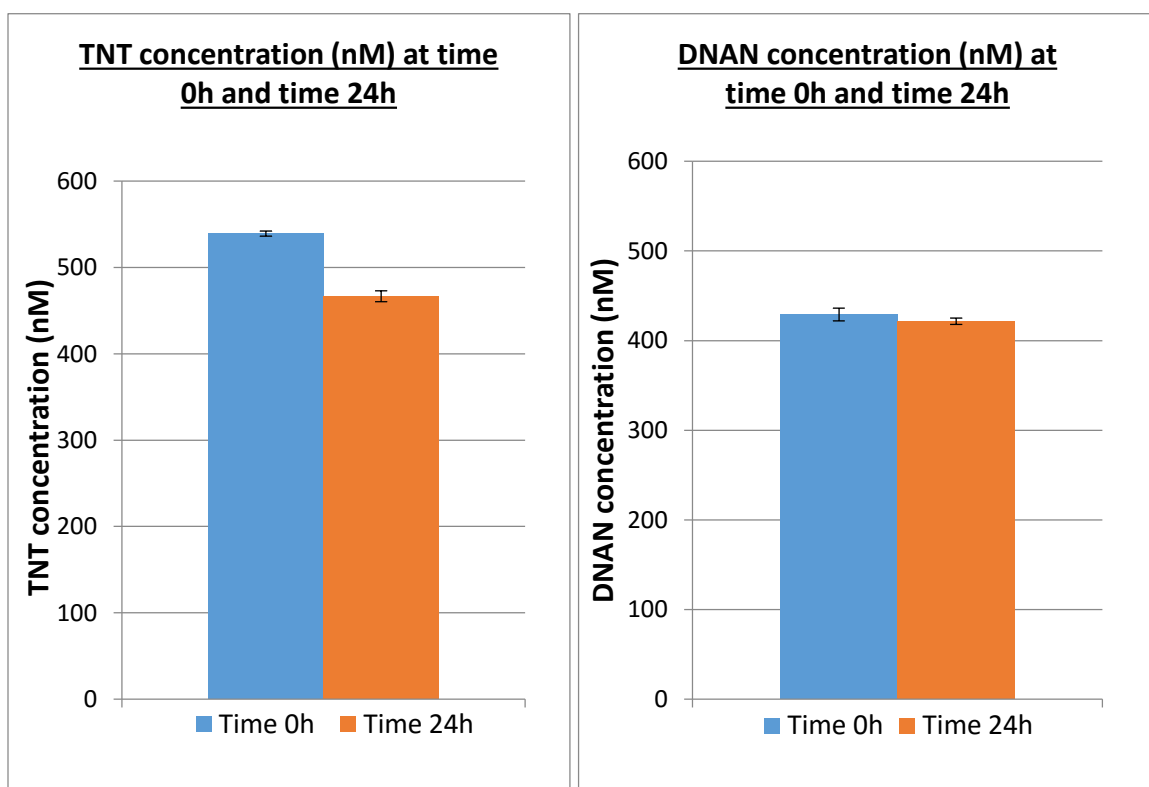
Figure 19. Assessment of the impact of incubation on TNT and DNAN concentrations. TNT and DNAN concentrations at the beginning and at the end of a 24 hour incubation period in co-culture medium in an IdMOC chamber. Error bars are standard deviations.

In order to determine the cause of loss of soluble TNT, a second experiment was designed using 500 nM of TNT in co-culture media according to three conditions (2 replicates per condition): 1) in amber glass tubes; 2) in clear glass tubes; 3) an IdMOC

62

chamber plated with vascular endothelial cells. The incubation times were 0, 1, 2, 6, and 24 hours. Figure 20 shows the concentration over incubation time of TNT and 4-amino-2,6-DNT in the condition with the amber glass tubes. Of all the TNT degradation by-products analyzed, only 4-amino-2,6-DNT was detected for all the conditions. A constant degradation of TNT over time was observed for the TNT media incubated in amber glass tubes. Therefore, even in a low-light environment, TNT in co-culture media degrades gradually to reach 25% degradation after 24 hours. The presence of 4-amino-2,6-DNT was also noticed at time zero. Consequently, TNT used in this project is not entirely pure and contains approximately 14% of 4-amino-2,6-DNT. This is not surprising considering that weapon grade TNT was used in the current project for logistical reasons. Figure 20 also shows that while the concentration of TNT decreases over time, the concentration of 4-amino-2,6-DNT remains constant, meaning that other undetected by-products are produced.
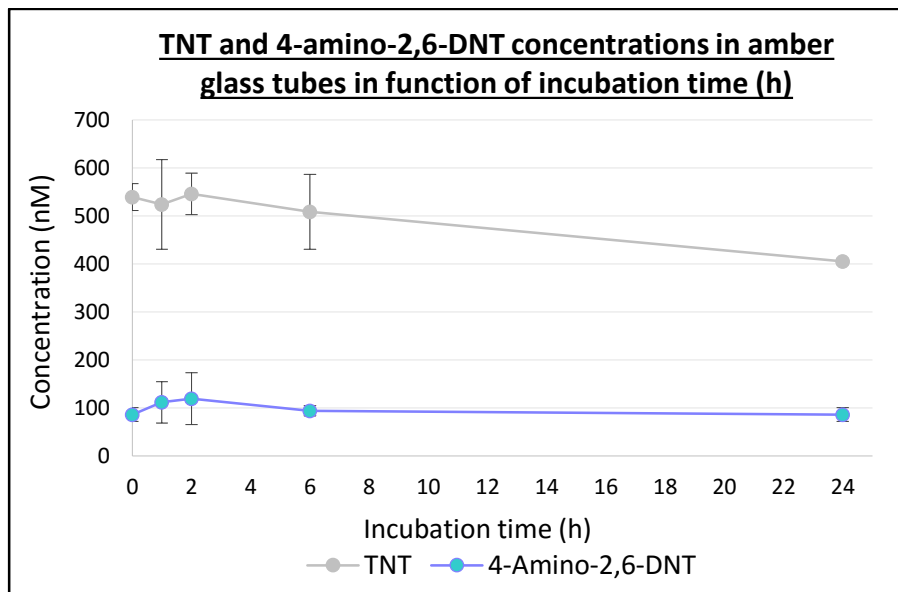
Figure 20. TNT and 4-amino-2,6-DNT concentrations from a TNT/co-culture media
solution in amber glass tubes in function of incubation time (h).
The error bars represent the standard deviations.

Figure 21 shows the concentration of TNT and of 4-amino-2,6-DNT over incubation time for the co-culture media in clear tubes. While the concentration of TNT remained constant, the concentration of 4-amino-2,6-DNT decreased over time, being degraded into other undetected by-product(s). Therefore, light could have played a role in the degradation of this by-product in co-culture media. However, the steady concentration of TNT can hardly be explained, considering that it decreased in a light-controlled environment (amber tubes). The TNT/DNAN solubility experiments having been designed to give a general idea of a potential limitation of this project, this observation can be reflective of the low confidence interval resulting from this experiment where only 2 replicates were used per condition. In Figure 22, the initial amount of 4-amino-2,6-DNT in the co-culture media decreases more quickly in the IdMOC plate than in the clear glass tubes, suggesting a potential implication of the vascular endothelial cells in the degradation of this TNT by-product. Overall, the results of the experiments assessing TNT concentration over a 24h incubation period suggest a TNT light-independent degradation and the presence of 4-amino-2,6-DNT and of its light-dependent degradation.
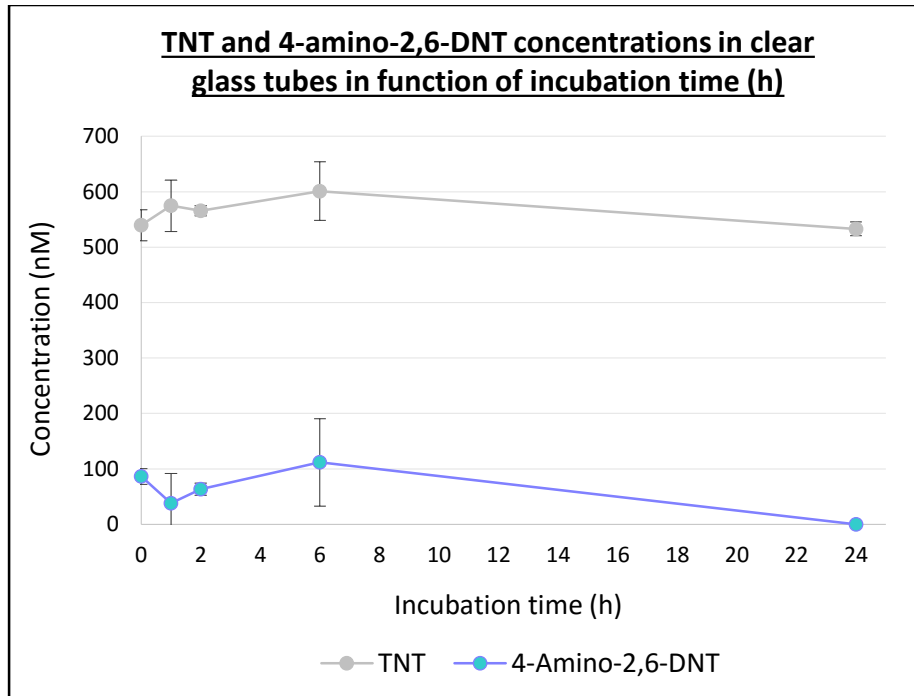
Figure 21. TNT and 4-amino-2,6-DNT concentrations from a TNT/co-culture media
solution in clear glass tubes in function of incubation time (h). The error bars
represent the standard deviations.
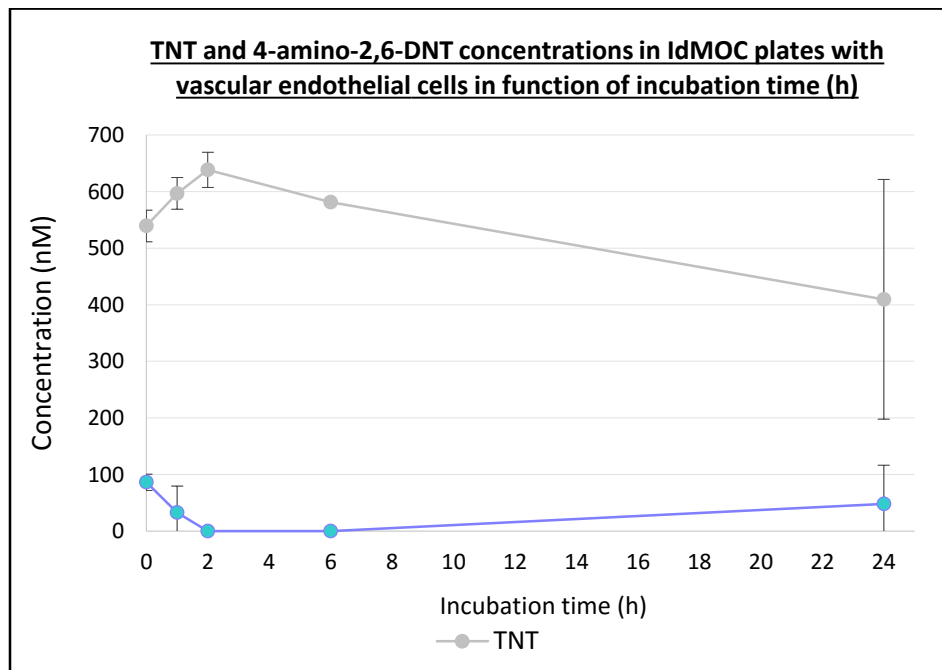
Figure 22. TNT and 4-amino-2,6-DNT concentrations from a TNT/co-culture media
solution in IdMOC plates containing vascular endothelial cells in function of
incubation time (h). The error bars represent the standard deviations.

DETERMINATION OF THE RANGE OF TNT/DNAN CONCENTRATIONS

Before collecting the cell media from the range finding experiment, it was noticed that the wells corresponding to the liver cells exposed to the highest TNT concentrations (1 mM, 10 mM and 100 mM) were darker than the other wells (Figure 23). This observation was not correlated with the liver cells exposed to DNAN. As described previously, the liver is highly involved in the detoxification of TNT, while its role in the detoxification of DNAN is less known.
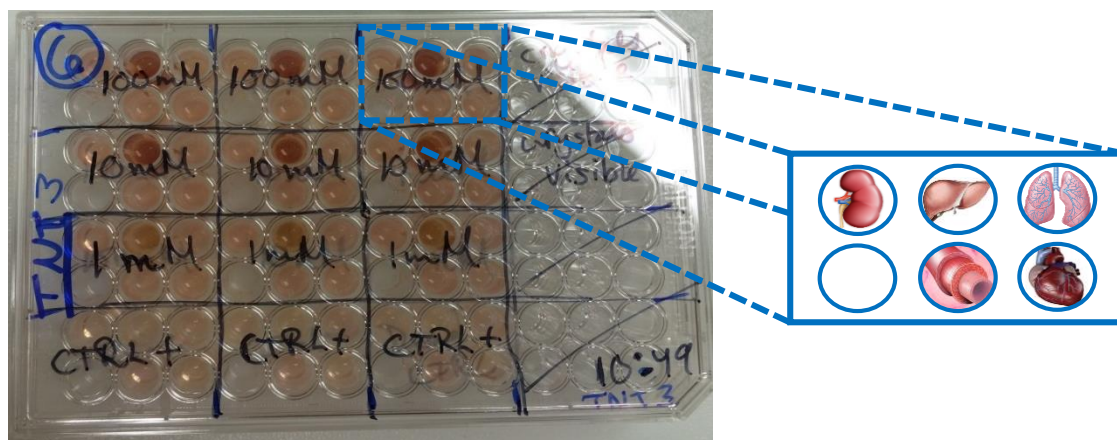
Figure 23. Picture of the plate containing the cell lines exposed to different concentrations of TNT and DMSO (control). In the plate presented, cells were exposed to 1, 10 and 100 mM of TNT (plus DMSO+ control) for a 24 hour incubation period as part of the range finding experiment.

Figures 24 to 28 show the results of the cell viability tests completed on all five cell lines exposed to a concentration range of TNT and DNAN, from 1 nM to 100 mM. The results are presented in terms of cell mortality in order to reflect typical dose-response curves. The range finding experiment included two controls: DMSO+ and DMSO- since TNT and DNAN were first dissolved in DMSO. The DMSO- controls were set as the zero mortality standards. Consequently, depending on the condition, cell

66

mortality (%) can be negative or over 100% for conditions causing a variation of absorbance greater than the difference between the controls and the blanks. Such variability can be explained by subtle differences in the number of cells platted or in the volume of reagents.

At 1 mM, TNT toxicity is such that no cells survived for any of the cell lines. There is a strong decrease of survivability from 100 µM to 1 mM of TNT, with all cell lines passing from a viability above 65% to 0%. Until this toxicity effect is reached, the lung cells (Figure 26) appear to be the least affected by TNT, while the liver cells (Figure 25) are the most affected. It can be noted that crystals had formed in the co-culture medium with the TNT and DNAN concentrations of 10 mM and 100 mM. Consequently, for those conditions, the concentrations of soluble TNT is expected to be less than the total concentration. Furthermore, for the concentrations of 100 mM of TNT and DNAN, the media included 10% DMSO in order to fully dissolve the related amount of chemical. Overall, the variability of the results, as depicted by the standard deviations, is relatively low. As per Figure 25, DMSO appears to decrease the viability of the liver cells. However, cell viability increases to 80% with the first concentration of TNT (1 nM), and remains between 65% and 85% until the TNT concentration of 100 µM. Due to variability between both experiments (TNT vs DNAN), the viability decrease of the liver cells when exposed to 1% DMSO during the range finding experiment with DNAN is not as distinct as the decrease obtained with the TNT range finding experiment, even though both conditions are identical and experiments were carried out at the exact same time with cells from the same culture vessels.

Compared to TNT, DNAN toxicity led to dose-response curves where effects were initiated at 10 mM rather than 1 mM for the lung and vascular endothelial cells (Figures 26 and 27). Even though effects were initiated at 1 mM for the kidney, liver and heart cells, the initial response was weaker and gradual with DNAN as opposed to TNT (Figures 24, 25 and 28). Even at 100 mM of DNAN, all cell lines were approximately 15 to 20% viable. Similarly to TNT, it can be noted that not all DNAN was at the soluble state at this concentration.

Cell mortality (%) of kidney cells exposed to TNT/DNAN
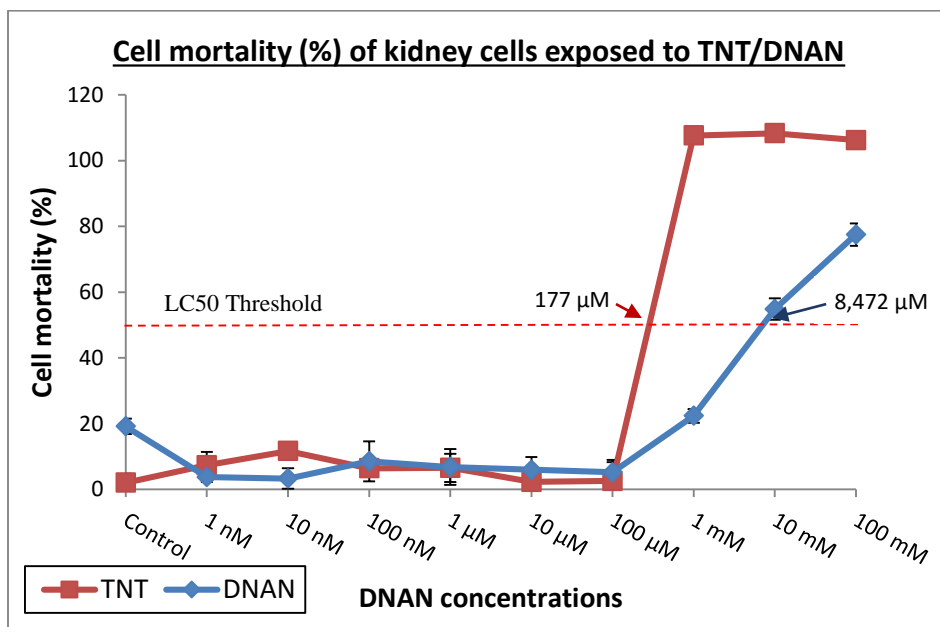
Figure 24. Mortality (%) of the kidney cells exposed to TNT/DNAN for 24 hours in co-culture media. The error bars represent the standard deviation.
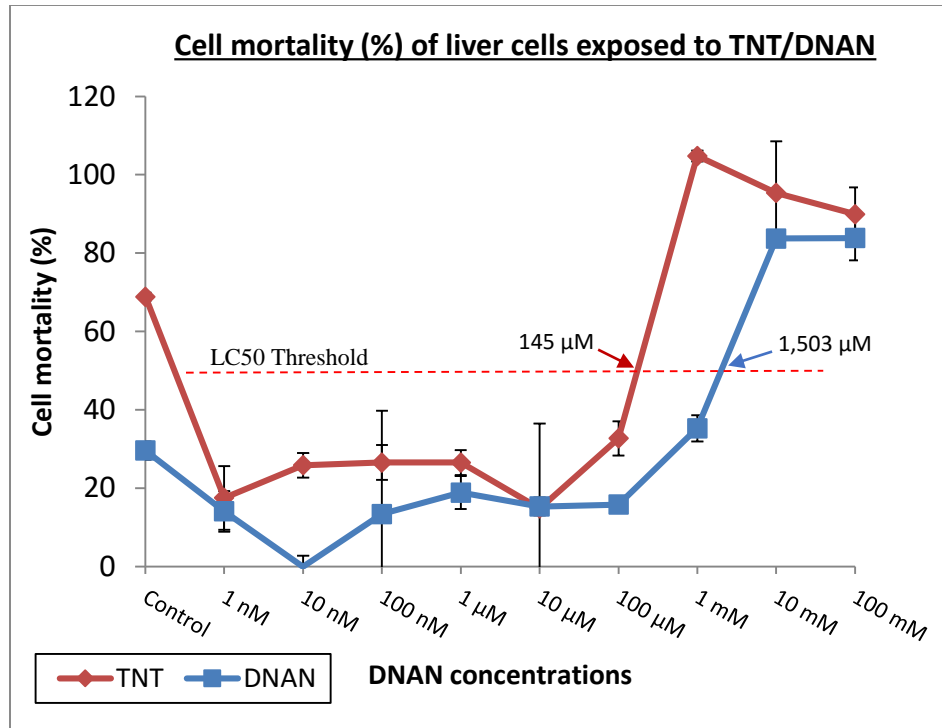
Figure 25. Mortality (%) of the liver cells exposed to TNT/DNAN for 24 hours in co-culture media. The error bars represent the standard deviation.
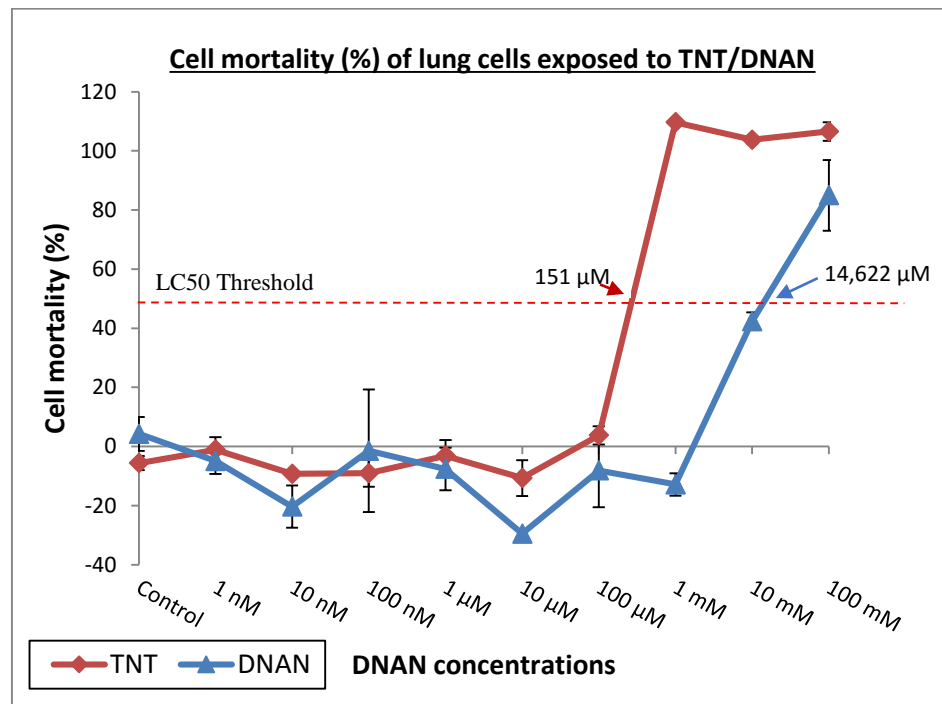
Figure 26. Mortality (%) of the lung cells exposed to TNT/DNAN for 24 hours in co-culture media. The error bars represent the standard deviation.
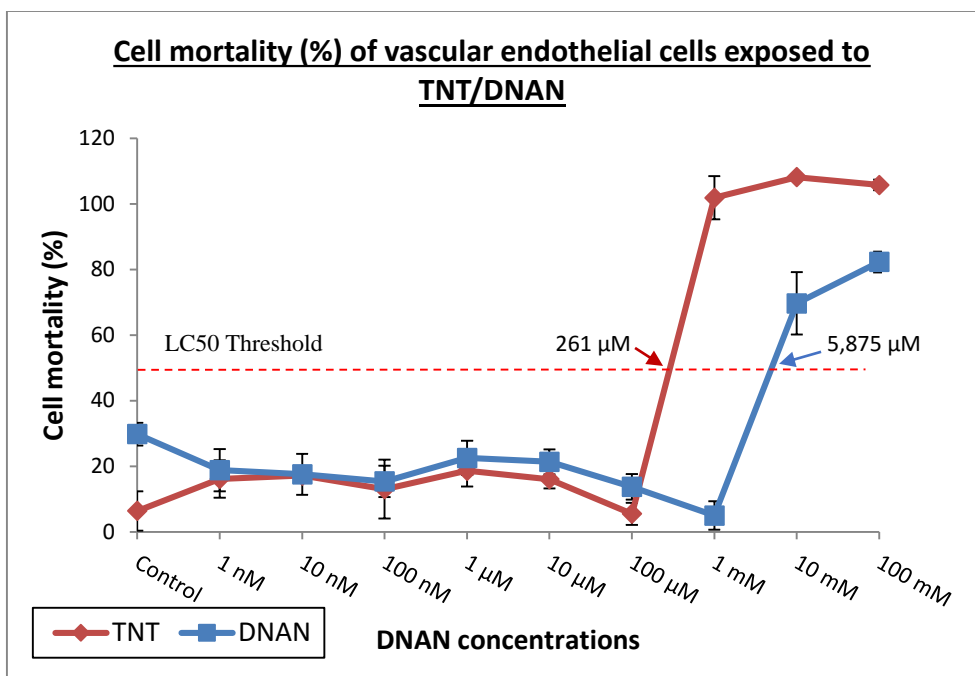
Figure 27. Mortality (%) of the vascular endothelial cells exposed to TNT/DNAN for 24 hours in co-culture media. The error bars represent the standard deviation.
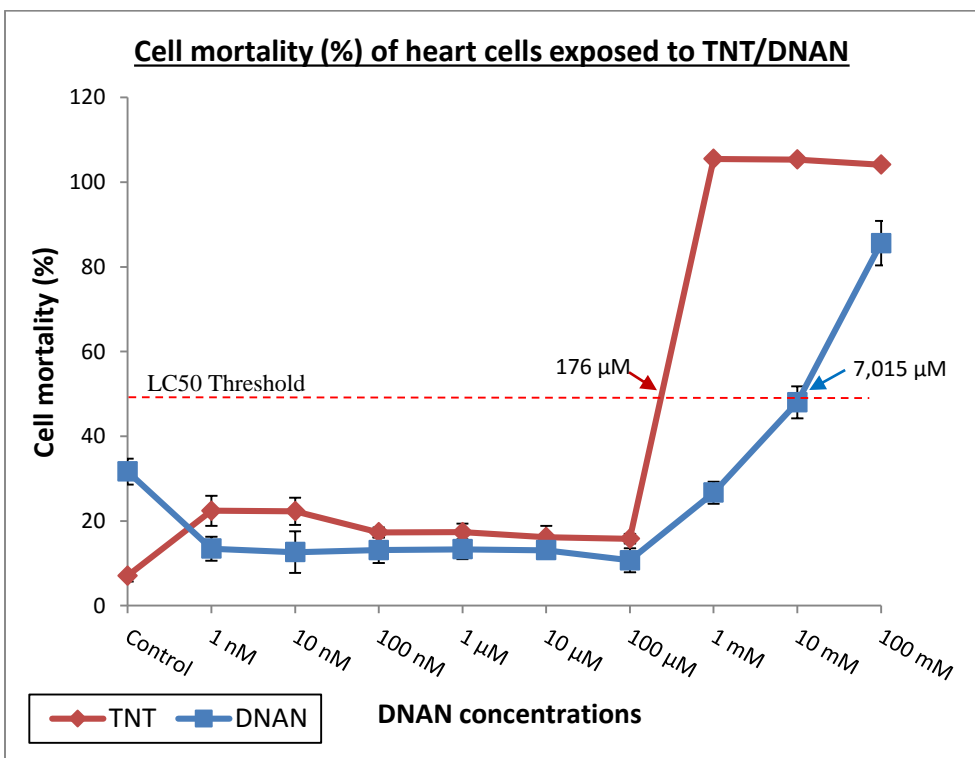
Figure 28. Mortality (%) of the heart cells exposed to TNT/DNAN for 24 hours in co-culture media. The error bars represent the standard deviation.

70

For each cell line, a two-way ANOVA was conducted testing the effects of TNT and DNAN across equivalent dose ranges. The results from this analysis demonstrated that both the toxicant used (TNT or DNAN) and the concentrations differently affected cell viability for all cell types tested ($p < 0.001$ for all conditions except for the effect of toxicants on vascular endothelial cell viability where $p = 0.009$). Table 6 shows the calculated LC_{50}s for each pair of toxicant and cell line with the 95% confidence interval.

Table 6. Calculated LC_{50}s of human cells exposed to TNT and DNAN.

Toxicant	Cell line	LC_{50} (μM)	95% Confidence interval* (μM)	
			Lower bound	Upper bound
TNT	Kidney	177	-	+
	Liver	145	36	577
	Lung	151	-	+
	Vasc. endo.	261	71	962
	Heart	176	15	2,051
DNAN	Kidney	8,472	5,093	14,060
	Liver	1,503	520	4,345
	Lung	14,622	7,870	27,164
	Vasc. endo.	5,875	2,559	13,521
	Heart	7,015	2,630	18,664

* - sign indicates that the calculated lower bound is smaller than 10^{-50} μM; + sign indicates that the calculated upper bound is greater than 10^{50} μM.

In order to better select the four concentrations of TNT and DNAN to use for the IdMOC experiment, the level of each biomarker was assessed for the samples collected from the hepatocytes of the range finding experiment. The hepatocytes did not produce any significant amount of NGAL, SP-B, endothelin I and cardiac troponin I (results not shown). As expected, the hepatocytes produced significant amount of albumin (Appendix B, Figure B1). The analyzed samples for DNAN were from the 10 nM to 1 mM concentrations, and for TNT from 1 nM to 100 μM due the higher toxicity of TNT.

No significant change in the production of albumin was observed. Consequently, the

selection of the chemical concentrations was based specifically on the results from the

viability assay. For TNT, the selected concentrations were 100 nM, 1 μM, 10 μM and

100 μM; and for DNAN the selected concentrations were 1 μM, 10 μM, 100 μM and 1

mM.

LEVEL OF PRODUCTION OF BIOMARKERS BY HUMAN CELLS EXPOSED TO TNT AND DNAN

Following the IdMOC experiment, the concentrations of the five pre-selected

biomarkers in the media collected from each condition were assessed.

NGAL

NGAL production by kidney cells decreased significantly ($p < 0.001$) with the

increase of TNT concentration and is undetectable for a TNT exposure of 100 μM

(Appendix B, Figure B2).   The average NGAL production of all cell lines exposed to

TNT increased initially before decreasing close to undetectable levels at 100 μM of TNT.

It can be noted that, other than the kidney cells, only lung cells produced a detectable

level of NGAL. NGAL concentration from culture media collected from the cell lines

exposed to TNT in a co-culture setting did not change significantly with higher TNT

concentrations as shown in Figure 29.
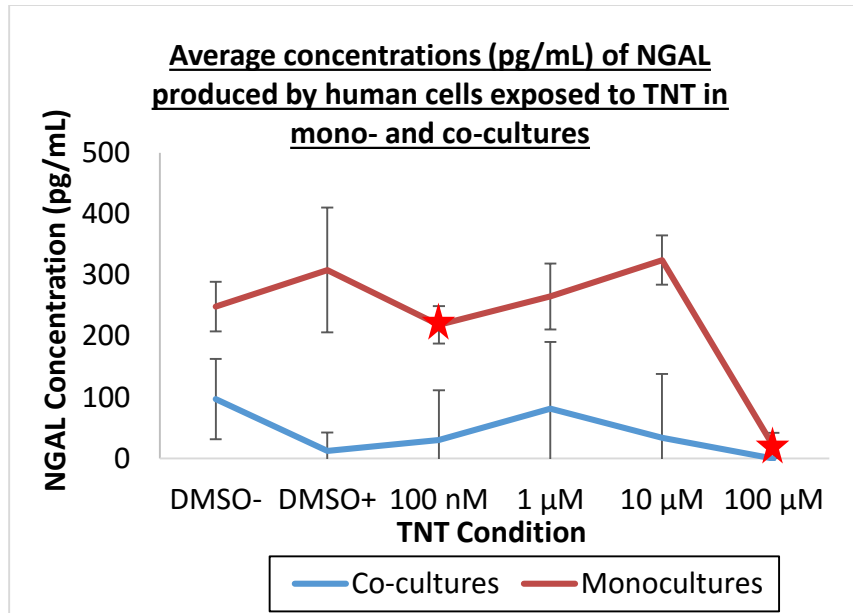
Figure 29. NGAL concentration (pg/mL) of culture media collected from the five cell lines exposed to TNT in a co-culture setting, and average NGAL concentrations (pg/mL) of all culture media collected from the five cell lines exposed to TNT in monoculture setting. Error bars represent the 95% confidence interval. Stars represent conditions for which there was a significant change compared to positive control (DMSO+).

NGAL production by kidney cells exposed to DNAN significantly ($p < 0.001$) decreased at 100 µM and 1mM (Appendix B, Figure B3). Similarly, the average NGAL production by all cell lines significantly ($p < 0.001$) decreased at the same two concentrations. However, there was no significant change of NGAL concentration in culture media collected from the five cell lines exposed to DNAN in a co-culture setting (Appendix B, Figure B4).

Albumin

No significant change of albumin production was detected for liver cells exposed to TNT in monocultures (Appendix B, Figure B5). However, the average albumin concentration found in culture media from all cells exposed to TNT in monoculture setting is significantly ($p = 0.002$) lower for the highest TNT concentration of 100 µM

than for the other TNT exposures and control (Figure 30). No significant change in

albumin levels was detected for the co-cultures exposed to TNT (Figure 30).
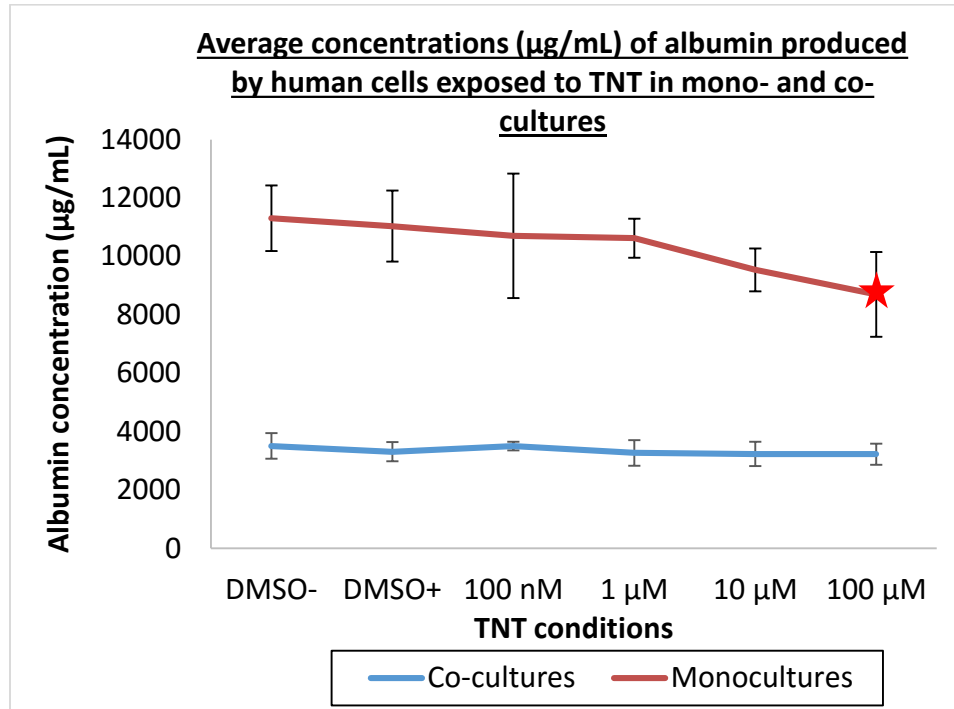
Figure 30. Albumin concentration (µg/mL) of culture media collected from the five cell
lines exposed to TNT in a co-culture setting, and average albumin
concentrations (µg/mL) of all culture media collected from the five cell lines
exposed to TNT in monoculture setting. Error bars represent the 95%
confidence interval. Stars represent conditions for which there was a
significant change compared to positive control (DMSO+).

The albumin level of liver cells exposed to DNAN in monocultures significantly

($p < 0.001$) increased at the lowest DNAN concentration of 100 nM and did not

significantly change thereafter with increasing DNAN concentrations (Appendix B,

Figure B6). The same trend was observed for the average albumin level of all cells

exposed to DNAN in monocultures ($p < 0.001$). However, there was no significant

change in the albumin level of cells exposed to DNAN in co-culture (Figure 31).
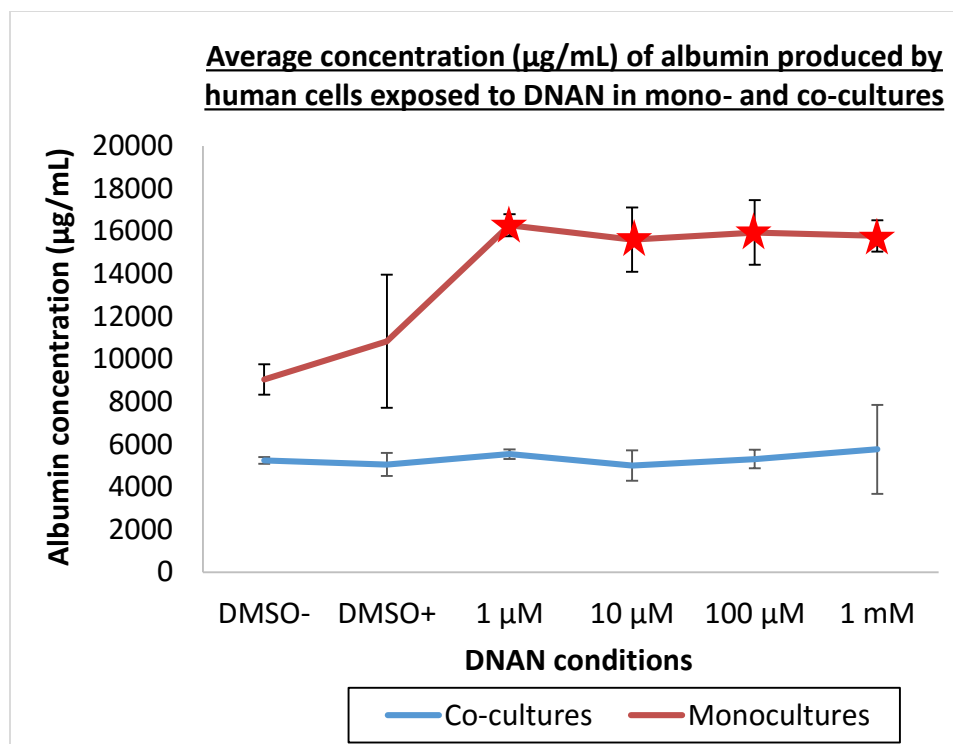
Figure 31. Albumin concentration (μg/mL) of culture media collected from the five cell lines exposed to DNAN in a co-culture setting, and average albumin concentrations (μg/mL) of all culture media collected from the five cell lines exposed to DNAN in monoculture setting. Error bars represent the 95% confidence interval. Stars represent conditions for which there was a significant change compared to positive control (DMSO+).

It can be noted that the level of production of albumin for most of the samples analyzed was over the highest concentration of the standard used (200 μg/mL), which represents a limitation in the interpretation of the results.

Surfactant Protein B

While the level of SP-B produced by the lung cells did not significantly increased when cells were exposed to increasing concentrations of TNT (Appendix B, Figure B7), the overall SP-B average concentration for all monocultures increased at 1 μM and 100 μM (Figure 32; $p < 0.001$). This increase came mainly from the liver and vascular

endothelial cells, and to a lesser extent from the heart cells (results not shown). The co-cultures exposed to TNT did not lead to any significant change in SP-B production, except for a light increase for the 100 nM TNT exposure.
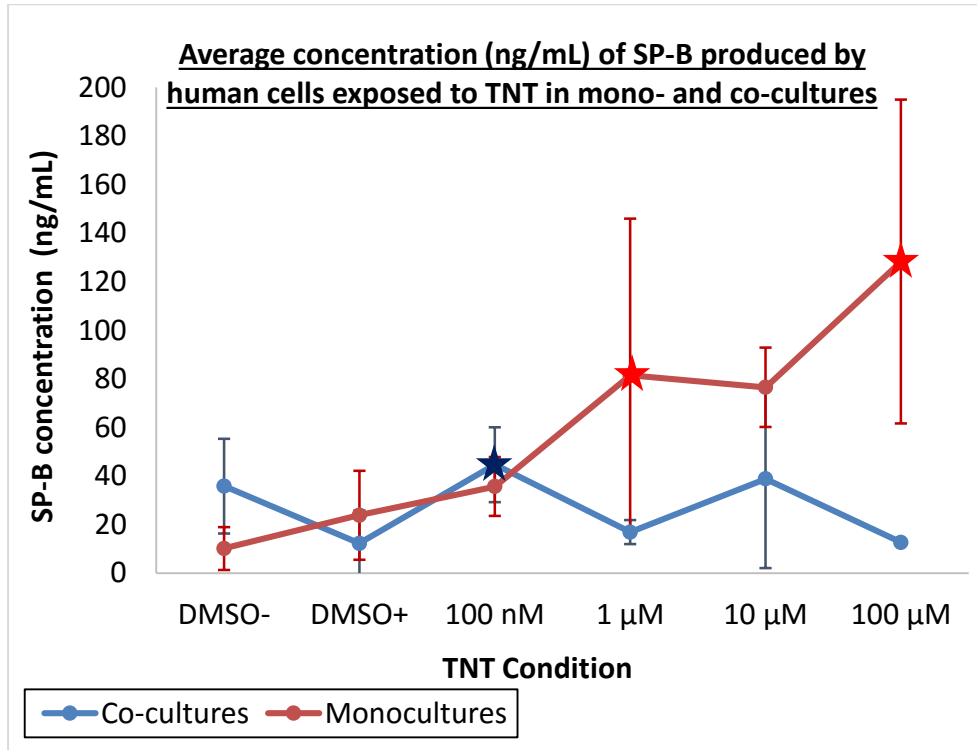
Figure 32. SP-B concentration (ng/mL) of culture media collected from the five cell lines exposed to TNT in a co-culture setting, and average SP-B concentrations (ng/mL) of all culture media collected from the five cell lines exposed to TNT in monoculture setting. Error bars represent the 95% confidence interval. Stars represent conditions for which there was a significant change compared to positive control (DMSO+).

SP-B concentration in culture media from all monocultures exposed to DNAN decreased significantly ($p < 0.001$) at the lowest DNAN concentration, and remained at zero for all other conditions (Figure 33). The latter trend is also observed for lung cells exposed to DNAN in monocultures (Appendix B, Figure B8). In the co-cultures exposed

to DNAN, SP-B levels did not change significantly with increasing DNAN

concentrations (Figure 33).
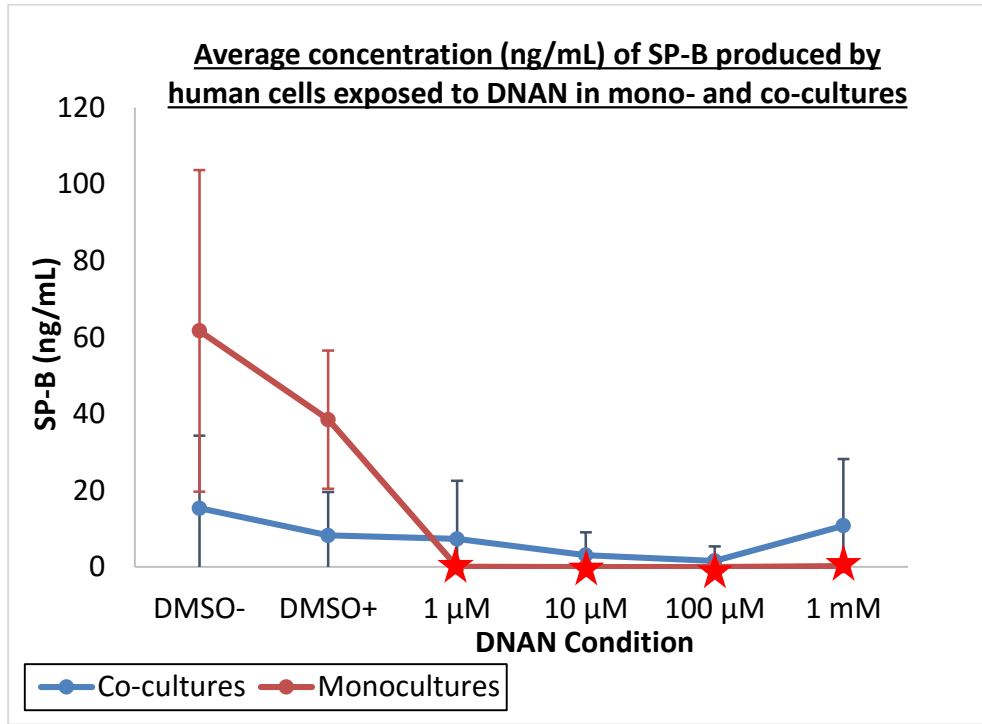
Figure 33. SP-B concentration (ng/mL) of culture media collected from the five cell lines
exposed to DNAN in a co-culture setting, and average SP-B concentrations
(ng/mL) of all culture media collected from the five cell lines exposed to
DNAN in monoculture setting. Error bars represent the 95% confidence
interval. Stars represent conditions for which there was a significant change
compared to positive control (DMSO+).

Endothelin I

Compared to the DMSO+ controls, endothelin I production by vascular

endothelial cells initially increased with exposure to increasing TNT concentrations

before going back to its original value at the highest TNT concentration exposure

(Appendix B, Figure B9; $p = 0.001$). The same trend is observed for the average

endothelin I production by all cell lines exposed to TNT ($p < 0.001$). However, cells

exposed to increasing concentrations of TNT in co-culture produced an increasing level

of endothelin I (Figure 34; $p < 0.001$).
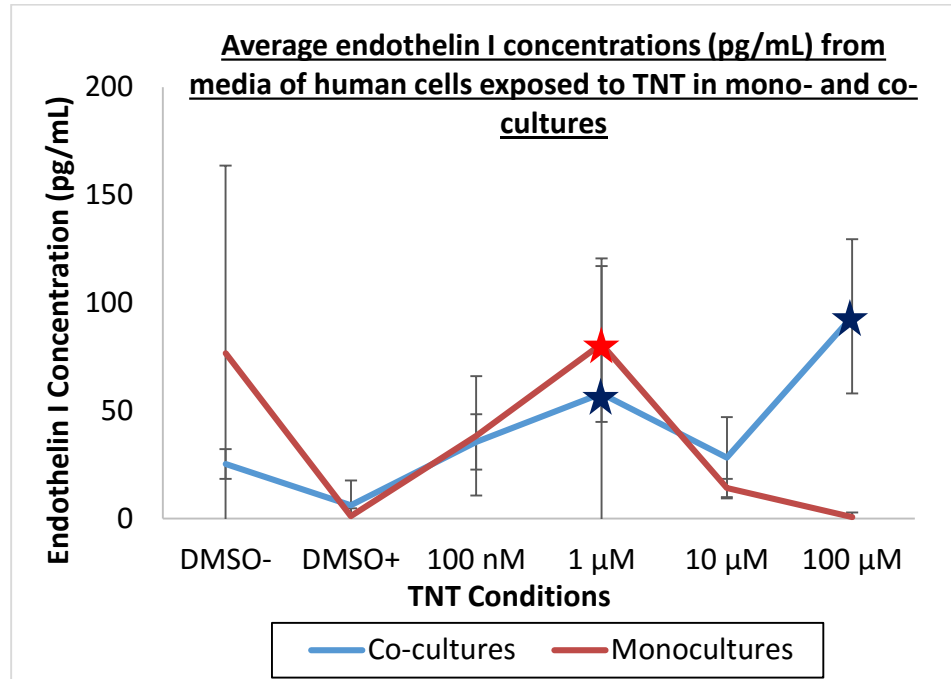
Figure 34. Endothelin I concentrations (pg/mL) in culture media collected from all five
cell lines exposed to TNT in co-culture setting, and average endothelin I
concentration from all culture media collected from the five cell lines exposed
to TNT in monoculture setting. Error bars represent the 95% confidence
interval. Stars represent conditions for which there was a significant change
compared to positive control (DMSO+).

No significant change in the level of production of endothelin I was observed in

vascular endothelial cells exposed to DNAN (Appendix B, Figure B10). However, the

average concentration of endothelin I in culture media from all cell lines exposed to

DNAN initially increased with increasing DNAN concentrations before going back to its

original value ($p = 0.001$). The same observation can be made for cells exposed to

DNAN in co-culture (Figure 35; $p = 0.015$).
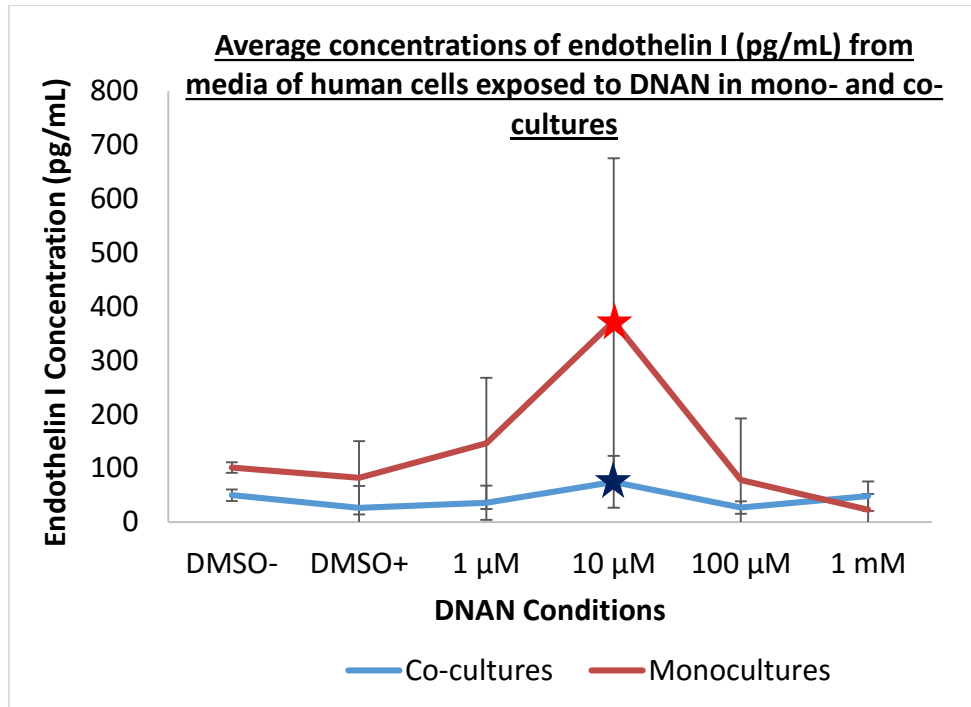
Figure 35. Endothelin I concentrations (pg/mL) in culture media collected from all five cell lines exposed to DNAN in co-culture setting, and average endothelin I concentration from all culture media collected from the five cell lines exposed to DNAN in monoculture setting. Error bars represent the 95% confidence interval. Stars represent conditions for which there was a significant change compared to positive control (DMSO+).

Cardiac Troponin I

Cardiac troponin I was not detected in any of the cultures (mono- and co-) exposed to TNT, including controls. However, troponin production increased in monocultures exposed to increasing concentrations of DNAN (Figure 36; $p < 0.001$). A troponin increase was observed with the heart cells exposed in monocultures to 10 µM DNAN (Figure 36, $p < 0.001$). Cardiac troponin was not detected in any of the co-cultures exposed to DNAN.
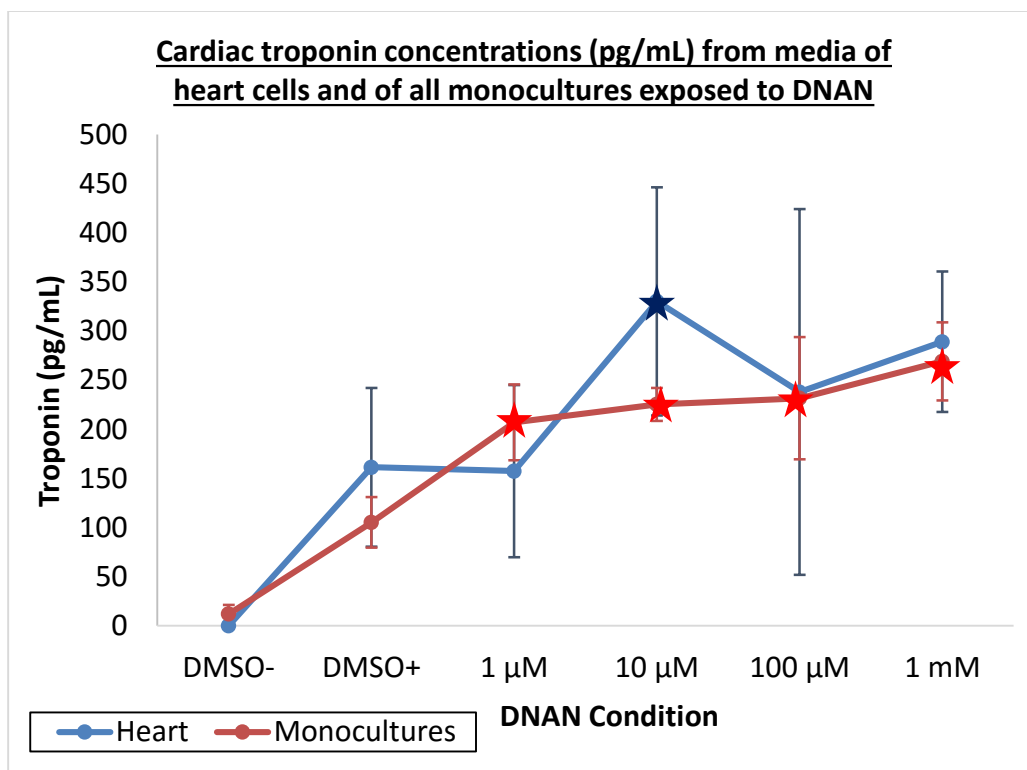
Figure 36. Cardiac troponin concentrations (pg/mL) in culture media collected from all five cell lines exposed to DNAN in co-culture setting, and average cardiac troponin concentration from all culture media collected from the five cell lines exposed to DNAN in monoculture setting. Error bars represent the 95% confidence interval. Stars represent conditions for which there was a significant change compared to positive control (DMSO+).

EFFECT OF TNT AND DNAN ON GLOBAL TRANSCRIPT EXPRESSION IN KIDNEY CELLS

Global transcript expression was investigated from both monocultures and IdMOC co-cultures for both DNAN and TNT exposures where the RNA from kidney cells was extracted from a total of 48 samples. Specifically, for both TNT and DNAN, the experiments investigated the effect of the culture method which included 2 conditions (mono- and co-cultures) x 3 exposure levels (the DMSO+ controls and the 2 highest exposure concentrations for each chemical) x 4 replicates per condition. It can be noted

that the microarray of one replicate from the controls of the co-cultures exposed to TNT was compromised and, therefore removed from the data analysis for a total of 47 microarray samples. PCA demonstrated that the concentration of TNT has a greater influence on the transcript expression profiles than the setting of the cultures (i.e. mono- versus co-).

TNT - GLOBAL TRANSCRIPT EXPRESSION

PCA was conducted as a means to provide a visual overview of the transcript expression results. Given that the TNT treatment caused a far greater number of transcripts to have significant differential expression relative to the culture treatment, 5,618 relative to 37 (of which 30 of the 37 were differentially expressed in-common among treatments), PCA was conducted based on transcripts significantly affected in the TNT treatment.   The PCA results (Figure 37) demonstrate clear separation of the TNT treatments (i.e. Control, 10μM and 100μM) regardless of the culture treatment (i.e. mono- versus co-culture) where 75.2% of the overall variation is described by the 3 principle components.

Figure 37. Three dimension principal component analysis representation for the targets differentially expressed in response to the exposure to TNT. Individual data points within the plot represent each biological replicate where n = 4 for each treatment combination (i.e. monocultures x control, etc.).

Transcripts differently expressed in common among the mono- and co-cultures are represented in Figures 38 (10 μM) and 39 (100 μM). In both cases, the co-cultures led to more differently expressed transcripts than the monocultures. Furthermore, a higher proportion of differently expressed transcripts in common between the mono- and co-cultures was observed at the highest TNT concentration. Consequently, while more than one third of the enriched transcripts in the monocultures were also differentially expressed in the co-cultures at TNT concentration 10 μM, this proportion increased to 77% at TNT concentration 100 μM. Furthermore, the highest TNT concentration led to a larger number of differently expressed transcripts for both mono- and co-cultures.
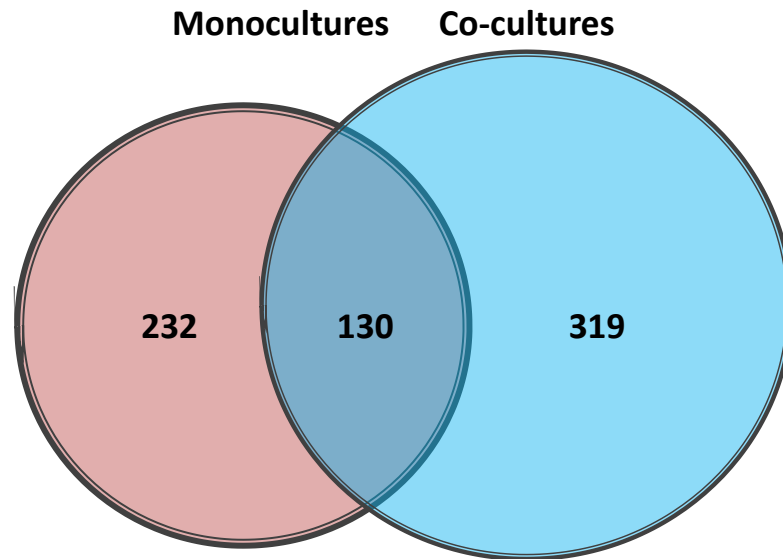
Figure 38. Differently expressed transcripts in common within kidney cell monocultures and co-cultures exposed to TNT (10 μM).

Figure 39. Differently expressed transcripts in common within kidney cell monocultures and co-cultures exposed to TNT (100 μM).

Table 7 shows the statistically enriched pathways within kidney cells exposed to

TNT detected by DAVID based on the Kyoto Encyclopedia of Genes and Genomes

(KEGG). The p values presented in the table refer to a modified Fisher Exact Test used

by DAVID to measure the level of pathway enrichment. The smaller the p value is, the

more associated to the related pathway a selected list of transcripts is. The cut-off point

used is a p value of 0.1. The enriched pathways are presented from pathways with the

smallest p values to pathways with the highest p values. Also presented in Table 7 are

the differently expressed transcripts (number and percentage) per enriched pathway.

Table 7. Enriched KEGG pathways within kidney cells exposed to TNT in mono- and co-
cultures.

Condition	Enriched pathway	Count	%	P Value
Co-culture 100 µM	Systemic lupus erythematosus	30	1.6	1.5E-06
	Ribosome	26	1.3	1.2E-05
	p53 signaling pathway	17	0.9	0.004
	Metabolism of xenobiotics by cytochrome P450	14	0.7	0.019
	Glutathione metabolism	12	0.6	0.027
	Ascorbate and aldarate metabolism	6	0.3	0.041
	Proteasome	11	0.6	0.042
	Bladder cancer	10	0.5	0.051
	ECM-receptor interaction	16	0.8	0.062
	Focal adhesion	32	1.7	0.064
	ABC transporters	10	0.5	0.065
	Porphyrin and chlorophyll metabolism	8	0.4	0.084
	Arginine and proline metabolism	11	0.6	0.085
	Tryptophan metabolism	9	0.5	0.089
	Cysteine and methionine metabolism	8	0.4	0.095
Monoculture 100 µM	Systemic lupus erythematosus	27	1.4	3.7E-05
	Proteasome	17	0.9	4.1E-05
	ECM-receptor interaction	20	1.0	0.003
	Ascorbate and aldarate metabolism	7	0.4	0.009
	p53 signaling pathway	15	0.8	0.022
	ABC transporters	11	0.6	0.026
	Porphyrin and chlorophyll metabolism	9	0.5	0.031
	Focal adhesion	33	1.7	0.036
	Metabolism of xenobiotics by cytochrome P450	13	0.7	0.040
	Endocytosis	30	1.5	0.050

	Nicotinate and nicotinamide metabolism	7	0.4	0.051
	Circadian rhythm	5	0.3	0.054
	Pathways in cancer	48	2.4	0.068
	Glycerolipid metabolism	10	0.5	0.069
	MAPK signaling pathway	40	2.0	0.072
	Amyotrophic lateral sclerosis (ALS)	11	0.6	0.080
	Tryptophan metabolism	9	0.5	0.084
	Cysteine and methionine metabolism	8	0.4	0.091
Co-culture 10 µM	Systemic lupus erythematosus	14	4.1	3.7E-07
	Metabolism of xenobiotics by cytochrome P450	7	2.1	0.003
	Arachidonic acid metabolism	6	1.8	0.010
	Steroid hormone biosynthesis	5	1.5	0.022
	Porphyrin and chlorophyll metabolism	4	1.2	0.041
	Pathogenic Escherichia coli infection	5	1.5	0.044
	TGF-beta signaling pathway	6	1.8	0.052
	Gap junction	6	1.8	0.057
	p53 signaling pathway	5	1.5	0.074
	Pancreatic cancer	5	1.5	0.087
Monoculture 10 µM	Metabolism of xenobiotics by cytochrome P450	5	1.8	0.022
	Ascorbate and aldarate metabolism	3	1.1	0.036
	Steroid hormone biosynthesis	4	1.4	0.048

Table 8 compares for each condition a selected list of statistically enriched pathways with the related differently expressed transcripts. The selection was based on evidence from the literature involving the enrichment of the pathways following TNT exposure in *in vivo* and *in vitro* studies. The enriched pathways were selected from the KEGG database, but also from the Reactome and BioCarta databases used by DAVID when determining the enrichment of pathways. Among the pathways presented, there tended to be a higher number of differently expressed transcripts within the co-cultures exposed to TNT when compared to the exposed monocultures.

Table 8. Number of differently expressed transcripts within statistically enriched
pathways observed in cultures exposed to TNT.

	Mono (10 uM)	Co (10 uM)	Mono (100 uM)	Co (100 uM)
P53	2	5	15	17
P450	5	7	13	14
Biological Oxidative Stress	4	8	19	22
Glutathione Metabolism	3	3	8	12
Bladder Cancer	1	3	7	10
Telomere maintenance	0	12	21	22
Metabolism of proteins	3	4	11	36
Metabolism of amino acids	10	7	41	35
Focal adhesion	2	3	33	32
Apoptosis	1	3	33	27

DNAN - GLOBAL TRANSCRIPT EXPRESSION

As was done for TNT, PCA was conducted as a means to provide a visual
overview of the transcript expression results in the DNAN exposure experiment. Given
that the DNAN treatment caused a greater number of transcripts to have significant
differential expression relative to the culture treatment, 969 relative to 199 (of which 72
of the 199 were differentially expressed in-common among treatments), PCA was
conducted based on transcripts significantly affected in the DNAN treatment.   The PCA
results (Figure 40) demonstrate clear separation of the DNAN treatments (i.e. Control,
10μM and 100μM) regardless of the culture treatment (i.e. mono- versus co-culture)
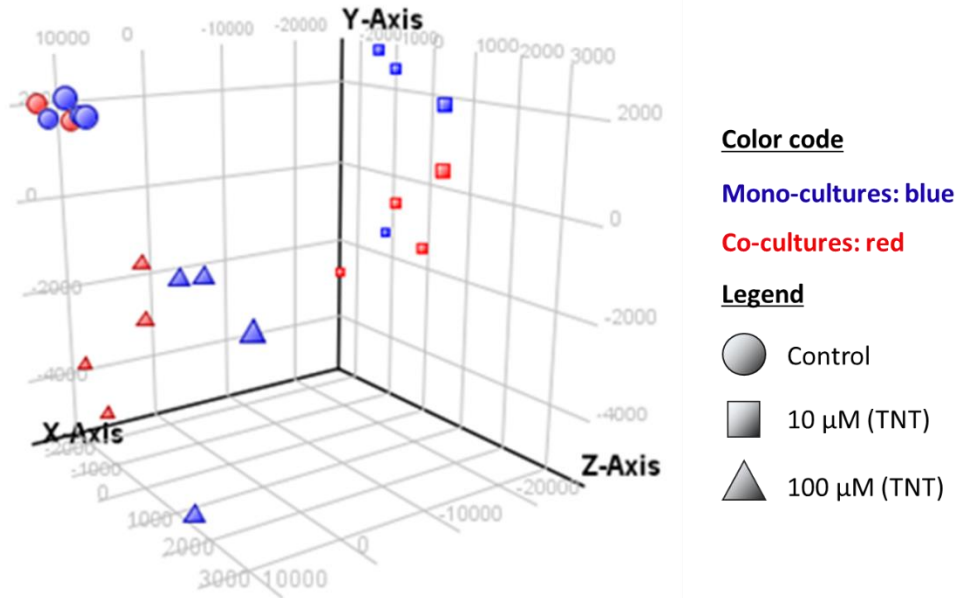where 75.8% of the overall variation is described by the 3 principle components.
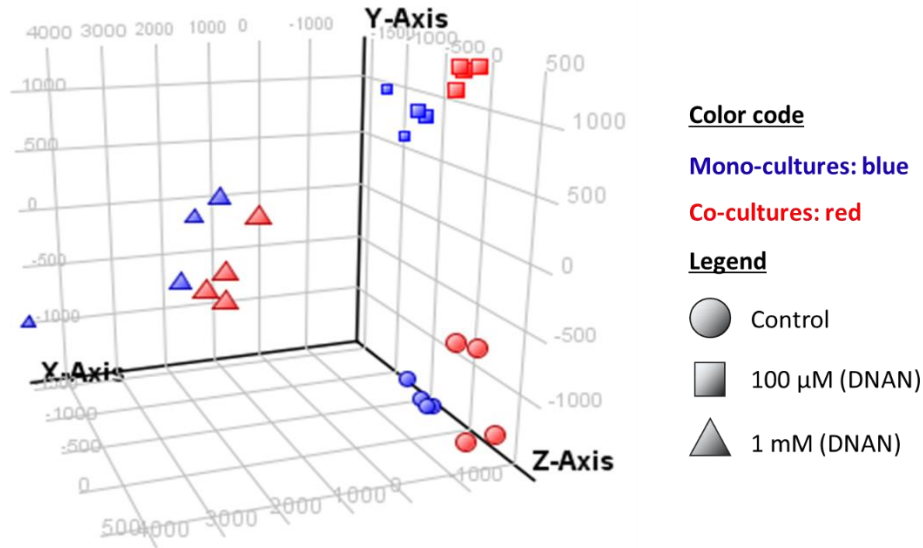
Figure 40. Three dimension principal component analysis representation for the targets differentially expressed in response to the exposure to DNAN.

Figures 41 and 42 present the commonly enriched gene-transcripts between the mono- and co-cultures exposed to 100 μM and 1 mM of DNAN respectively. For these two concentrations, using the number of differently expressed transcripts from the monocultures as denominator, the proportion of transcripts differently expressed in common between mono- and co-cultures are 66% and 75%, respectively.
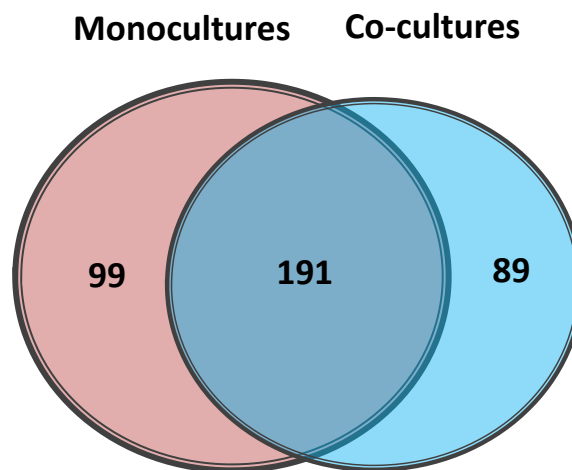
Figure 41. Differently expressed transcripts in common within kidney cells exposed in co-cultures and monocultures to DNAN (100 μM).

Monocultures   **Co-cultures**
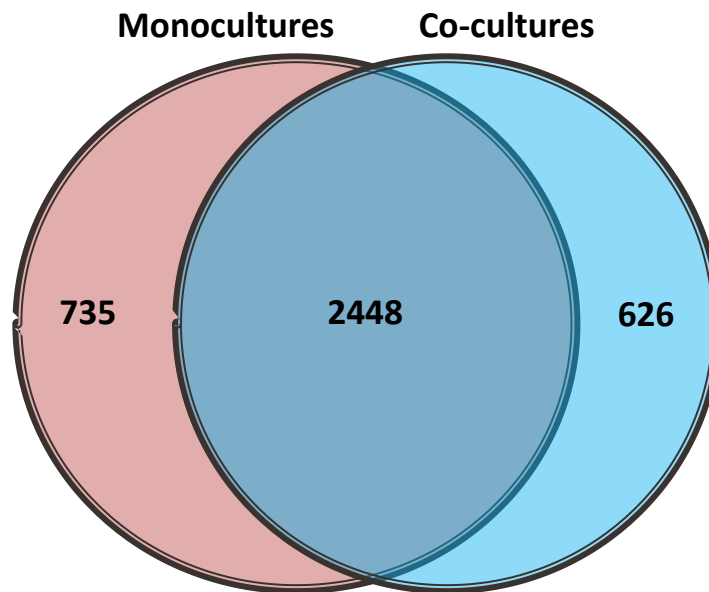
112   326   175
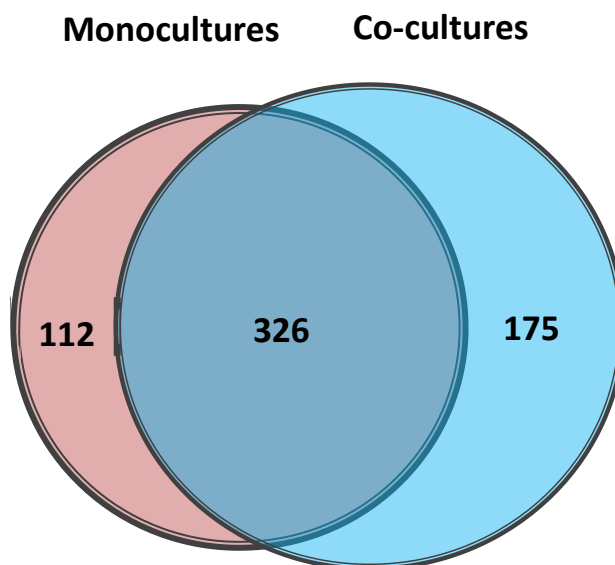
Figure 42. Differently expressed transcripts in common within kidney cells exposed in co-cultures and monocultures to DNAN (1 mM).

Table 9 shows the statistically enriched pathways within kidney cells exposed to DNAN and detected by DAVID based on KEGG. The enriched pathways are presented from pathways with the smallest p values to the pathways with the highest p values.

Table 10 compares for each condition a selected list of statistically enriched pathways with the related differently expressed transcripts. The same literature-based selection process was used as for TNT exposures. It can be noted that the apoptosis associated pathway was not detected as an enriched pathway by DAVID, but the related differently expressed transcripts are nevertheless presented for comparison with TNT exposure.

Table 9. Enriched KEGG pathways within kidney cells exposed to DNAN in mono- and co-cultures.

Condition	Term	Count	%	PValue
Co-culture 1 mM	Cytokine-cytokine receptor interaction	14	3.5	0.010
	Nitrogen metabolism	4	1.0	0.017
	TGF-beta signaling pathway	7	1.8	0.018
	Alanine, aspartate and glutamate metabolism	4	1.0	0.038
	Graft-versus-host disease	4	1.0	0.067
	p53 signaling pathway	5	1.3	0.081
	D-Glutamine and D-glutamate metabolism	2	0.5	0.093
	Cell adhesion molecules (CAMs)	7	1.8	0.099
Monoculture 1 mM	Pantothenate and CoA biosynthesis	3	0.9	0.035
	Steroid hormone biosynthesis	4	1.2	0.062
	Antigen processing and presentation	5	1.4	0.082
	Purine metabolism	7	2.0	0.083
Co-culture 100 µM	Natural killer cell mediated cytotoxicity	7	3.3	0.006
	Leukocyte transendothelial migration	6	2.8	0.015
	Regulation of actin cytoskeleton	8	3.8	0.016
	Type II diabetes mellitus	4	1.9	0.020
	Apoptosis	5	2.3	0.022
	TGF-beta signaling pathway	5	2.3	0.022
	Cell adhesion molecules (CAMs)	6	2.8	0.023
	Hypertrophic cardiomyopathy (HCM)	4	1.9	0.088
Monoculture 100 µM	Cell adhesion molecules (CAMs)	8	3.493	0.004
	ECM-receptor interaction	6	2.620	0.009
	TGF-beta signaling pathway	6	2.620	0.010
	Regulation of actin cytoskeleton	9	3.930	0.015
	Focal adhesion	8	3.493	0.032
	Hypertrophic cardiomyopathy (HCM)	5	2.183	0.039
	Dilated cardiomyopathy	5	2.183	0.050

Table 10. Number of enriched genes per selected pathways observed in co-cultures
exposed to DNAN.

	Mono (100 uM)	Co (100 uM)	Mono (1 mM)	Co (1mM)
P53 metabolism	2	0	1	5
TGF-Beta signaling pathway	6	5	4	7
Metabolism of amino acids	0	1	7	8
Nitrogen metabolism	1	0	2	4
Glutamine/glutamate metabolism	0	0	1	2
Integrin cell surface interactions	9	6	2	5
Cell adhesion molecules (CAMs)	8	6	-	7
Apoptosis*	3	5	2	3

* Not statistically enriched pathway

While not included in any of the enriched pathways, two transcripts with a
potential implication in DNAN toxicity had an increased expression: CHAC1 and KCNJ2
(Table 11). The former is coding for glutathione-specific gamma-
glutamylcyclotransferase, while KCNJ2 translation leads to member 2 of the potassium
channel, inwardly rectifying subfamily J.

Table 11. Differently expressed transcripts of particular interest within the cultures
exposed to DNAN - CHAC1 and KCNJ2 – and their increased factor relative
to controls.

Transcript	100 uM		1 mM	
	Monocultures	Co-cultures	Monocultures	Co-cultures
CHAC1	1.60	ND*	6.71	2.23
KCNJ2	ND*	ND*	3.57	3.92

*ND: Non-differently expressed transcript

TNT vs DNAN - GLOBAL TRANSCRIPT EXPRESSION IN KIDNEY CELLS

As gene expression changes often occur before the onset of toxicity (27), it is

interesting to compare the number of differently expressed transcripts between exposures

to TNT and DNAN. First, the number of transcripts differently expressed in common

among co-cultures exposed to 100 μM of TNT and 100 μM of DNAN is presented in

Figure 43. For a same concentration, TNT led to 11 times more differently expressed

transcripts than DNAN.
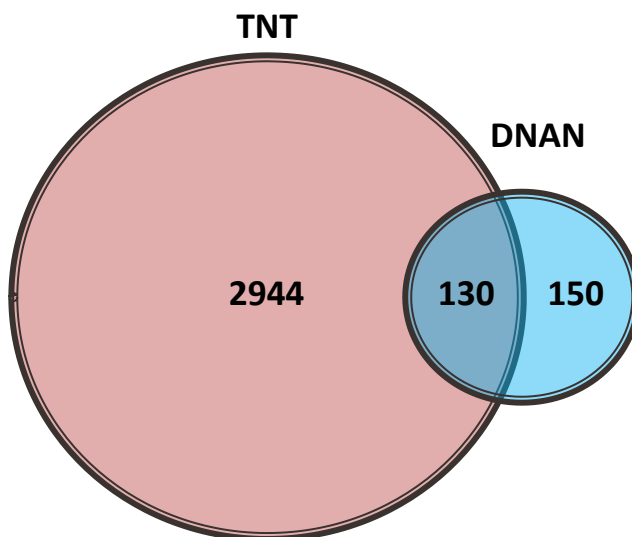
Figure 43. Differently expressed transcripts in common within kidney cells exposed in
co-cultures to TNT (100 μM) and to DNAN (100 μM).

Such a result is not surprising considering the difference in potency between the

two compounds observed during the range finding experiment (Table 6). Since the

observed potency for DNAN was approximately 10 times less than TNT for cell viability,

the comparison between the highest concentrations assessed for each xenobiotic can

provide a more informative comparison of each compound's toxicity at concentrations

leading to a similar potency. Therefore, Figure 44 shows the number of transcripts

differently expressed in common among co-cultures exposed to 100 μM of TNT and 1 mM of DNAN. While the number of differently expressed transcripts within the co-cultures exposed to 1 mM of DNAN almost doubled compared to the 100 μM DNAN exposure, it is still well below the number of differently expressed transcripts from the co-cultures exposed to 100 μM of TNT. Furthermore, at 44 %, the proportion of commonly expressed transcripts between the two co-cultures remains similar.
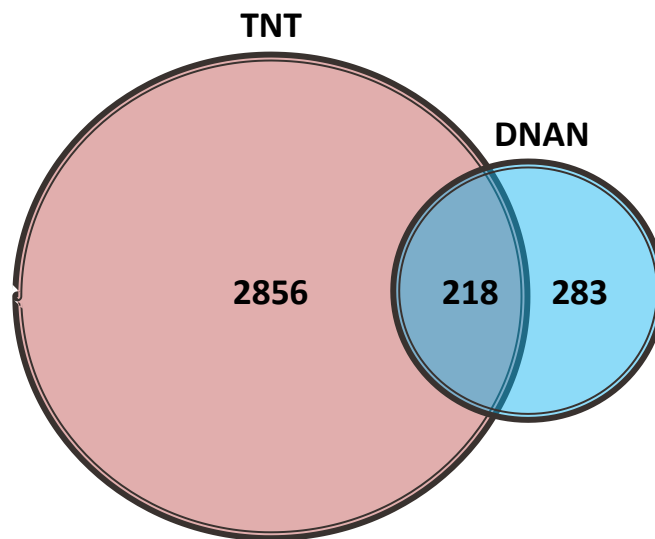
Figure 44. Differently expressed transcripts in common within kidney cells exposed in co-cultures to TNT (100 μM) and to DNAN (1 mM).

CHAPTER 4: DISCUSSION

VALIDATION OF THE IdMOC SYSTEM

Cell Culture Considerations

In a co-culture system using up to six cell lines such as the IdMOC system, it is highly likely that at least one of the cell lines will have a growing rate that is significantly slower than the other cell lines. In the current project, this cell line was the THLE-3 (liver) cells, which reached its growing rate peak only after six days following inoculation, making it difficult to have a constant supply of hepatocytes. However, such limitation can be overcome by keeping a greater quantity of those cells in stock, which necessitates time upon starting the culture. Therefore, such measure needs to be taken into consideration in any IdMOC project timeline.

Another important consideration with regards to the IdMOC system is the determination of the number of cells to use per well. For each cell line, the number of cells providing a confluent layer in a 96 well plate was determined. While this number differs from one cell line to another, this allows to maximize the response to the toxicant and the yield of RNA for subsequent microarray analysis. Furthermore, it also leads to a surface of tissue that is identical for each organ represented in the system.

High-N Compound Solubility and Purity

The solubility of high-N compounds varies from one chemical to another and among other factors with temperature and salinity, influencing the accessibility of these compounds to cells. While this solubility can be estimated using mathematical models, direct measurements remain the most accurate mean to assess it (90). The above results

showed that TNT concentration decreased by approximately 13.5% (Figure 16) to 25% (Figures 17, 18 and 19) after a 24h incubation in co-culture media. The level of soluble DNAN, however, was not affected. In order to assess if the loss of soluble TNT over time was caused by TNT degradation, further investigation was conducted. Among the known TNT degradation by-products tested, only 4-ADNT was detected, to include in the source product at about 14%. Light was not a factor in the degradation of TNT (Figure 21). The solubility experiment conducted in an IdMOC plate with vascular endothelial cells did not lead to any significant conclusion because of results variability. Heat and binding to the culture vessel surface could have contributed to the loss of soluble TNT (24; 31; 202). When combining the impurity of the source compound with its natural degradation, a final concentration of approximately 64% to 74% of TNT originally calculated value can be expected. Such TNT degradation needs to be taken into consideration when comparing results from TNT exposure to results from DNAN exposure. Overall, these results show the importance of testing for the loss or chemical breakdown of every high-N compound being assessed with the IdMOC system. Ideally, this testing should be conducted before the range finding experiment so that concentrations can be adjusted accordingly.

Efficacy of Each Biomarker / Cell Line Pair for the Assessment of Cellular Stress

NGAL / Kidney Cells

The initial assessment of the cell lines led to the detection of NGAL in culture media from kidney cells and lung cells mainly (Figure 8). Those results were later confirmed with the DMSO+ controls of the experiment with the reference compounds (Figures 15 and 16). NGAL, also known as lipocalin-2, was originally identified as a

94

component of neutrophil granules (85). Since then, most tissues have been shown to express NGAL, including kidney and lung. Therefore, it is highly likely that the obtained results are not caused by a lack of specificity of the ELISA assay, but rather because both HK-2 (kidney) and NULI-1 (lung) cells are producing the protein.

Against expectations, cyclosporin A decreased the production of NGAL by both the kidney and lung cells. While NGAL is a recognized *in vivo* biomarker of nephrotoxicity (160), a recent study assessing the potential of known *in vivo* biomarkers as *in vitro* biomarkers for the screening of drug-induced nephrotoxicity showed that traditional cytotoxicity assays and biomarker assays (to include NGAL) using HK-2 cells were both unsuitable for the prediction of nephrotoxicity (80). The authors of the study demonstrated an upregulation of NGAL in HK-2 cells exposed to toxicants, but with only scattered significant dose-dependent responses.   Such a conclusion is further reinforced by the observed significant decrease of NGAL in HK-2 cells exposed to the toxicants daunorubucin and troglitazon. With the HK-2 cell line being one of the only commercially available immortalized kidney cell line derived from normal human tissue, the use of primary kidney cells for the IdMOC system could represent a more suitable option, though being more resource intensive. Another alternative could be the creation of other normal human cell lines from diverse genetic backgrounds.

Albumin / Liver Cells

The initial assessment of the cell lines led to the detection of albumin in culture media from the liver cells, but also to a lesser extent with all other cell lines, particularly from the lung and heart cells (Figure 9). The detection of albumin in the culture media from the lung cells can be explained by its presence in the bronchial epithelial cell growth

kit that is supplementing the media. The kit includes human serum albumin leading to a final concentration of 500 µg/mL. This can explain why the albumin level from the lung cell culture media considerably decreased after 48 hours of incubation, the lung cells not replacing the albumin that is naturally degrading in the media. While the liver represents the chief source of albumin, other tissues are known to produce small quantities. As such, mRNA has previously been detected in kidney, though there is no evidence that this mRNA is translated (49). There is also no evidence that cardiac muscle cells produce albumin. Therefore, the albumin detected in the heart cell culture media is likely coming from the heat inactivated FBS used in the medium. Even though heat inactivation of serum deactivates most labile proteins, some albumin can remain in the culture medium (116). The albumin level detected in heart cell medium significantly decreased three days after inoculation as heart muscle cells do not produce albumin.

A high level of albumin was detected in all samples analyzed from the experiment with the reference compounds. In this experiment, the cells were exposed to the reference compounds in UPC plating media. While there is little information provided with regards to the content of the UPC plating media, the manufacturer later confirmed that the media contain heat-inactivated bovine serum. Consequently, the majority of the albumin detected in any sample containing UPC plating media, to include the IdMOC samples, is coming from the bovine serum contained in the media. Therefore, other potential *in vitro* hepatotoxicity biomarkers should be used as an alternative to albumin, such as aldo-keto reductase 1C1, heterogeneous nuclear ribonucleoprotein D and glucose-regulated protein (178). Since they are not secreted, the assessment of these biomarkers would need to be conducted through reverse transcription polymerase chain

96

reaction or as part of the microarrays. Other potential liver-specific biomarkers are those found in hepatocyte-derived extracellular vesicles, such as carbamoyl phosphate synthetase 1, S-adenosyl methionine synthetase 1, and catechol-O-methyltransferase (151).

SP-B / Lung Cells

SP-B was detected as expected in culture media from lung cells, but to a greater extent in culture media from kidney cells, and to a lesser extent in culture media from liver cells (Figure 10). A possible explanation is cross reaction of the ELISA assay with other proteins, which is recognized as a possibility by the assay manufacturer. For instance, surfactant proteins bind to toll-like receptors and the latter are not only expressed by lung cells, but also by kidney and liver cells (26; 114). It is therefore possible that hepatocytes produce a protein that is similar to surfactant protein B. Nevertheless, this limitation of specificity is overcome by the having monocultures as controls during the IdMOC experiment.

Endothelin I / Vascular Endothelial Cells

Endothelin I was initially detected mainly in culture media from vascular endothelial cells, with negligible levels observed from the other cell lines (Figure 11). However, while mainly produced by vascular endothelial cells, endothelin I can also be produced by various tissues and cells (96). The latter was confirmed by the experiment with the reference compounds as endothelin I was detected in culture media from every cell line, with the vascular endothelial cells producing a minimum of five times the production of any other cell line (Figure 18). The low production of endothelin I by

kidney, liver, lung and heart cells was not influenced by any of the reference compounds assessed. However, cyclosporin A and daunorubicun, and to a lesser extent VEGF-121, decreased the production of endothelin I by vascular endothelial cells. The latter is reflective of the role of VEGF-121. This growth factor is thought to promote vascular health by decreasing endothelin I production in human microvascular endothelial cells (169). The decrease of endothelin I by cyclosporin A does not reflect the literature. It is suggested that cyclosporin A causes hypertension through the release of vascular constrictors, such as endothelin I, by vascular endothelial cells (146; 172; 205). The observed decrease of endothelin I by vascular endothelial cells exposed to daunorubicin is also contradicting with the literature. Daunorubicin and doxorubicin, two structurally related anti-neoplastic drugs, are known for their potential cardiac toxicity (174). Doxorubicin increases the plasma level of endothelin I in humans (19).

Cardiac Troponin I / Heart Muscle Cells

The initial assessment of the cell lines shows a production of cardiac troponin I by heart cells (Figure 12). However, the ELISA assay used also detected troponins produced by the liver and lung cells, and to a lesser extent by the vascular endothelial and kidney cells, suggesting cross-reactivity. While cardiac troponin I is mainly produced by heart muscle cells, other non-muscle tissues can also produce significant amounts, such as the liver and the brain as observed in a study with chicken (65). Furthermore, while normal lung cells do not produce cardiac troponin I, non-small cell lung cancer tissues have been shown to produce the protein in significant amount (25). Even though the lung cell line used in the current project comes from normal tissue, the immortalization of the

cell line combined to the observation of chromosomal abnormalities by the manufacturer can explain the level of cardiac troponin I produced by the NULI-1 cells.

Summary of the Assessment of the Biomarkers of Cellular Stress

Table 12 summarizes the results obtained from the monocultures exposed to the reference compounds. The table indicates for each pair of reference compound and target cell, whether or not the reference compound led to the expected effect on the biomarker production.

Table 12. Assessment of the cell lines response to reference compounds.

Reference Compound (Target Cell)	Biomarker (Expected Production Change)	Was the expected change in biomarker production observed?
Cyclosporin A (Kidney)	NGAL (Increase)	No
Troglitazone (Liver)	Albumin (Decrease)	No
VEGF-121 (Vasc. endo.)	Endothelin I (Decrease)	Yes

As we can see, only endothelin I showed a response to stress corresponding to the expected change based on the literature. Therefore, the combination cell-biomarker for the selected kidney and liver cells are not ideal for the assessment of cellular stress. Moreover, cross-reactivity of the ELISA assays could have highly contributed to the unexpected results. This is taken into consideration in the discussion about the assessed biomarkers from the cultures exposed to TNT and DNAN.

TNT Toxicity Based on the Biomarkers of Cellular Stress

Initial assessment of the cell lines shows that each selected biomarker of cellular stress, except endothelin I, is not specific to a single cell line, thus showing the

99

importance of having appropriate monocultures serving as controls. By having controls in monocultures when conducting an IdMOC experiment, any difference observed in the production of the biomarkers in co-culture can be better evaluated and the potential cause identified. When comparing the average concentrations of a biomarker in media from monocultures versus co-cultures, one needs to take into consideration that cells are twice more diluted in co-culture than in monoculture. Therefore, the trend observed within each condition can be compared to each other, but not the direct values.

NGAL

Similarly to the decreased production of NGAL by kidney and lung cells exposed to cyclosporin A, NGAL production by these two cell lines in monocultures was significantly lower at the highest TNT concentrations compared to the controls as assessed by pairwise comparisons (Figure 29). Such results support the conclusion of the above study with regards to the poor reliability of HK-2 cells for the prediction of nephrotoxicity (80). Nevertheless, NGAL is not significantly produced by any cell line exposed to TNT in co-culture which is a notable difference with the results obtained from the monocultures. This could be caused by the detoxification of TNT in the co-cultures by the liver cells.

Albumin

Based on the literature, albumin levels decrease for hepatocytes exposed to toxicants (33; 57; 100; 207). Such decrease of albumin was observed from all monocultures exposed to increasing TNT concentrations (Figure 30). However, no change in albumin level was observed for human cells exposed to TNT in co-culture.

These results suggest a lower TNT toxicity for cells in co-culture settings. The fact that no change in albumin level was observed in co-culture could also have been caused by the cells being more diluted and the presence of albumin in the UPC plating media.

SP-B

The increase of SP-B in culture media from three of the cell lines exposed to TNT is consistent with the hypothesis that cross-reactivity occurred during the ELISA assay. While surfactant protein B is only produced in lung tissues, the saposin-like protein family to which it belongs is composed of 200 members with several proteins being found in lysosomes (191). Furthermore, saposin-like proteins share some key structural features, such as hydrophobic amino acid distribution and a pattern of three intra-molecular disulphide bridges formed by six cysteines (126; 134). As TNT concentrations increase, apoptosis triggers the release of the content of lysosomes, including the saposin-like proteins (134). Therefore, besides the toll-like receptors ligands mentioned above, saposin-like proteins could be an additional source of cross-reactivity when cells are exposed to TNT. This would be consistent with the decreased TNT toxicity in co-culture settings, since the level of SP-B (and possible analogues) remained constant (Figure 32). While no cell viability testing was done with the cells from the co-cultures, this could be done in the future in order to compare with the results obtained from the monocultures. Considering the above results, either a different SP-B ELISA kit or a different lung cell toxicity biomarker could be selected. A potential candidate for lung cell toxicity is the glycoprotein Krebs von den Lungen-6 (KL-6) (124). The fact that, in co-cultures, no change in SP-B concentration was observed between the highest concentration of TNT and the controls is consistent with the detoxification role of hepatocytes.

Endothelin I

The production of endothelin I initially increased in monocultures exposed to the lowest concentrations of TNT, particularly for vascular endothelial cells (Figure 34). However, as the concentrations of TNT increased, the level of endothelin decreased close to its original value. These results suggest a possible feedback control mechanism once a certain concentration of endothelin I is reached. Such mechanism has been suggested by Giraldo and his colleagues and involves the activating transcription factor 3 (Atf3) and early growth response 1 (Egr1) factor (62). Furthermore, cardiac hypertrophy and dysfunction stimulated by sustained pressure overload of Sprague-Dawley male rats' hearts led to the observation of an initial increase of endothelin I before decreasing continuously from day 8 of pressure overload (166). A negative feedback loop mechanism could also be responsible for the decreased level of endothelin I caused by cyclosporin A and daunorubicin (131). However, this dose-response relationship was not observed in co-cultures exposed to TNT as endothelin I concentration increased with increasing concentrations of TNT, even at the highest TNT concentration. A possible explanation is that the high detoxifying metabolic capacity of the co-cultured liver cells could suffice to cell survival, keeping the endothelin I negative feedback loop inactivated.

Cardiac Troponin I

No significant production of cardiac troponin was detected in any cultures (mono and co-) exposed to TNT, including controls. This is contradictory to the initial assessment of cardiac troponin production by the five cell lines. Considering that the controls in monocultures exposed to TNT and those from monocultures exposed to DNAN were the same, and that in only one of these controls was cardiac troponin

observed, a low replicability of the ELISA assay could be the cause. Even though all samples were processed at the same time, each ELISA plate only allows for the assessment of 96 samples, which led to use more than one plate for the analysis of the samples from the IdMOC experiment. In the case of cardiac troponin, some noticeable change in detected troponin was observed from one plate to another. This reliability issue can be added to the possibility of cross-reactivity that was addressed above.

Summary of TNT Effects on Biomarkers

Table 13 summarizes the above discussion and shows, for each selected biomarker of cytotoxic stress, whether or not TNT toxicity was observed. Overall, endothelin I appears to be the most effective biomarker of cytotoxic stress for the IdMOC system.   The fact that no significant change in SP-B was observed in culture media of lung cells exposed to TNT can be partially explained by the high variance of the related controls. Consequently, SP-B has the potential to be an effective biomarker for IdMOC experiments should an assay with no cross-reactivity be found.

Table 13. Toxicity of TNT as assessed by the detection of biomarkers.

Biomarker (Target Cell)	TNT Toxicity on Target Cell	TNT Toxicity in Co-Culture	Possible cross-reactivity observed
NGAL (kidney)	No	No	Yes
Albumin (liver)	No	No	Inconclusive
SP-B (lung)	No	No	Yes
Endothelin I (vasc. endo.)	Yes	Yes	No
Cardiac troponin I (heart)	No	No	Yes

Effects of TNT on Global Transcript Expression

At the highest TNT concentration (100 μM), kidney cells in mono- and co-cultures had 7 and 8 times, respectively, more differently expressed transcripts than within the cultures exposed at the lowest concentration (10 μM). This could be attributed to sublethal effects on cells near the concentration threshold where mortality was induced (Figure 24). Enrichment analysis indicated the activation of several pathways in response to the high concentration of TNT, including p53 signaling pathway and biological oxidation.

Enriched pathways that had, at the highest TNT concentration, more differently expressed transcripts within the co-cultures versus the monocultures include:

- p53 signaling pathway, which is involved in DNA repair and apoptosis;

- Metabolism of xenobiotics by cytochrome P450, a phase I enzyme family;

- Biological oxidative stress mitigation pathway;

- Glutathione metabolism, which includes the glutathione S-transferase, a phase II enzyme known to be involved in TNT detoxification;

- Bladder cancer associated pathway;

- Telomere maintenance pathway, which is essential to prevent genomic instability such as genomic copy addition, deletion, mutation, and translocation; and

- Pathways associated to metabolism of proteins and ribosomes.

The transcription factor p53 acts on damaged DNA and stalls cell division in order to either contribute to repairing DNA or, if the damages are high, to promoting apoptosis (30). The results obtained with the IdMOC system are reflective of a study that

showed that 2A-DNT, one of the most common TNT metabolites, leads to accumulation

of p53 proteins in MCF-7 human breast cancer cells (12). Furthermore, the TNT

metabolites hydroxilamino-dinitrotoluenes are known to lead to DNA damage (76).

Consequently, the enrichment of the p53 pathway in the IdMOC system could be

explained by the TNT metabolites from the hepatocytes. The difference between mono-

and co-cultures in p53 enrichment is more noticeable at the lowest TNT concentration.

This could be due to the saturation of the cells by TNT at highest concentration, leading

to the activation of proapoptotic signaling pathways. This hypothesis is supported by the

observation, in the mono- and co-cultures exposed to 100 µM of TNT, of change in

expression of 3 transcripts coding for BCL2 binding component 3, tumor protein p53

inducible protein 3, and scotin, all from the p53 pathway and involved in apoptosis.

None of these transcripts were differently expressed in the mono- and co-cultures

exposed to the lowest TNT concentration. Furthermore, as demonstrated previously from

the range finding experiment, no cells survived above the concentration of 1 mM. It can

therefore be advanced that the cells were preparing for apoptosis at 100 µM of TNT.

The observed enrichment of the P450 pathway in co-cultures exposed to TNT is

consistent with the implication of the amino- and hydroxylamino metabolites of TNT as

substrates for the single-electron transferring NADPH:P-450 reductase described

previously (156). The increase of this reductase has also been observed *in vivo* (37), and

has been correlated with a decrease in CYPA1 activities. The latter is further reinforced

by the observed decrease of the phase I CYP1A catalytic activities in European eels

exposed to TNT (179). From our results, a closer look at the 14 enriched genes of the

cytochrome P450 pathway indicates that 12 of the genes had decreased expression,

including the two cytochromes P450 CYP1B1 and CYP2C18. Furthermore, at the highest TNT concentration (100 µM), NADPH:P450 reductase transcript expression increased by a factor of 3.6 in the co-culture versus 2.7 in the monoculture.

DAVID also identified significant enrichment within the biological oxidative stress mitigation pathway where 22 differently expressed transcripts were observed within the co-cultures exposed to the highest TNT concentration. And, similarly to P450 and p53 enriched pathways, the difference between the mono- and co-cultures is greater within the lowest TNT concentration. These results are in line with the literature and the known oxidative stress caused by TNT metabolites (156). Furthermore, a study demonstrated the production of hydrogen peroxide in mitochondria of kidneys from monkeys exposed to TNT (92). One important pathway involved in oxidative stress and detoxification response towards nitro-aromatics is NRF-2-mediated oxidative stress response pathway. NRF2 is a transcription factor leading to reduce toxicity and reduced carcinogenesis (39). However, for both concentrations of TNT, the number of differently expressed transcripts within this enriched pathway was the same for both mono- and co-cultures.

The results also indicated significant enrichment of the glutathione metabolism associated pathway, which is consistent with the TNT biotransformation by the phase II enzyme glutathione-S-transferase. Among the 12 differently expressed transcripts was microsomal glutathione-S-transferase 1, which had a four-fold increase in expression within the co-cultures exposed to 100 µM TNT. Such increase was observed in an *in vivo* study with European eels (*Anguilla anguilla*) exposed to TNT (37). In a different *in vivo* study with rainbow trout (*Oncorhynchus mykiss*), the increase of glutathione S-

transferase activity in TNT treated fish was correlated with an increase in glutathione reductase as well (46). Gene-transcript expression for the latter was increased by 3.1-fold in the co-cultures, as opposed to 2.3-fold increase in the monocultures. However, while the microsomal glutathione-S-transferase 1 transcript had increased expression within the co-cultures exposed to 100 μM TNT, three non-microsomal glutathione-S-transferase transcripts had decreased expression: GSTZ1, GSTO2 and GSTK1.

Another enriched pathway in TNT exposed co-cultures is associated to bladder cancer. As discussed in the introduction, TNT is a known carcinogen (199). Even though liver cancer is the malignancy the most associated to the level of exposure to TNT, risks of developing other cancers have also been reported. As such, 21.8 % of female Fisher-344 rats fed with 50 mg/kg/day of TNT developed urinary bladder carcinomas (150). This was further supported by the observation of renal and urinary bladder hyperplasia in the treated animals. The 10 differently expressed transcripts associated to bladder cancer and detected by DAVID are related to cell cycle. Among those is CDKN2A, encoding for p14ARF, which had decreased expression in our co-culture exposed to the highest TNT concentration. Inactivation of the CDKN2A is known to be an early event in transitional cell carcinoma in bladder cancer (17). The decreased expression of CDKN2A was not observed in the monocultures.

The microarray data analysis identified telomere maintenance as an enriched function from co-cultures exposed to 100 μM TNT. A closer look determined that from the 22 genes identified in this case, 20 of them are part of histone clusters and all had decreased expression. Several natural and industrial toxicants, including heavy metals and ethanol, are known to decrease the level of expression of genes encoding for histones

(41). In some instances, this decrease was associated with carcinogenesis (41). The only transcript having increased expression within the enriched telomere maintenance function was the telomeric repeat binding factor 2, for which an overexpression has been correlated to lung, liver and gastric tumors (58; 137). From the 22 differently expressed transcripts involved in telomere maintenance and identified from the co-cultures exposed to 100 µM TNT, 16 of them were also differently expressed within the monocultures exposed to 100 µM TNT, none for the monocultures exposed to 10 µM TNT, and 8 for the co-cultures exposed to 10 µM.

As mentioned in the introduction, the liver and more specifically cytochrome P450, is responsible for the bioactivation of hydroxylamines which are then binding to sulfhydryl proteins (152). While on one hand hydroxylamino-metabolites can lead to a faster degradation of protein adducts, on the other hand oxidative stress causes the down-regulation of translation and protein synthesis (187). The co-cultures exposed to 100 µM of TNT led to 36 differently expressed transcripts directly involved in protein metabolism. Among those, 25 that coded for ribosomal proteins had decreased expression. Consequently, taking into account the observed enrichment of the oxidative stress related genes, the results from TNT-exposed cells within the IdMOC system corroborate the repression of protein translation under such oxidative stress.

Among the most enriched pathways within both mono- and co-cultures exposed to TNT was the focal adhesion pathway. This is another observation that is reflective of the literature with regards to TNT toxicity based on *in vivo* studies. Indeed, a recent study looking at the mechanistic impacts of 2A-DNT (a TNT metabolite) exposure in Northern Bobwhite found that the most highly enriched pathway from the kidney tissues

from the exposed female subjects was involved in signal molecules/interactions (68). Among the differently expressed transcripts were 6 transcripts involved in collagen metabolism which all had a decreased expression within the pathway. Interestingly, the enriched focal adhesion pathway from the co-cultures exposed to the highest TNT concentration contained 3 differently expressed transcripts related to collagen metabolism which also had a decreased expression: COL4A1, COL4A2 and COL5A1. Within the present study, from these 3 transcripts only COL4A1 and COL4A2 were differently expressed within the monocultures exposed to the highest TNT concentration. They had a decreased expression but to a lesser extent than within the co-cultures. The same study also found that the most enriched pathway from the kidney of the male subjects exposed to 2-ADNT was involved in amino acid metabolism. The enrichment of the latter was also observed within both mono- and co-cultures exposed to TNT.

The different signs of toxicity observed through the enriched pathways within the kidney cells exposed in co-culture to TNT can also be compared against a study that observed morphological effects on the kidney and nephrotoxicity caused by TNT exposure. Western fence lizard (Sceloporus occidentalis) gavaged with 45 mg/kg/day of TNT for 60 days had a 170% increase in kidney size relative to controls (120). Furthermore, significant incidence of renal tubular degeneration, characterized by vacuolation, cellular swelling, increased eosinophilia, and tubular necrosis, were also observed along with renal mineralization. In a study where adult male bullfrogs were fed with TNT; 2,4-DNT and 2,6-DNT, kidney necrosis was also observed within the three exposure groups (135). These morphological and histopathological observations are in line with the different enriched pathways found within kidney cells exposed to TNT in

the current study. As such, the transcription factor p53 has been found to be a mediator of transcriptional responses to ischemia-reperfusion kidney injury (55) and to accumulate in injured renal tubular cells (95). Oxidative stress is also strongly associated to renal injury by damaging molecular components of the kidney (180), potentially leading to cell necrosis (204). Furthermore, acetyl-histone H3 decreases in injured kidneys from septic mice and is correlated to increased expression of histone deacetylase 5 (HDAC5), which was also observed in the current project within kidney cells exposed to TNT in co-culture (20). With regards to acute kidney injury biomarkers, GST has served as a predicting indicator for renal replacement therapy in acute tubular necrosis patients (121).

Taken all together, the above observations provide evidence of the increased predictive value of the IdMOC system as opposed to monocultures in the assessment of high-nitrogen compounds' toxicity. The higher number of differently expressed transcripts, supported by a smaller p value for pathway enrichment, within kidney cells exposed to TNT in co-cultures versus monocultures for pathways related to p53 signaling, xenobiotic metabolism by cytochrome P450, ribosome, glutathione metabolism and bladder cancer, shows the impact of TNT metabolites on cell response to stress. Consequently, the cell-specific toxicity of parent compounds and of metabolites generated by other cells within the IdMOC system is contributing to the improved representation of human metabolism of xenobiotics. However, focal adhesion associated pathway was more enriched in monocultures than co-cultures. Microarray data analysis from cells not highly involved in the metabolism of xenobiotics and used in the IdMOC system could lead to an increased difference in terms of enriched pathways between co-

110

cultures and monocultures in favor of the former. However, literature would provide only scarce information about TNT effects on the related tissues.

EFFECTS OF DNAN ON GLOBAL TRANSCRIPT EXPRESSION

Statistically enriched pathways within kidney cells exposed to DNAN included pathways related to cytokine-cytokine receptor interaction; nitrogen metabolism; TGF-β signaling; glutamate metabolism; p53 signaling; metabolism of amino acids, cell adhesion; pantothenate and co-enzyme A biosynthesis; steroid hormone biosynthesis; antigen processing and presentation; and purine metabolism. Among those, five had, at the highest DNAN concentration, more differently expressed transcripts within the co-cultures versus the monocultures and are related to:

- p53 signaling;

- TGF-β signaling, which is involved in several cellular functions, such as differentiation, apoptosis and extracellular matrix production;

- Metabolism of amino acids;

- Nitrogen metabolism; and

- Glutamine-glutamate metabolism.

From these five pathways, only TGF-β signaling associated pathway was enriched at the lowest DNAN concentration within both mono- and co-cultures. Overall, the lowest DNAN concentration led to different enriched pathways compared to the highest concentration, including pathways related to natural killer cell mediated cytotoxicity, leucocyte transendothelial migration and regulation of actin cytoskeleton. The following discussion focuses on the five pathways that were more enriched within kidney cells

exposed to the highest concentration of DNAN in co-cultures and for which literature provided etiological insight.

The enrichment of the p53 pathway in the co-cultures exposed to 1 mM of DNAN is consistent with the known inhibition of p53 degradation by dinitrophenol, the primary DNAN metabolite (66).

Tumor growth factor (TGF) beta signaling pathway had a higher number of transcripts that had increased expression in the co-culture compared to the monocultures exposed to the highest DNAN concentration. The principal metabolite of DNAN, DNP, while under the form of 2,4-dinitrophenol glycine has been found to increase the level of detectable TGF-β from t-cell-derived antigen-binding molecules isolated from a toluene-sensitive patient (88). TGF-β family is involved in several cellular functions, such as differentiation, apoptosis and extracellular matrix production (3). Dysregulation of TGF-β has long been associated with various liver diseases (203) as well as cancer (108). In the latter, TGF- β can either suppress tumorigenesis or promote it depending, among others, on the stage of the cancer.

The enrichment of pathways involved in amino acid metabolism within the co-cultures exposed to 1 mM of DNAN may contribute to explaining a recent study where rats treated with 2,4-dinitrophenol showed an increased metabolism of tyrosine, lysine and phenylalanine (109). Another recent study that looked at the effect of dinitrophenol on kidney metabolism of male Sprague-Dawley rats showed an increase of proteinuria in treated animals, which is reflective of chronic kidney malfunction (54). More specifically, the authors of the study demonstrated that dinitrophenol led to increased kidney oxygen consumption possibly causing intrarenal hypoxia which resulted in

proteinuria. Among the 8 differently expressed transcripts related to amino acid

metabolism in co-cultures exposed to 1 mM of DNAN, four had increased expression and

coded for solute carrier (SLC) family members: one (member 12) from the SLC family 6,

and three (members 5, 11 and 10) from the SLC family 7. The transcript coding for

member 5 of the SLC family 7 (SLC7A5) leads to a subunit that is part of the cell surface

antigen CD98, which can be found on both epithelial membranes of kidney proximal

tubule (115). This transporter participates in the recovery of amino acids from the

primary filtrate. Therefore, the increase of amino acids may have contributed to the

elevated expression of the transcripts coding for SLC families 6 and 7. The monocultures

exposed to 1 mM of DNAN led to only 3 of the 4 SLC identified transcripts, which had

significantly increased expression, but to a lesser extent than in the co-cultures.

The co-cultures exposed to the highest concentration of DNAN had enrichment of

nitrogen metabolism associated pathway, within which four transcripts were differently

expressed. Among those was asparagine synthetase which catalyzes the conversion of L-

aspartate and L-glutamine into L-asparagine and L-glutamate (11). The observed

increase of asparagine synthetase transcript may be due to the acceleration of

phenylalanine metabolism by the presence of dinitrophenol, which basic process leads to

the formation of phenyl-acetylglutamine (109). The enrichment of the asparagine

synthetase was not observed in the monocultures.

Interestingly, while the increased expression of transcripts coding for asparagine

synthetase was observed in co-cultures exposed to 1 mM of DNAN, decreased expression

of glutamate dehydrogenases 1 and 2 (GLUD1 and GLUD2) transcripts was also noticed.

Glutamate dehydrogenase catalyzes the oxidative deamination of L-glutamate to 2-

oxoglutarate (105). While low concentrations of dinitrophenol is known to increase the deamination of glutamate in rat liver mitochondria, concentrations above 0.2 mM have been found to lead to the inhibition of the reaction (145). This correlates our observation with regards to the decreased expression of GLUD1 and GLUD2 in co-cultures exposed to 1 mM of DNAN. Only the decreased expression of GLUD2 was observed in the monoculture exposed to 1 mM of DNAN.

The co-cultures exposed to DNAN had an increased expression of the glutathione-specific gamma-glutamylcyclotransferase 1 transcript (CHAC1), which is a mammalian proapoptic protein catalyzing the cleavage of glutathione (94). The latter is known to have a reduced production in justaglomerular cells treated *in vitro* with dinitrophenol (70). In this study, when compared with the effects of the resulting reactive oxygen species, apoptosis in the treated cells was rather correlated with the rapid change of intracellular glutathione. This is consistent with the observed enriched pathways of the present project, as no pathway directly related to oxidative stress mitigation was enriched within the cultures exposed to DNAN. CHAC1 had also an increased expression in the monocultures exposed to the highest concentration of DNAN. It is worth noting that CHAC1 was not differently expressed in the co-cultures exposed to TNT.

The transcript of potassium channel inwardly rectifying subfamily J, member 2 (KCNJ2) had increased expression in the mono- and co-cultures exposed to the highest concentration of DNAN. This observation supports a study that showed that potassium accumulates in rabbit kidney provided with oral administration of dinitrophenol (125). In the study, the accumulation of potassium was found proportional to the dinitrophenol concentration, which could explain why KCNJ2 was not differently expressed at the

114

lowest DNAN concentration within both mono- and co-cultures. The accumulation of potassium caused by dinitrophenol was recently associated with hyperkalaemia, which contributed to the xenobiotic toxicity (84). Interestingly, KCNJ2 had a slight decreased expression within the co-cultures exposed to the highest TNT concentration.

In a study where Sprague-Dawley SPF rats where fed with 80 mg/kg/day of dinitrophenol for 28 days, the exposed group showed an increased mass of the kidneys and mineralization of the corticomedullary junction (91). Minor cortical tubular necrosis has also been observed in rats treated with 20 mg/day of dinitrophenol (4). The toxicity effects observed in the current project through enriched pathways within kidney cells exposed to DNAN in co-cultures support the known nephrotoxicity of dinitrophenol, more specifically based on the enrichment of three pathways related to p53 signaling, TGF-β signaling, and amino acid metabolism. As mentioned previously, the transcription factor p53 is a mediator of transcriptional responses to ischemia-reperfusion kidney injury (55) and accumulates in injured renal tubular cells (95). TGF-β has multifunctional effects on kidney. On one hand, TGF-β can promote renal fibrosis, and on the other hand it can confer some protective effects, including the inhibition of inflammation and induction of autophagy (171). The increased expression of transcripts coding for solute carrier proteins within the enriched pathway related to amino acid metabolism is consistent with the key role of these proteins in drug handling and nephrotoxicity (130). Solute carrier proteins have been shown to handle environmental toxins, potentially contributing to nephrotoxicity by exposing renal tubules to toxic metabolites (5; 40; 48).

EFFECTS COMPARISON FOR TNT AND DNAN

DNAN LC$_{50}$ versus TNT LC$_{50}$

Range finding experiments that need to be conducted for each high-N compound being assessed by the IdMOC system also provide a unique opportunity to compare the LC$_{50}$s obtained for each toxicant. The LC$_{50}$s calculated from TNT exposures are, for each cell line, at least one log scale less than those calculated for DNAN exposures, though only the differences for the liver, vascular endothelial and heart cells were significant. This difference demonstrates the importance of conducting a range finding experiment in order to better identify the scale of toxicant concentrations to assess with the IdMOC system. The resulting viability curve for DNAN showed a slope that is gradual, versus the abrupt slope obtained with TNT. Consequently, the dose-response curve for DNAN covers a broader range of concentrations as opposed to TNT. The observed differences in LC$_{50}$ between DNAN and TNT is reflective of the literature, particularly of a recent *in vivo* study comparing both compounds (168). The authors showed that LC$_{50}$ for leopard frogs exposed to DNAN for 96 hours (123 μM) was close to 4 times higher than the value obtained from TNT exposure (33 μM).

For both TNT and DNAN exposures, the liver cells have the lowest concentration threshold to elicit mortality. It is well documented that the liver is the primary organ metabolizing TNT. Hepatocytes are responsible for the bioactivation, from TNT metabolism, of hydroxylamines, which increase protein turn-over and oxidative stress (150). A study by Liu et al. (1992) showed that the binding of TNT metabolites was not observed as much in *in vitro* monocultures as *in vivo* because of plasma proteins (mainly albumin) in systemic circulation being in close contact with liver cells, trapping active

electrophilic metabolites produced in the liver more effectively. However, the IdMOC system used here involved THLE-3 (liver) cells producing albumin. Furthermore, the UPC plating media contains albumin as demonstrated by the functional assays.   As for DNAN, it is suggested that the metabolism of this compound starts, when ingested, in the lumen or villi where it is converted into dinitrophenol, possibly by P450 (77). Since hepatocytes, but also kidney cells, are producing P450, it is highly likely that these cells contributed to the conversion of DNAN into dinitrophenol within the IdMOC system (110). However, relative to the liver, the kidney is 60% as efficient in metabolizing dinitrophenol, which could explain the observed elevated cell mortality of hepatocytes exposed to DNAN (136).

No studies that looked at LC_{50}s from human cells exposed to DNAN in an *in vitro* setting were found. The LC_{50}s obtained in the current project and varying from 1,503 to 14,622 µM are at least 7 times higher than those observed in a previous *in vivo* study with *Pimephales promelas* (fish) and 2 cladocerans (i.e. water fleas: *Ceriodaphnia dubia* and *Daphnia pulex*), which were varying from 71.6 to 211.7 µM for an acute (48h) exposure (87). Another study also demonstrated DNAN microbial toxicity with LC_{50}s varying from 40-55 µM (*A. fischeri*) to 388 µM (aerobic heterotrophs) (107). A study by Donard and colleagues (44) showed that DNAN, in water, decreases green algae *Pseudokirchneriella subcapitata* growth with a half maximal effective concentration (EC_{50}) of 20 µM, and bacteria *Vibrio fischert* bioluminescence (EC_{50} = 303 µM). Therefore, the LC_{50}s obtained in the current project are considerably higher than those previously observed *in vivo*.

The observed $LC_{50}s$ for human cells exposed to TNT for 24 hours, varying between 145 μM and 261 μM, are reflective of previous *in vitro* studies where values from 17.6 μM to 197 μM were obtained for diverse mammalian cells exposed to TNT for 24 hours (128). Furthermore, compared to DNAN, the observed $LC_{50}s$ for TNT are closer to those observed in *in vivo* studies, such as the 33 μM mentioned above for leopard frogs exposed to TNT (168). The results presented in the current project suggest that a factor of approximately 4 to 200 needs to be applied in order to have an estimate of the ecotoxicological EC_{50} of high-N compounds. The assessment of other high-N compounds with the IdMOC system could provide more resolution regarding the effects comparisons between IdMOC and *in vivo* studies.

Biomarkers of Cellular Stress

NGAL

Similarly to TNT exposure, NGAL production by kidney and liver cells exposed to DNAN in monocultures was significantly lower at the highest DNAN concentrations compared to the controls as assessed by pairwise comparisons. NGAL was detected in co-cultures of cells exposed to DNAN, but increasing concentrations of the toxicant did not influence NGAL production. Consequently, such observation could be explained by the detoxification role of hepatocytes present in the IdMOC system, reinforcing the importance of toxicity testing in a co-culture setting.

Albumin

No decrease in albumin production was observed for cells exposed to DNAN in monoculture settings, which may be the result of the previously mentioned factors

affecting the detection of potential change in albumin levels. Nonetheless, this result is compatible with the expected lower toxicity of DNAN compared to TNT, for which a decrease of albumin was observed in monocultures. No change in albumin level was observed for human cells exposed to DNAN in co-culture.

SP-B

The decrease of SP-B (and possible analogues) in mono- and co-cultures exposed to DNAN, compared to the observed increase within monocultures exposed to TNT, is consistent with the expected lower toxicity of the former. Indeed, with DNAN leading to a lower activation of apoptosis, lysosomes are not releasing the saposin-like proteins. Again, a cell viability test could further support such hypothesis.

Endothelin I

For both monocultures and co-cultures exposed to DNAN, a significant increase in endothelin I production was only observed at 10 µM, but did not come from the vascular endothelial cells. This response reflects the same trend observed for the monocultures exposed to TNT and supports the possible involvement of the feedback loop mechanism mentioned previously. However, the changes in endothelin I production from monocultures and co-cultures exposed to DNAN were not as evident as for TNT. Again, this lighter response is reflective of the expected lower toxicity of DNAN compared to TNT.

Cardiac Troponin I

While no significant production of cardiac troponin was observed with cultures (mono- and co-) exposed to TNT, troponin increased in monocultures exposed to

increasing DNAN concentrations. This increase of cardiac troponin is consistent with the expected response from heart cells to a toxic stress. Furthermore, the fact that no troponin was detected in the co-cultures reflects the potential involvement of hepatocytes in detoxification.

Summary of DNAN Effects on Biomarkers

Table 14 summarizes the above discussion and shows, for each selected biomarker of cytotoxic stress, whether or not DNAN toxicity was observed. As we can see, cytotoxicity on biomarker producing cells was only observed with heart cells (through cardiac troponin). Considering the information that can be found in the literature with regards to DNAN toxicity, this is the first time that such stress response is reported. Compared to TNT, for which toxicity was only observed through the increase of endothelin I in mono- and co-cultures, DNAN did not cause an increase in endothelin I in monocultures. However, as for TNT, DNAN caused an increase in endothelin I levels in co-cultures, though lighter.

Table 14. Toxicity of DNAN as assessed by the detection of biomarkers.

Biomarker (Target Cell)	Toxicity on Target Cell	Toxicity in Co-Culture
NGAL (kidney)	No	No
Albumin (liver)	No	No
SP-B (lung)	No	No
Endothelin I (vasc. endo.)	No	Yes
Cardiac troponin I (heart)	Yes	No

DNAN Toxicity versus TNT Toxicity Based on Transcript Expression Profiles

For a concentration of 100 μM, TNT led to approximately 11 times more differently expressed transcripts than DNAN within the co-cultures. Even when comparing the highest concentration of TNT (100 μM) with the highest assessed concentration of DNAN (1 mM), each at exposure concentrations just prior to observations of decreased cell viability, TNT still led to 6 times more differently expressed transcripts within the co-cultures. This may be reflective of DNAN's lower potency and potentially more diverse adverse impacts in the TNT exposure given the diverse effects described in the Introduction. As transcript expression changes reflect underlying mechanism of toxicity, this work has made mechanistic connections to known adverse effects of TNT and has provided literature-backed hypotheses describing the potential mechanisms of action for DNAN.

TNT and DNAN led to similarities but also differences among enriched pathways within co-cultures exposed to each xenobiotic. Concerning the similarities, both compounds led to the enrichment of the p53 signaling pathway. Nevertheless, the five differently expressed transcripts within the enriched pathway resulting from the co-cultures exposed to DNAN were different than those from the exposure to TNT. Furthermore, TNT and DNAN led to two enriched pathways in common though the co-cultures did not had a higher enrichment than the monocultures: pathways related to amino acid metabolism and apoptosis. DNAN and TNT led to 2 transcripts differently expressed in common related to apoptosis: tumor necrosis factor (TNF) and proteasome activator subunit 1 (PSME1). A similar observation was made for the amino acid metabolism associated pathway, with 3 differently expressed transcripts in common:

PSME1, and members 5 and 11 of the solute carrier family 7. In all cases, the transcripts had a greater magnitude of differential expression within the co-cultures exposed to the highest TNT concentration. Consequently, not only the difference in transcript expression profiles between TNT and DNAN is reflected by the number of differently expressed transcripts, but also in terms of intensity.

CHAPTER 5: CONCLUSIONS

SUMMARY AND HYPOTHESIS DRIVEN CONCLUSIONS

The purpose of this project was to assess the toxicity of DNAN, as the latter is expected to replace TNT in many insensitive munitions. In order to do so, the IdMOC system, a recently developed assessment tool relying on the capability of an *in vitro* organ system to effectively represent human metabolism of xenobiotics, was used. Through TNT as a model chemical, the system offered a unique opportunity to compare both compounds' toxicity. Moreover, the project allowed for contributing in the development of an efficient and rapid tool for high-N hazard assessment capitalizing on multiple organ metabolism and organ-specific response. As national and international regulation towards the use of *in vivo* studies in chemical hazard assessment becomes stricter, the demand for practical alternatives will increase.

Five cell lines from different tissues were used in order to represent an organ system. Following the assessment of the system variables, including cell growth rate, biomarker production, RNA yield, cell response to stress and chemical degradation, a range finding experiment led to the selection of 4 concentrations of TNT and DNAN to be assessed through the IdMOC system. This selection of concentrations was based on their low impact on cell mortality and on their potential to lead to differently expressed transcripts within the exposed cells. The IdMOC experiment was then conducted where cells were exposed in mono- and co-cultures to TNT and DNAN with the appropriate controls. The culture media was harvested for the assessment of the biomarkers while the kidney cells were used for microarray analysis following RNA extraction. A two-way

ANOVA (p = 0.01) with Benjamini-Hochberg multiple-testing correction including a 1.5 fold-change cutoff led to the identification of differently expressed transcripts. Finally, a principal component analysis helped determining the influence of the xenobiotic concentrations and of the culture setting on the expression of the transcripts.

The results obtained in this project support the hypothesis that human cell types representative of multiple organs exposed to TNT and DNAN in co-culture have unique responses relative to monocultures, thus contributing to the validation of the IdMOC system as a chemical hazard assessment tool. TNT toxicity, based on endothelin I specific feedback loop mechanism, was lower within co-cultures as opposed to monocultures. This could be attributed to the detoxification role of hepatocytes within the IdMOC system. In both culture settings, the number of differently expressed transcripts was relatively similar for both concentrations assessed. Nonetheless, the co-cultures presented had more significant statistical enriched or KEGG pathways which contained a higher number of differently expressed transcripts. At the highest TNT concentration, the most enriched pathways were related to p53 signaling pathway, metabolism of xenobiotics by P450, ribosome, glutathione, and bladder cancer. Based on evidence from the literature, the observed increased activities of the p53 signaling pathway, of the oxidative stress mitigation pathway, of glutathione-S-transferase and of glutathione reductase were correlated with the action of TNT metabolites, particularly hydroxylamino-dinitrotoluenes. Similarly, the decreased expression of differently expressed transcripts within the pathways related to cytochrome P450 metabolism and protein metabolism was also correlated with TNT metabolites. Moreover, the enrichment of the pathway related to bladder cancer reflects *in vivo* observations of TNT toxicity and

124

the associated status of TNT as carcinogen impacting the urinary tract. Taken together, these observations are not only in line with the known mechanisms of action of TNT and TNT metabolites, but also reflect an improved detection of transcript expression for genes involved in xenobiotic metabolism by the IdMOC system as opposed to monocultures. Nevertheless, the principal component analysis showed that TNT exposure was the primary driver to differential expression relative to culturing method (mono- versus co-cultures). This can be explained by the increased expression, within kidney cells exposed to TNT in co-cultures and in monocultures, of the transcripts coding for the TNT metabolizing enzymes NADPH:P450 reductase (phase I) and microsomal-S-transferase 1 (phase II). Consequently, TNT was metabolized in both mono- and co-cultures.

DNAN toxicity was mainly observed by microarray data analysis considering the poor reliability of the functional assays. The global transcript expression profiles obtained support the hypothesis that human cell types representative of multiple organs exposed to TNT and DNAN in co-culture have unique chemical-exposure specific gene-transcript expression profiles indicative of systemic toxicity and of the lower relative toxicity of DNAN compared to TNT. The number of differently expressed transcripts was higher in the co-cultures exposed to 1 mM of DNAN compared to the monocultures, indicating a possible greater toxicity within the co-culture. Based on evidence from the literature, the most statistically significant enriched pathways were those related to p53 signaling, TGF-β signaling, amino acids metabolism, nitrogen metabolism and glutamine-glutamate metabolism, within the co-cultures exposed to DNAN. They were all correlated with dinitrophenol, the major metabolite of DNAN. Furthermore, the

increase expression of CHAC1 and KCNJ2 transcripts was also consistent with cell

exposure to dinitrophenol. Compared to TNT, DNAN showed a lower toxic potency for

cell viability. Indeed, the range finding experiment led to LC_{50}s for DNAN that were

significantly higher for three cell lines (liver, vascular endothelial, and heart cells).

Furthermore, kidney cells exposed in co-culture to DNAN had a number of differently

expressed transcripts that was well below the one from the exposure to a same

concentration of TNT. Even for a DNAN concentration (1 mM) 10 times higher than

TNT concentration, the former led to less differently expressed transcripts. Similarities

observed between DNAN and TNT toxicities include the enrichment of pathways related

to p53 signaling, amino acid metabolism and apoptosis. However, the intensity of the

changes in the expression of the transcripts was greater within cells exposed to TNT.

LIMITATIONS

While the IdMOC system offers several advantages compared to *in vivo* toxicity

testing, including rapidity of the assessment and the use of less resources, some

limitations are worth noting. The metabolism of toxicants within the IdMOC system

shows differences from human metabolism. First, while the vascular endothelial and

liver cells are among the first cells to be exposed to an ingested xenobiotic (because of

the first pass effect) and to potentially metabolize it, all cell lines of the IdMOC system

are equally exposed to the toxicant. Secondly, immortalized cells can be metabolically

less competent than their *in vivo* counterparts or primary cells. While the use of primary

cells could be considered for the IdMOC system, the scarcity of suitable human tissue

samples would make impractical the conduct of regular toxicity testing involving all five

tissues of the system. Therefore, immortalized cells represent the optimal option for an

eventual wide use of the IdMOC system. Furthermore, the solubility and degradation of high-N compounds in culture media need to be considered when comparing results from one toxicant to another. In the current project, TNT is expected to have an even higher toxicity than what was observed since soluble TNT decreased significantly in culture media after a 24h incubation. Also, the purity of the toxicant can impact the significance of *in vitro* toxicity testing.

Endothelin I was the only selected biomarker to provide an expected response to cellular stress. Therefore, the selected biomarkers were not necessarily reflective of cellular stress, and the assessment of TNT and DNAN toxicity was mainly based on the microarray results and on the range finding experiment. Particular aspects of the IdMOC system may have impacted the detection of the biomarkers of cellular stress, starting with the media-to-cell ratio which is twice as much within the co-cultures as within the monocultures, leading to a more diluted cytokine production within the former. This 2-fold dilution factor cannot be decreased as a maximum of media is used in the monocultures, and a minimum of media is used in the co-cultures. Also, secondary cell lines have a decreased capacity to produce biomarkers compared to the source tissues. Finally, cross-reactivity within the ELISA assays is highly likely to have contributed to the unexpected results.

FUTURE WORK

The IdMOC system used in this project represents a unique opportunity for assessing the toxicity of the multitude of high-N compounds developed recently. Future work is required in order to fully take advantage of the IdMOC system for such purpose:

1) The dosing of TNT metabolites within mono- and co-culture media from kidney cells exposed to TNT would support the conclusions made with regards to TNT toxicity. As the kidney cells used within the IdMOC system expressed transcripts coding for phase I and Phase II enzymes metabolizing TNT, metabolites of the latter should be found within both mono- and co-cultures. Such dosing could become part of every IdMOC experiment.

2) Microarray analysis of cells not directly involved in the metabolism of xenobiotics, such as lung or cardiac muscle cells, could better demonstrate the increased representation of human metabolism by the IdMOC system as opposed to monocultures.

3) The system can be further validated with traditional explosive compounds used in insensitive munitions, such as RDX and HMX. Such experimentation, besides the IdMOC experiment, would include the testing for loss of soluble chemical and the range finding experiment.

4) The integration of the system with the other components of the RHAAC project – the ecological hazard assay and the computational toxicokinetics/toxicodynamics predictive models – will lead to a hazard assessment tool more representative of human metabolism of high-N compounds.

5) In parallel to the above efforts, another range finding experiment using TNT concentrations covering a narrower range than the current project (i.e. between 100 μM and 1 mM) could provide more precise LC_{50}s.

As demonstrated in the current project with the IdMOC system, DNAN, with a lower potency than TNT, represents a more suitable option for melt cast formulations of

insensitive munitions. But the capacity of the system to assess chemical hazards is not limited to high-N compounds only. As chemical hazard assessment using *in vivo* techniques has led so far to the establishment of only a few hundred occupational exposure limits by national agencies, there is definitely room for a more efficient alternative. The IdMOC system could be part of the solution especially for initial hazard screening. However, several barriers lay ahead before the system becomes profitable, and they are not only physical. As John Maynard Keynes (1883-1946) once said: "The difficulty lies, not in the new ideas, but in escaping from the old ones."

REFERENCES

1.   ABCC. 2015. *DADID: Functional Annotation Bioinformatics Microarray Analysis*. http://david.abcc.ncifcrf.gov

2.   Adamcova M, Simunek T, Kaiserova H, Popelova O, Sterba M, et al. 2007. *In vitro* and *in vivo* examination of cardiac troponins as biochemical markers of drug-induced cardiotoxicity. *Toxicology* 237:218-28

3.   Akhurst RJ, Hata A. 2012. Targeting the TGFbeta signalling pathway in disease. *Nature reviews. Drug discovery* 11:790-811

4.   Arnold L, Collins C, Starmer GA. 1976. Studies on the modification of renal lesions due to aspirin and oxyphenbutazone in the rat and the effects on the kidney of 2:4 dinitrophenol. *Pathology* 8:179-84

5.   Aslamkhan AG, Han YH, Yang XP, Zalups RK, Pritchard JB. 2003. Human renal organic anion transporter 1-dependent uptake and toxicity of mercuric-thiol conjugates in Madin-Darby canine kidney cells. *Molecular pharmacology* 63:590-6

6.   ATCC. 2015. *General information on HK-2 cell line*. http://www.atcc.org/products/all/CRL-2190.aspx#generalinformation

7.   ATCC. 2015. *General information on NuLi-1 cell line*. http://www.atcc.org/products/all/CRL-4011.aspx#generalinformation

8.   ATCC. 2015. *General information on TeloHAEC cell line*. http://www.atcc.org/products/all/CRL-4052.aspx#generalinformation

9.   ATCC. 2015. *General information on THLE-3 cell line*. http://www.atcc.org/products/all/CRL-11233.aspx

10.   Badgujar DM, Talawar MB, Asthana SN, Mahulikar PP. 2008. Advances in science and technology of modern energetic materials: an overview. *Journal of hazardous materials* 151:289-305

11.   Balasubramanian MN, Butterworth EA, Kilberg MS. 2013. Asparagine synthetase: regulation by cell stress and involvement in tumor biology. *American journal of physiology. Endocrinology and metabolism* 304:E789-99

12.   Banerjee H, Hawkins Z, Dutta S, Smoot D. 2003. Effects of 2-amino-4,6-dinitrotoluene on p53 tumor suppressor gene expression. *Molecular and cellular biochemistry* 252:387-9

13.   Baron RM, Carvajal IM, Fredenburgh LE, Liu X, Porrata Y, et al. 2004. Nitric oxide synthase-2 down-regulates surfactant protein-B expression and enhances

endotoxin-induced lung injury in mice. *FASEB journal : official publication of the Federation of American Societies for Experimental Biology* 18:1276-8

14.   Basketter DA, Clewell H, Kimber I, Rossi A, Blaauboer B, et al. 2012. A roadmap for the development of alternative (non-animal) methods for systemic toxicity testing - t4 report*. *Altex* 29:3-91

15.   Bein K, Wesselkamper SC, Liu X, Dietsch M, Majumder N, et al. 2009. Surfactant-Associated Protein B Is Critical to Survival in Nickel-Induced Injury in Mice. *American Journal of Respiratory Cell and Molecular Biology* 41:226-36

16.   Beltz LA, Neira DR, Axtell CA, Iverson S, Deaton W, et al. 2001. Immunotoxicity of explosives-contaminated soil before and after bioremediation. *Archives of environmental contamination and toxicology* 40:311-7

17.   Berggren P, Kumar R, Sakano S, Hemminki L, Wada T, et al. 2003. Detecting homozygous deletions in the CDKN2A(p16(INK4a))/ARF(p14(ARF)) gene in urinary bladder cancer using real-time quantitative PCR. *Clinical cancer research : an official journal of the American Association for Cancer Research* 9:235-42

18.   Bhattacharya S, Zhang Q, Carmichael PL, Boekelheide K, Andersen ME. 2011. Toxicity testing in the 21 century: defining new risk assessment approaches based on perturbation of intracellular toxicity pathways. *PloS one* 6:e20887

19.   Bien S, Riad A, Ritter CA, Gratz M, Olshausen F, et al. 2007. The endothelin receptor blocker bosentan inhibits doxorubicin-induced cardiomyopathy. *Cancer research* 67:10428-35

20.   Bomsztyk K, Denisenko O. 2013. Epigenetic alterations in acute kidney injury. *Seminars in nephrology* 33:327-40

21.   Bruning T, Chronz C, Thier R, Havelka J, Ko Y, Bolt HM. 1999. Occurrence of urinary tract tumors in miners highly exposed to dinitrotoluene. *Journal of occupational and environmental medicine / American College of Occupational and Environmental Medicine* 41:144-9

22.   Cardoso WV, Williams MC, Mitsialis SA, Joyce-Brady M, Rishi AK, Brody JS. 1995. Retinoic acid induces changes in the pattern of airway branching and alters epithelial cell differentiation in the developing lung *in vitro*. *Am J Respir Cell Mol Biol* 12:464-76

23.   Cenas N, Nemeikaite-Ceniene A, Sergediene E, Nivinskas H, Anusevicius Z, Sarlauskas J. 2001. Quantitative structure-activity relationships in enzymatic single-electron reduction of nitroaromatic explosives: implications for their cytotoxicity. *Biochimica et biophysica acta* 1528:31-8

24.   Chaffee-Cipich MN, Sturtevant BD, Beaudoin SP. 2013. Adhesion of Explosives. *Analytical Chemistry* 85:5358-66

25. Chen C, Liu JB, Bian ZP, Xu JD, Wu HF, et al. 2014. Cardiac troponin I is abnormally expressed in non-small cell lung cancer tissues and human cancer cells. *International journal of clinical and experimental pathology* 7:1314-24

26. Chen K, Huang J, Gong W, Iribarren P, Dunlop NM, Wang JM. 2007. Toll-like receptors in inflammation, infection and cancer. *International Immunopharmacology* 7:1271-85

27. Chen M, Zhang M, Borlak J, Tong W. 2012. A decade of toxicogenomic research and its contribution to toxicological science. *Toxicological sciences : an official journal of the Society of Toxicology* 130:217-28

28. Cherkasskaia RG, Razumov VV, Semenikhin VA, Briukhova AR. 1993. [Toxic melanoderma in chronic intoxication with trinitrotoluene]. *Meditsina truda i promyshlennaia ekologiia*:39-41

29. Chuang HC, Fan CW, Chen KY, Chang-Chien GP, Chan CC. 2012. Vasoactive alteration and inflammation induced by polycyclic aromatic hydrocarbons and trace metals of vehicle exhaust particles. *Toxicology letters* 214:131-6

30. Clewell RA, Sun B, Adeleye Y, Carmichael P, Efremenko A, et al. 2014. Profiling dose-dependent activation of p53-mediated signaling pathways by chemicals with distinct mechanisms of DNA damage. *Toxicological sciences : an official journal of the Society of Toxicology* 142:56-73

31. Cohen R, Zeiri Y, Wurzberg E, Kosloff R. 2007. Mechanism of thermal unimolecular decomposition of TNT (2,4,6-trinitrotoluene): a DFT study. *The journal of physical chemistry. A* 111:11074-83

32. Cole SD, Madren-Whalley JS, Li AP, Dorsey R, Salem H. 2014. High content analysis of an *in vitro* model for metabolic toxicity: results with the model toxicants 4-aminophenol and cyclophosphamide. *Journal of biomolecular screening* 19:1402-8

33. Das J, Ghosh J, Roy A, Sil PC. 2012. Mangiferin exerts hepatoprotective activity against D-galactosamine induced acute toxicity and oxidative/nitrosative stress via Nrf2-NFkappaB pathways. *Toxicology and applied pharmacology* 260:35-47

34. Davidson MM, Nesti C, Palenzuela L, Walker WF, Hernandez E, et al. 2005. Novel cell lines derived from adult human ventricular cardiomyocytes. *Journal of molecular and cellular cardiology* 39:133-47

35. Davies PJ, Provatas, A. 2006. Characterisation of 2,4-Dinitroanisole: An Ingredient for use in Low Sensitivity Melt Cast Formulations, Australian Government - Department of Defence

36. Della Torre C, Corsi I, Arukwe A, Alcaro L, Amato E, Focardi S. 2008. Effects of 2,4,6-trinitrotoluene (TNT) on phase I and phase II biotransformation enzymes in

European eel Anguilla anguilla (Linnaeus, 1758). *Marine environmental research* 66:9-11

37.   Della Torre C, Corsi I, Arukwe A, Valoti M, Focardi S. 2008. Interactions of 2,4,6-trinitrotoluene (TNT) with xenobiotic biotransformation system in European eel Anguilla anguilla (Linnaeus, 1758). *Ecotoxicology and Environmental Safety* 71:798-805

38.   Deng Y, Johnson DR, Guan X, Ang CY, Ai J, Perkins EJ. 2010. *In vitro* gene regulatory networks predict in vivo function of liver. *BMC systems biology* 4:153

39.   Deng Y, Meyer SA, Guan X, Escalon BL, Ai J, et al. 2011. Analysis of common and specific mechanisms of liver function affected by nitrotoluene compounds. *PloS one* 6:e14662

40.   Di Giusto G, Anzai N, Ruiz ML, Endou H, Torres AM. 2009. Expression and function of Oat1 and Oat3 in rat kidney exposed to mercuric chloride. *Archives of toxicology* 83:887-97

41.   Dik S, Scheepers PT, Godderis L. 2012. Effects of environmental stressors on histone modifications and their relevance to carcinogenesis: a systematic review. *Critical reviews in toxicology* 42:491-500

42.   Dilley JV, Tyson CA, Spanggord RJ, Sasmore DP, Newell GW, Dacre JC. 1982. Short-term oral toxicity of 2,4,6-trinitrotoluene in mice, rats, and dogs. *Journal of toxicology and environmental health* 9:565-85

43.   Djerassi L. 1998. Hemolytic crisis in G6PD-deficient individuals in the occupational setting. *International archives of occupational and environmental health* 71 Suppl:S26-8

44.   Dodard SG, Sarrazin M, Hawari J, Paquet L, Ampleman G, et al. 2013. Ecotoxicological assessment of a high energetic and insensitive munitions compound: 2,4-dinitroanisole (DNAN). *Journal of hazardous materials* 262:143-50

45.   Dodd DE, McDougal, J.N. 2002. Recommendation of an Occupational Exposure Level for PAX-21, AFRL-HE-WP-TR-2001-0103

46.   Ek H, Dave G, Sturve J, Almroth BC, Stephensen E, et al. 2005. Tentative biomarkers for 2,4,6-trinitrotoluene (TNT) in fish (Oncorhynchus mykiss). *Aquatic Toxicology* 72:221-30

47.   Elferink MG, Olinga P, Draaisma AL, Merema MT, Bauerschmidt S, et al. 2008. Microarray analysis in rat liver slices correctly predicts *in vivo* hepatotoxicity. *Toxicology and applied pharmacology* 229:300-9

48. Engstrom K, Ameer S, Bernaudat L, Drasch G, Baeuml J, et al. 2013. Polymorphisms in genes encoding potential mercury transporters and urine mercury concentrations in populations exposed to mercury vapor from gold mining. *Environmental health perspectives* 121:85-91

49. Fanali G, di Masi A, Trezza V, Marino M, Fasano M, Ascenzi P. 2012. Human serum albumin: From bench to bedside. *MOLECULAR ASPECTS OF MEDICINE* 33:209-90

50. Federoff BT. 1960. Encyclopedia of Explosives and Related Items. Dover, New Jersey: Picatinny Arsenal

51. Ferrara N. 2004. Vascular endothelial growth factor: basic science and clinical progress. *Endocrine reviews* 25:581-611

52. Fournier D, Bride JM, Poirie M, Berge JB, Plapp FW, Jr. 1992. Insect glutathione S-transferases. Biochemical characteristics of the major forms from houseflies susceptible and resistant to insecticides. *The Journal of biological chemistry* 267:1840-5

53. Fox SI. 2012. *Human Physiology*. McGraw-Hill Science. 832 pp.

54. Friederich-Persson M, Persson P, Fasching A, Hansell P, Nordquist L, Palm F. 2013. Increased kidney metabolism as a pathway to kidney tissue hypoxia and damage: effects of triiodothyronine and dinitrophenol in normoglycemic rats. *Advances in experimental medicine and biology* 789:9-14

55. Fujino T, Muhib S, Sato N, Hasebe N. 2013. Silencing of p53 RNA through transarterial delivery ameliorates renal tubular injury and downregulates GSK-3beta expression after ischemia-reperfusion injury. *American journal of physiology. Renal physiology* 305:F1617-27

56. G R, Chandra SAM, W LJ, W QC. 2000. Toxicity of 2,4,6-Trinitrotoluene (TNT) in Hispid Cotton Rats (Sigmodon hispidus): Hematological, Biochemical, and Pathological Effects. *International Journal of Toxicology* 19:169-77

57. Gaiser BK, Hirn S, Kermanizadeh A, Kanase N, Fytianos K, et al. 2013. Effects of silver nanoparticles on the liver and hepatocytes *in vitro*. *Toxicological sciences : an official journal of the Society of Toxicology* 131:537-47

58. Gao J, Zhang J, Long Y, Lu X. 2011. Expression of telomere binding proteins in gastric cancer and correlation with clinicopathological parameters. *Asia-Pacific journal of clinical oncology* 7:339-45

59. Garcia-Reyero N, Habib T, Pirooznia M, Gust KA, Gong P, et al. 2011. Conserved toxic responses across divergent phylogenetic lineages: a meta-analysis of the neurotoxic effects of RDX among multiple species using toxicogenomics. *Ecotoxicology (London, England)* 20:580-94

134

60.   George PM, Cunningham ME, Galloway-Phillipps N, Badiger R, Alazawi W, et al. 2012. Endothelin-1 as a mediator and potential biomarker for interferon induced pulmonary toxicity. *Pulmonary circulation* 2:501-4

61.   George TN, Snyder JM. 1997. Regulation of surfactant protein gene expression by retinoic acid metabolites. *Pediatric research* 41:692-701

62.   Giraldo A, Barrett OP, Tindall MJ, Fuller SJ, Amirak E, et al. 2012. Feedback regulation by Atf3 in the endothelin-1-responsive transcriptome of cardiomyocytes: Egr1 is a principal Atf3 target. *The Biochemical journal* 444:343-55

63.   Gong P, Guan X, Inouye LS, Deng Y, Pirooznia M, Perkins EJ. 2008. Transcriptomic analysis of RDX and TNT interactive sublethal effects in the earthworm Eisenia fetida. *BMC genomics* 9 Suppl 1:S15

64.   Gong P, Guan X, Inouye LS, Pirooznia M, Indest KJ, et al. 2007. Toxicogenomic analysis provides new insights into molecular mechanisms of the sublethal toxicity of 2,4,6-trinitrotoluene in Eisenia fetida. *Environmental science & technology* 41:8195-202

65.   Grewal JS, Bag J. 1996. Slow troponin C gene expression in chicken heart and liver is regulated by similar enhancers. *FEBS Letters* 383:267-72

66.   Gronostajski RM, Goldberg AL, Pardee AB. 1984. Energy requirement for degradation of tumor-associated protein p53. *Molecular and cellular biology* 4:442-8

67.   Grundlingh J, Dargan PI, El-Zanfaly M, Wood DM. 2011. 2,4-dinitrophenol (DNP): a weight loss agent with significant acute toxicity and risk of death. *Journal of medical toxicology : official journal of the American College of Medical Toxicology* 7:205-12

68.   Gust KA, Nanduri B, Rawat A, Wilbanks MS, Ang CY, et al. 2015. Systems toxicology identifies mechanistic impacts of 2-amino-4,6-dinitrotoluene (2A-DNT) exposure in Northern Bobwhite. *BMC genomics* 16:587

69.   Haase M, Bellomo R, Haase-Fielitz A. 2010. Neutrophil gelatinase-associated lipocalin. *Current opinion in critical care* 16:526-32

70.   Han YH, Kim SZ, Kim SH, Park WH. 2008. 2,4-Dinitrophenol induces apoptosis in As4.1 juxtaglomerular cells through rapid depletion of GSH. *Cell biology international* 32:1536-45

71.   Hantson P, Weynand B, Doyle I, Bernand A, Hermans C. 2008. Pneumoproteins as markers of paraquat lung injury: A clinical case. *Journal of Forensic and Legal Medicine* 15:48-52

72.   Harkonen H, Karki M, Lahti A, Savolainen H. 1983. Early equatorial cataracts in workers exposed to trinitrotoluene. *American journal of ophthalmology* 95:807-10

73.   Hassman P, Hassmanova V. 1976. Exposure tests in trinitrotoluene workers. *Sbornik vedeckych praci Lekarske fakulty Karlovy university v Hradci Kralove* 19:51-60

74.   Hatzinger PB, Schaefer CE, Sheehan P, Leeson A, Environmental Security Technology Certification Program Office Arlington VA. 2012. In Situ Bioremediation of Energetic Compounds in Groundwater.

75.   Hirose S, Hosoda Y, Furuya S, Otsuki T, Ikeda E. 2000. Expression of vascular endothelial growth factor and its receptors correlates closely with formation of the plexiform lesion in human pulmonary hypertension. *Pathology International* 50:472-9

76.   Homma-Takeda S, Hiraku Y, Ohkuma Y, Oikawa S, Murata M, et al. 2002. 2,4,6-trinitrotoluene-induced reproductive toxicity via oxidative DNA damage by its metabolite. *Free radical research* 36:555-66

77.   Hoyt N, Brunell M, Kroeck K, Hable M, Crouse L, et al. 2013. Biomarkers of oral exposure to 3-nitro-1,2,4-triazol-5-one (NTO) and 2,4-dinitroanisole (DNAN) in blood and urine of rhesus macaques (Macaca mulatta). *Biomarkers : biochemical indicators of exposure, response, and susceptibility to chemicals* 18:587-94

78.   Huang da W, Sherman BT, Lempicki RA. 2009. Systematic and integrative analysis of large gene lists using DAVID bioinformatics resources. *Nature protocols* 4:44-57

79.   Huang DW, Sherman BT, Tan Q, Collins JR, Alvord WG, et al. 2007. The DAVID Gene Functional Classification Tool: a novel biological module-centric algorithm to functionally analyze large gene lists. *Genome Biology* 8:R183-R

80.   Huang JX, Kaeslin G, Ranall MV, Blaskovich MA, Becker B, et al. 2015. Evaluation of biomarkers for *in vitro* prediction of drug-induced nephrotoxicity: comparison of HK-2, immortalized human proximal tubule epithelial, and primary cultures of human proximal tubular cells. *Pharmacology Research & Perspectives* 3:n/a-n/a

81.   Huang YC, Ghio AJ. 2006. Vascular effects of ambient pollutant particles and metals. *Current vascular pharmacology* 4:199-203

82.   Hwang P, Chow T, Adrian NR, Construction Engineering Research Lab Champaign IL. 1998. Transformation of TNT to Triaminotoluene by Mixed Cultures Incubated Under Methanogenic Conditions.

83.   International A. 2014. Standard Guide for Assessing the Environmental and Huan Health Impacts of New Energetic Compounds. West Conshohocken, PA

84.   Jiang J, Yuan Z, Huang W, Wang J. 2011. 2, 4-dinitrophenol poisoning caused by non-oral exposure. *Toxicology and industrial health* 27:323-7

85.   Kalousek I, Roselova P, Otevrelova P. 2006. [NGAL--neutrophil gelatinase associated lipocalin in biochemistry, physiology and clinical praxis]. *Casopis lekaru ceskych* 145:373-6

86.   Kavlock R, Dix D. 2010. Computational toxicology as implemented by the U.S. EPA: providing high throughput decision support tools for screening and assessing chemical exposure, hazard and risk. *Journal of toxicology and environmental health. Part B, Critical reviews* 13:197-217

87.   Kennedy AJ, Laird JG, Lounds C, Gong P, Barker ND, et al. 2014. Inter- and intraspecies chemical sensitivity: A case study using 2,4-dinitroanisole. *Environmental toxicology and chemistry / SETAC*

88.   Khalil Z, Georgiou GM, Ogedegbe H, Cone RE, Simpson F, Little CH. 2000. Immunological and in-vivo neurological studies on a benzoic acid-specific T cell-derived antigen-binding molecule from the serum of a toluene-sensitive patient. *Archives of environmental health* 55:304-18

89.   Khan MI, Lee J, Park J. 2013. A toxicological review on potential microbial degradation intermediates of 2,4,6-trinitrotoluene, and its implications in bioremediation. *KSCE Journal of Civil Engineering* 17:1223-31

90.   Kholod YA, Gryn'ova G, Gorb L, Hill FC, Leszczynski J. 2011. Evaluation of the dependence of aqueous solubility of nitro compounds on temperature and salinity: a COSMO-RS simulation. *Chemosphere* 83:287-94

91.   Koizumi M, Yamamoto Y, Ito Y, Takano M, Enami T, et al. 2001. Comparative study of toxicity of 4-nitrophenol and 2,4-dinitrophenol in newborn and young rats. *The Journal of toxicological sciences* 26:299-311

92.   Kong LY, Jiang QG, Qu QS. 1989. Formation of superoxide radical and hydrogen peroxide enhanced by trinitrotoluene in rat liver, brain, kidney, and testicle *in vitro* and monkey liver *in vivo*. *Biomedical and environmental sciences : BES* 2:72-7

93.   Kozuka H, Mori M, Naruse Y. 1979. Studies on the metabolism and toxicity of dinitrotoluenes. Toxicological study of 2,4-dinitrotoluene (2, 4-DNT) in rats in long term feeding. *The Journal of toxicological sciences* 4:221-8

94.   Kumar A, Tikoo S, Maity S, Sengupta S, Sengupta S, et al. 2012. Mammalian proapoptotic factor ChaC1 and its homologues function as gamma-glutamyl cyclotransferases acting specifically on glutathione. *EMBO reports* 13:1095-101

95. Lee CG, Kang YJ, Kim HS, Moon A, Kim SG. 2015. Phlda3, a urine-detectable protein, causes p53 accumulation in renal tubular cells injured by cisplatin. *Cell biology and toxicology* 31:121-30

96. Lee LK, Kim JH, Kim MY, Lee JU, Yang SM, et al. 2014. A Review of Signal Transduction of Endothelin-1 and Mitogen-activated Protein Kinase-related Pain for Nanophysiotherapy. *Journal of physical therapy science* 26:789-92

97. Lefebvre MH, Falmagne, B., and B. Smedts. 2004. Sensitivities and performances of non-regular explosives. In *New Trends in Research of Energetic Materials Seminar*, ed. FoCT- Pardubice, p. 10

98. Lent E. 2012. The subchronic oral toxicity of 2,4-dinitroanisole (DNAN) in rats, Aberdeen Proving Ground (MD)

99. Letzel S, Goen T, Bader M, Angerer J, Kraus T. 2003. Exposure to nitroaromatic explosives and health effects during disposal of military waste. *Occupational and environmental medicine* 60:483-8

100. Letzsch S, Hänel, F., Böttcher, K. and J. Kelm. 2014. Application Note: Cellular Imaging and Analysis, PerkinElmer, Maltham, MA, USA

101. Leung KH, Yao M, Stearns R, Chiu SH. 1995. Mechanism of bioactivation and covalent binding of 2,4,6-trinitrotoluene. *Chemico-biological interactions* 97:37-51

102. Levine BS, Furedi EM, Gordon DE, Lish PM, Barkley JJ. 1984. Subchronic toxicity of trinitrotoluene in Fischer 344 rats. *Toxicology* 32:253-65

103. Li AP. 2009. The use of the Integrated Discrete Multiple Organ Co-culture (IdMOC) system for the evaluation of multiple organ toxicity. *Alternatives to laboratory animals : ATLA* 37:377-85

104. Li AP, Bode C, Sakai Y. 2004. A novel *in vitro* system, the integrated discrete multiple organ cell culture (IdMOC) system, for the evaluation of human drug toxicity: comparative cytotoxicity of tamoxifen towards normal human cells from five major organs and MCF-7 adenocarcinoma breast cancer cells. *Chemico-biological interactions* 150:129-36

105. Li M, Li C, Allen A, Stanley CA, Smith TJ. 2014. Glutamate dehydrogenase: structure, allosteric regulation, and role in insulin homeostasis. *Neurochemical research* 39:433-45

106. Li Y, Jiang QG, Yao SQ, Liu W, Tian GJ, Cui JW. 1993. Effects of exposure to trinitrotoluene on male reproduction. *Biomedical and environmental sciences : BES* 6:154-60

107. Liang J, Olivares C, Field JA, Sierra-Alvarez R. 2013. Microbial toxicity of the insensitive munitions compound, 2,4-dinitroanisole (DNAN), and its aromatic amine metabolites. *Journal of hazardous materials* 262:281-7

108. Lin RL, Zhao LJ. 2015. Mechanistic basis and clinical relevance of the role of transforming growth factor-beta in cancer. *Cancer biology & medicine* 12:385-93

109. Liu S, Wang N, Chen P, Li X, Liu C. 2013. Effect of huanglianjiedu tang on fever in rats induced by 2, 4-dinitrophenol. *Journal of traditional Chinese medicine = Chung i tsa chih ying wen pan / sponsored by All-China Association of Traditional Chinese Medicine, Academy of Traditional Chinese Medicine* 33:492-9

110. Liu S, Yao Y, Lu S, Aldous K, Ding X, et al. 2013. The role of renal proximal tubule P450 enzymes in chloroform-induced nephrotoxicity: utility of renal specific P450 reductase knockout mouse models. *Toxicology and applied pharmacology* 272:230-7

111. Liu YY, Lu AY, Stearns RA, Chiu SH. 1992. *In vivo* covalent binding of [14C]trinitrotoluene to proteins in the rat. *Chemico-biological interactions* 82:1-19

112. Liu YY, Yao M, Fang JL, Wang YW. 1995. Monitoring human risk and exposure to trinitrotoluene (TNT) using haemoglobin adducts as biomarkers. *Toxicology letters* 77:281-7

113. Lotufo GR, Biedenbach JM, Sims JG, Chappell P, Stanley JK, Gust KA. 2014. Bioaccumulation kinetics of the conventional energetics TNT and RDX relative to insensitive munitions constituents DNAN and NTO in Rana pipiens tadpoles. *Environmental toxicology and chemistry / SETAC*

114. Luangsay S, Ait-Goughoulte M, Michelet M, Floriot O, Bonnin M, et al. 2015. Expression and functionality of Toll- and RIG-like receptors in HepaRG cells. *Journal of hepatology* 63:1077-85

115. Makrides V, Camargo SM, Verrey F. 2014. Transport of amino acids in the kidney. *Comprehensive Physiology* 4:367-403

116. Marini I, Moschini R, Del Corso A, Mura U. 2005. Chaperone-like features of bovine serum albumin: a comparison with alpha-crystallin. *Cellular and molecular life sciences : CMLS* 62:3092-9

117. Markham DC, Simpson MJ, Baker RE. 2014. Choosing an Appropriate Modelling Framework for Analysing Multispecies Co-culture Cell Biology Experiments. *Bulletin of mathematical biology*

118.   Masubuchi Y. 2006. Metabolic and non-metabolic factors determining troglitazone hepatotoxicity: a review. *Drug metabolism and pharmacokinetics* 21:347-56

119.   Mc GL, Reed HL, et al. 1947. Metabolic disturbances in workers exposed to dinitrotoluene during World War II. *Gastroenterology* 8:293-5

120.   McFarland CA, Quinn MJ, Jr., Bazar MA, Remick AK, Talent LG, Johnson MS. 2008. Toxicity of oral exposure to 2,4,6-trinitrotoluene in the western fence lizard (Sceloporus occidentalis). *Environmental toxicology and chemistry / SETAC* 27:1102-11

121.   McMahon BA, Koyner JL, Murray PT. 2010. Urinary glutathione S-transferases in the pathogenesis and diagnostic evaluation of acute kidney injury following cardiac surgery: a critical review. *Current opinion in critical care* 16:550-5

122.   Meier R, van Griensven M, Pape HC, Krettek C, Chawda M, Seekamp A. 2003. Effects of cardiac contusion in isolated perfused rat hearts. *Shock (Augusta, Ga.)* 19:123-6

123.   Miliukiene V, Cenas N. 2008. Cytotoxicity of nitroaromatic explosives and their biodegradation products in mice splenocytes: implications for their immunotoxicity. *Zeitschrift fur Naturforschung. C, Journal of biosciences* 63:519-25

124.   Mokra D, Kosutova P. 2015. Biomarkers in acute lung injury. *Respiratory physiology & neurobiology* 209:52-8

125.   Mudge GH. 1951. Electrolyte and water metabolism of rabbit kidney slices; effect of metabolic inhibitors. *The American journal of physiology* 167:206-23

126.   Munford RS, Sheppard PO, O'Hara PJ. 1995. Saposin-like proteins (SAPLIP) carry out diverse functions on a common backbone structure. *Journal of lipid research* 36:1653-63

127.   N. Cenas AN-C, J. Sarlauskas, Z. Anusevicius, H. Nivinskas, L. Miseviciene, A. Maroziene. 2009. *Ecotoxicology of Explosives: Chapter 9 - Mechanisms of the Mammalian Cell Cytotoxicity of Explosives*. Taylor and Francis Group, LLC. 16 pp.

128.   Nemeikaitė-Čėnienė A, Miliukienė V, Šarlauskas J, Maldutis E, Čėnas N. 2006. Chemical aspects of cytotoxicity of nitroaromatic explosives: a review. *Chemija* 17:34-41

129.   Newby LK, Rodriguez I, Finkle J, Becker RC, Hicks KA, et al. 2011. Troponin measurements during drug development--considerations for monitoring and management of potential cardiotoxicity: an educational collaboration among the

Cardiac Safety Research Consortium, the Duke Clinical Research Institute, and the US Food and Drug Administration. *American heart journal* 162:64-73

130. Nigam SK, Wu W, Bush KT, Hoenig MP, Blantz RC, Bhatnagar V. 2015. Handling of Drugs, Metabolites, and Uremic Toxins by Kidney Proximal Tubule Drug Transporters. *Clinical journal of the American Society of Nephrology : CJASN* 10:2039-49

131. Nobori K, Ito H, Tamamori-Adachi M, Adachi S, Ono Y, et al. 2002. ATF3 inhibits doxorubicin-induced apoptosis in cardiac myocytes: a novel cardioprotective role of ATF3. *Journal of molecular and cellular cardiology* 34:1387-97

132. NRC. 2007. Toxicity Testing in the 21th Century: A Vision and a Strategy

133. Olivares C, Liang J, Abrell L, Sierra-Alvarez R, Field JA. 2013. Pathways of reductive 2,4-dinitroanisole (DNAN) biotransformation in sludge. *Biotechnology and bioengineering* 110:1595-604

134. Olmeda B, Garcia-Alvarez B, Perez-Gil J. 2013. Structure-function correlations of pulmonary surfactant protein SP-B and the saposin-like family of proteins. *European biophysics journal : EBJ* 42:209-22

135. Paden NE, Smith EE, Kendall RJ. 2008. Acute toxicity of 2,4,6-trinitrotoluene, 2,4-dinitrotoluene, and 2,6-dinitrotoluene in the adult bullfrog (Lithobates catesbeiana). *Bulletin of environmental contamination and toxicology* 80:487-91

136. Parker VH. 1952. Enzymic reduction of 2:4-dinitrophenol by rat-tissue homogenates. *The Biochemical journal* 51:363-70

137. Patel TN, Vasan R, Gupta D, Patel J, Trivedi M. 2015. Shelterin proteins and cancer. *Asian Pacific journal of cancer prevention : APJCP* 16:3085-90

138. Patil H, Vaidya O, Bogart D. 2011. A review of causes and systemic approach to cardiac troponin elevation. *Clinical cardiology* 34:723-8

139. Peacock WFt, Maisel A, Kim J, Ronco C. 2013. Neutrophil gelatinase associated lipocalin in acute kidney injury. *Postgraduate medicine* 125:82-93

140. Pennington JC, Brannon JM. 2002. Environmental fate of explosives. *Thermochimica Acta* 384:163-72

141. Perkins EJ, Ankley GT, Crofton KM, Garcia-Reyero N, LaLone CA, et al. 2013. Current perspectives on the use of alternative species in human health and ecological hazard assessments. *Environmental health perspectives* 121:1002-10

142. Perreault NN, Manno D, Halasz A, Thiboutot S, Ampleman G, Hawari J. 2012. Aerobic biotransformation of 2,4-dinitroanisole in soil and soil Bacillus sp. *Biodegradation* 23:287-95

143. Platten WE, 3rd, Bailey D, Suidan MT, Maloney SW. 2010. Biological transformation pathways of 2,4-dinitro anisole and N-methyl paranitro aniline in anaerobic fluidized-bed bioreactors. *Chemosphere* 81:1131-6

144. PSciences. *IdMOC Plates*. http://www.apsciences.com/ncatalog/index.php?main_page=index&cPath=67

145. Quagliariello E, Papa S, Saccone C, Palmieri F, Francavilla A. 1965. THE OXIDATION OF GLUTAMATE BY RAT-LIVER MITOCHONDRIA. *The Biochemical journal* 95:742-8

146. Ramzy D, Wallen J, Badiwala MV, Tumiati LC, Tepperman E, et al. 2011. Endothelin-1 antagonism and nitric oxide augmentation prevents cyclosporine-induced vasomotor impairment. *The Journal of heart and lung transplantation : the official publication of the International Society for Heart Transplantation* 30:77-85

147. Rao B, Wang W, Cai Q, Anderson T, Gu B. 2013. Photochemical transformation of the insensitive munitions compound 2,4-dinitroanisole. *The Science of the total environment* 443:692-9

148. Ravi P, Badgujar DM, Gore GM, Tewari SP, Sikder AK. 2011. Review on Melt Cast Explosives. *Propellants, Explosives, Pyrotechnics* 36:393-403

149. Rawat A, Gust KA, Deng Y, Garcia-Reyero N, Quinn MJ, Jr., et al. 2010. From raw materials to validated system: the construction of a genomic library and microarray to interpret systemic perturbations in Northern bobwhite. *Physiological genomics* 42:219-35

150. Registry USAfTSaD. 1995. Toxicological Profile for 2,4,6-Trinitrotoluene

151. Rodriguez-Suarez E, Gonzalez E, Hughes C, Conde-Vancells J, Rudella A, et al. 2014. Quantitative proteomic analysis of hepatocyte-secreted extracellular vesicles reveals candidate markers for liver toxicity. *Journal of proteomics* 103:227-40

152. Sabbioni G, Sepai O, Norppa H, Yan H, Hirvonen A, et al. 2007. Comparison of biomarkers in workers exposed to 2,4,6-trinitrotoluene. *Biomarkers : biochemical indicators of exposure, response, and susceptibility to chemicals* 12:21-37

153. Sabbioni G, Wei J, Liu YY. 1996. Determination of hemoglobin adducts in workers exposed to 2,4, 6-trinitrotoluene. *Journal of chromatography. B, Biomedical applications* 682:243-8

154. Samuels P. 2012. Characterization of 2,4-dinitroanisole (DNAN). ed. DaEC Armament Research. Picatinny Arsenal, New Jersey

155. Sarlauskas J, Dickancaite E, Nemeikaite A, Anusevicius Z, Nivinskas H, et al. 1997. Nitrobenzimidazoles as substrates for DT-diaphorase and redox cycling compounds: their enzymatic reactions and cytotoxicity. *Archives of biochemistry and biophysics* 346:219-29

156. Sarlauskas J, Nemeikaite-Ceniene A, Anusevicius Z, Miseviciene L, Julvez MM, et al. 2004. Flavoenzyme-catalyzed redox cycling of hydroxylamino- and amino metabolites of 2,4,6-trinitrotoluene: implications for their cytotoxicity. *Archives of biochemistry and biophysics* 425:184-92

157. Sarlauskas J, Nemeikaite-Ceniene A, Anusevicius Z, Miseviciene L, Maroziene A, et al. 2004. Enzymatic redox properties of novel nitrotriazole explosives implications for their toxicity. *Zeitschrift fur Naturforschung. C, Journal of biosciences* 59:399-404

158. Schumann R. 2002. The seventh amendment to the cosmetics directive: what does DG enterprise want from ECVAM? *Alternatives to laboratory animals : ATLA* 30 Suppl 2:213-4

159. Sheen YY, Owens IS, Kim SS, Kim JE. 1998. UDPGT cDNA expression and UDPGT1 in human liver. *The Journal of toxicological sciences* 23 Suppl 2:136-9

160. Shemin D, Dworkin LD. 2011. Neutrophil gelatinase-associated lipocalin (NGAL) as a biomarker for early acute kidney injury. *Critical care clinics* 27:379-89

161. Sherwood MW, Kristin Newby L. 2014. High-sensitivity troponin assays: evidence, indications, and reasonable use. *Journal of the American Heart Association* 3:e000403

162. Shinkai Y, Nishihara Y, Amamiya M, Wakayama T, Li S, et al. 2015. NADPH-cytochrome P450 reductase-mediated denitration reaction of 2,4,6-trinitrotoluene to yield nitrite in mammals. *Free radical biology & medicine* 91:178-87

163. Simon N, Barre J, Jolliet P, Urien S, Tillement JP. 1997. [Mediators involved in the nephrotoxicity of cyclosporin A]. *Therapie* 52:329-33

164. Simon S. 2004. *S-Shaped Curves*. http://www.pmean.com/04/scurve.html

165. Simunek T, Klimtova I, Kaplanova J, Sterba M, Mazurova Y, et al. 2005. Study of daunorubicin cardiotoxicity prevention with pyridoxal isonicotinoyl hydrazone in rabbits. *Pharmacological research : the official journal of the Italian Pharmacological Society* 51:223-31

166.   Sirvio ML, Uhlenius N, Stewen P, Metsarinne K, Fyhrquist F. 1995. The effect of aortic coarctation on expression of endothelin-1 and endothelin receptors in heart and lungs. *Blood pressure* 4:320-3

167.   Slonim DK, Yanai I. 2009. Getting started in gene expression microarray analysis. *PLoS computational biology* 5:e1000543

168.   Stanley JK, Lotufo GR, Biedenbach JM, Chappell P, Gust KA. 2015. Toxicity of the conventional energetics TNT and RDX relative to new insensitive munitions constituents DNAN and NTO in Rana pipiens tadpoles. *Environmental toxicology and chemistry / SETAC*

169.   Star GP, Giovinazzo M, Lamoureux E, Langleben D. 2014. Effects of vascular endothelial growth factor on endothelin-1 production by human lung microvascular endothelial cells *in vitro*. *Life sciences* 118:191-4

170.   Sun H, Xia M, Austin CP, Huang R. 2012. Paradigm shift in toxicity testing and modeling. *The AAPS journal* 14:473-80

171.   Sureshbabu A, Muhsin SA, Choi ME. 2016. TGF-beta Signaling in the Kidney: Pro-fibrotic and Protective Effects. *American journal of physiology. Renal physiology*:ajprenal.00365.2015

172.   Takeda Y, Miyamori I, Wu P, Yoneda T, Furukawa K, Takeda R. 1995. Effects of an endothelin receptor antagonist in rats with cyclosporine-induced hypertension. *Hypertension* 26:932-6

173.   Talley JW, Sleeper PM. 1997. Roadblocks to the implementation of biotreatment strategies. *Annals of the New York Academy of Sciences* 829:16-29

174.   Tan C, Tasaka H, Yu KP, Murphy ML, Karnofsky DA. 1967. Daunomycin, an antitumor antibiotic, in the treatment of neoplastic disease. Clinical evaluation with special reference to childhood leukemia. *Cancer* 20:333-53

175.   Taylor S, Park E, Bullion K, Dontsova K. 2015. Dissolution of three insensitive munitions formulations. *Chemosphere* 119:342-8

176.   Tchounwou PB, Wilson BA, Ishaque AB, Schneider J. 2001. Transcriptional activation of stress genes and cytotoxicity in human liver carcinoma cells (HepG2) exposed to 2,4,6-trinitrotoluene, 2,4-dinitrotoluene, and 2,6-dinitrotoluene. *Environmental toxicology* 16:209-16

177.   Thomas RS, Philbert MA, Auerbach SS, Wetmore BA, Devito MJ, et al. 2013. Incorporating new technologies into toxicity testing and risk assessment: moving from 21st century vision to a data-driven framework. *Toxicological sciences : an official journal of the Society of Toxicology* 136:4-18

178. Thome-Kromer B, Bonk I, Klatt M, Nebrich G, Taufmann M, et al. 2003. Toward the identification of liver toxicity markers: a proteome study in human cell culture and rats. *Proteomics* 3:1835-62

179. Torre CD, Corsi I, Alcaro L, Amato E, Focardi S. 2006. The involvement of cytochrome P450 system in the fate of 2,4,6-trinitrotoluene (TNT) in European eel [Anguilla anguilla (Linnaeus, 1758)]. *Biochemical Society transactions* 34:1228-30

180. Tucker PS, Scanlan AT, Dalbo VJ. 2015. Chronic kidney disease influences multiple systems: describing the relationship between oxidative stress, inflammation, kidney damage, and concomitant disease. *Oxidative medicine and cellular longevity* 2015:806358

181. U.S. Army Medical Research and Development Command. 1981. Species differences in the disposition and metabolism of 2,4,6-trinitrotoluene as a function of route of administration

182. U.S. Army Public Health Command. 2011. Revised preliminary occupational exposure level for 3-nitro-1,2,4-triazol-5-one (NTO), Aberdeen Proving Ground, MD

183. U.S. Environmental Protection Agency. 2014. Tehcnical Fact Sheet - 2,4,6-Trinitrotoluene. ed. OoSWaE Response, p. 8

184. Uranski T. 1984. *Chemistry and Technology of Explosives*. Oxford, UK. 160 pp.

185. Urbanski T. 1964. *Chemistry and Technology of Explosives*. Warszawa: PWN-Polish Scientific Publishers

186. Voegtlin C. HCW, and Johnson J.M. 1919. Trinitrotoluene poisoning. *U.S. Public Health Rep.* 34

187. Vogel C, Silva GM, Marcotte EM. 2011. Protein expression regulation under oxidative stress. *Molecular & cellular proteomics : MCP* 10:M111.009217

188. Vorisek V, Pour M, Ubik K, Hassmanova V, Korolova E, et al. 2005. Analytical monitoring of trinitrotoluene metabolites in urine by GC-MS. Part I. Semiquantitative determination of 4-amino-2,6-dinitrotoluene in human urine. *Journal of analytical toxicology* 29:62-5

189. Walsh MR, Walsh ME, Ramsey CA, Brochu S, Thiboutot S, Ampleman G. 2013. Perchlorate contamination from the detonation of insensitive high-explosive rounds. *Journal of hazardous materials* 262:228-33

190. Warner CM, Gust KA, Stanley JK, Habib T, Wilbanks MS, et al. 2012. A systems toxicology approach to elucidate the mechanisms involved in RDX species-specific sensitivity. *Environmental science & technology* 46:7790-8

191. Weaver TE, Whitsett JA. 1991. Function and regulation of expression of pulmonary surfactant-associated proteins. *The Biochemical journal* 273(Pt 2):249-64

192. Wilbanks MS, Gust KA, Atwa S, Sunesara I, Johnson D, et al. 2014. Validation of a genomics-based hypothetical adverse outcome pathway: 2,4-dinitrotoluene perturbs PPAR signaling thus impairing energy metabolism and exercise endurance. *Toxicological sciences : an official journal of the Society of Toxicology* 141:44-58

193. Williams ES, Panko J, Paustenbach DJ. 2009. The European Union's REACH regulation: a review of its history and requirements. *Critical reviews in toxicology* 39:553-75

194. Winczura A, Zdzalik D, Tudek B. 2012. Damage of DNA and proteins by major lipid peroxidation products in genome stability. *Free radical research* 46:442-59

195. Wintz H, Yoo LJ, Loguinov A, Wu YY, Steevens JA, et al. 2006. Gene expression profiles in fathead minnow exposed to 2,4-DNT: correlation with toxicity in mammals. *Toxicological sciences : an official journal of the Society of Toxicology* 94:71-82

196. Wu Y, Zang WD, Jiang W. 2014. Functional analysis of differentially expressed genes associated with glaucoma from DNA microarray data. *Genetics and molecular research : GMR* 13:9421-8

197. Xu J, Jing N. 2012. Effects of 2,4-dinitrotoluene exposure on enzyme activity, energy reserves and condition factors in common carp (Cyprinus carpio). *Journal of hazardous materials* 203-204:299-307

198. Yamazaki H, Hatanaka N, Kizu R, Hayakawa K, Shimada N, et al. 2000. Bioactivation of diesel exhaust particle extracts and their major nitrated polycyclic aromatic hydrocarbon components, 1-nitropyrene and dinitropyrenes, by human cytochromes P450 1A1, 1A2, and 1B1. *Mutation research* 472:129-38

199. Yan C, Wang Y, Xia B, Li L, Zhang Y, Liu Y. 2002. [The retrospective survey of malignant tumor in weapon workers exposed to 2,4,6-trinitrotoluene]. *Zhonghua lao dong wei sheng zhi ye bing za zhi = Zhonghua laodong weisheng zhiyebing zazhi = Chinese journal of industrial hygiene and occupational diseases* 20:184-8

200. Yen M, Ewald MB. 2012. Toxicity of weight loss agents. *Journal of medical toxicology : official journal of the American College of Medical Toxicology* 8:145-52

201. Zakhari AV, J.E. 1978. A Literature Review: Problem Definition Studies on Selected Chemicals, Philadelphia, PA

202. Zakon Y, Lemcoff NG, Marmur A, Zeiri Y. 2012. Adhesion of Standard Explosive Particles to Model Surfaces. *The Journal of Physical Chemistry C* 116:22815-22

203. Zhang S, Sun WY, Wu JJ, Wei W. 2014. TGF-beta signaling pathway as a pharmacological target in liver diseases. *Pharmacological research : the official journal of the Italian Pharmacological Society* 85:15-22

204. Zhao H, Hong J, Yu X, Zhao X, Sheng L, et al. 2013. Oxidative stress in the kidney injury of mice following exposure to lanthanides trichloride. *Chemosphere* 93:875-84

205. Zheng JP, Zhang X, Wang H, Wang Y, Cheng Z, et al. 2013. Vasomotor dysfunction in the mesenteric artery after organ culture with cyclosporin A. *Basic & clinical pharmacology & toxicology* 113:370-6

206. Zitting A, Szumańska G, Nickels J, Savolainen H. 1982. Acute toxic effects of trinitrotoluene on rat brain, liver and kidney: role of radical production. *Archives of toxicology* 51:53-64

207. Zucchini-Pascal N, Peyre L, de Sousa G, Rahmani R. 2012. Organochlorine pesticides induce epithelial to mesenchymal transition of human primary cultured hepatocytes. *Food and chemical toxicology : an international journal published for the British Industrial Biological Research Association* 50:3963-70

147

APPENDIX A: IdMOC SYSTEM CELL LINES

KIDNEY - HK-2 (ATCC CRL-2190): Human epithelial cells isolated from the cortex/proximal tubule of a normal kidney and immortalized by transduction with human papilloma virus 16 (HPV-16) (6).

Medium: Keratinocyte Serum Free Medium (Gibco™ from Thermo Fisher Scientific ®) with the supplied kit (catalog number 17005-042) which provides for a final concentration of 0.05 mg/mL of bovine pituitary extract (BPE) and 5 ng/mL of EGF.

LIVER - THLE-3 (ATCC CRL-11233): Human epithelial cells isolated from the left lobe of the liver of a healthy adult and immortalized using SV40 large T antigen (9).

Medium: Bronchial Epithelial Cell Growth Medium (BEGM) from Lonza/Clonetics Corporation, Walkersville, MD, USA, supplemented by the BEGM Bullet kit, CC3170 (Lonza/Clonetics®). Additionally to the kit, 5 ng/mL of epithelial growth factor (EGF) (Sigma®), 70 ng/mL of o-phosphoethanolamine (Sigma®), and 10% of heat-inactivated fetal bovine serum are added.

Flask Coating: At least 16 hours before use, the flasks were coated with a mixture of 0.01 mg/mL fibronectin (Sigma®), 0.03 mg/mL bovine collagen type 1 (Sigma®) and 0.01 mg/mL fraction V bovine serum albumin (BSA) (Sigma® A2153). The freshly coated vessels were incubated at 37ºC until use.

LUNG - NULI-1 (ATCC CRL-4011): Human epithelial-like cells isolated from the normal lung of an adult subject and immortalized by dual retroviral infection with HPV-16/E7-LXSN (7).

Medium: Airway Epithelial Cell Basal Medium (ATCC® PCS-300-030) and Bronchial Epithelial Cell Growth Kit (ATCC PCS-300-040) additives.

Flask Coating: At least 18 hours before use, the flasks were coated with a 60 µg/mL solution of Human Placental Collagen Type IV (Sigma®) in Dulbecco's Phosphate Buffered Saline. Prior to use, the flasks were then rinsed twice with Dulbecco's Phosphate Buffered Saline.

CARDIAC MUSCLE - AC10 (ATCC PTA-1501): Immortalized human undifferentiated cardiomyocyte cell line (34).

Medium: Ham's F12 Nutrient mixture (Gibco™) with 12.5% heat-inactivated FBS (LifeTechnologies®).

VASCULAR ENDOTHELIUM - TeloHAEC (ATCC CRL-4052): Human endothelial cell line cloned from the aorta of a healthy subject and immortalized by stably expressing human telomerase catalytic subunit hTERT (8).

Medium: Vascular Cell Basal Medium (ATCC PCS-100-030), supplemented with Vascular Endothelial Cell Growth Kit-VEGF (ATCC PCS-100-041).
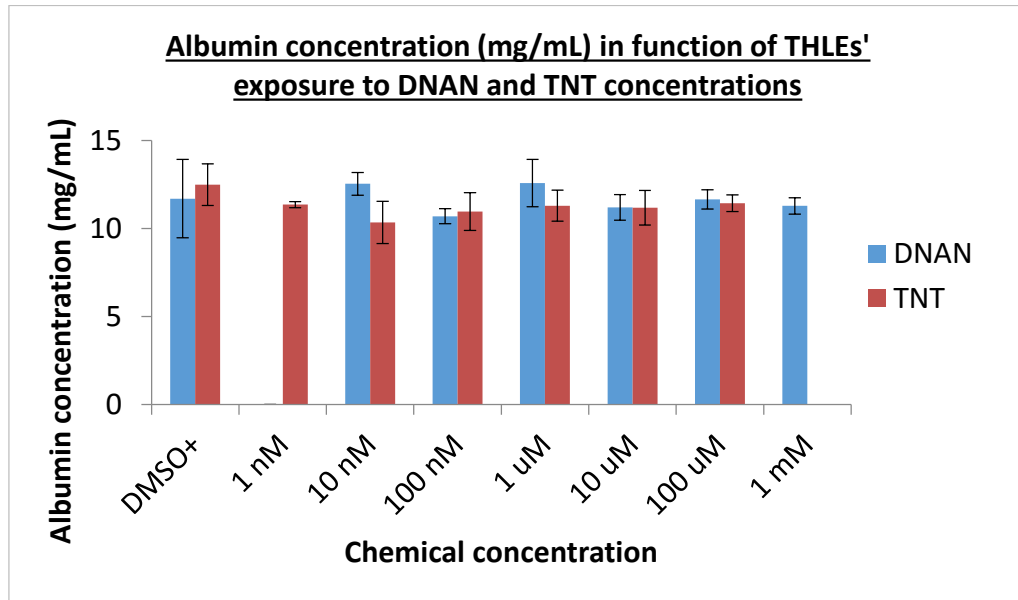
Figure B1. Level of albumin production of hepatocytes exposed to TNT and DNAN. The tested conditions were during a 24 hour incubation in co-culture medium. The error bars represent the respective standard deviations.
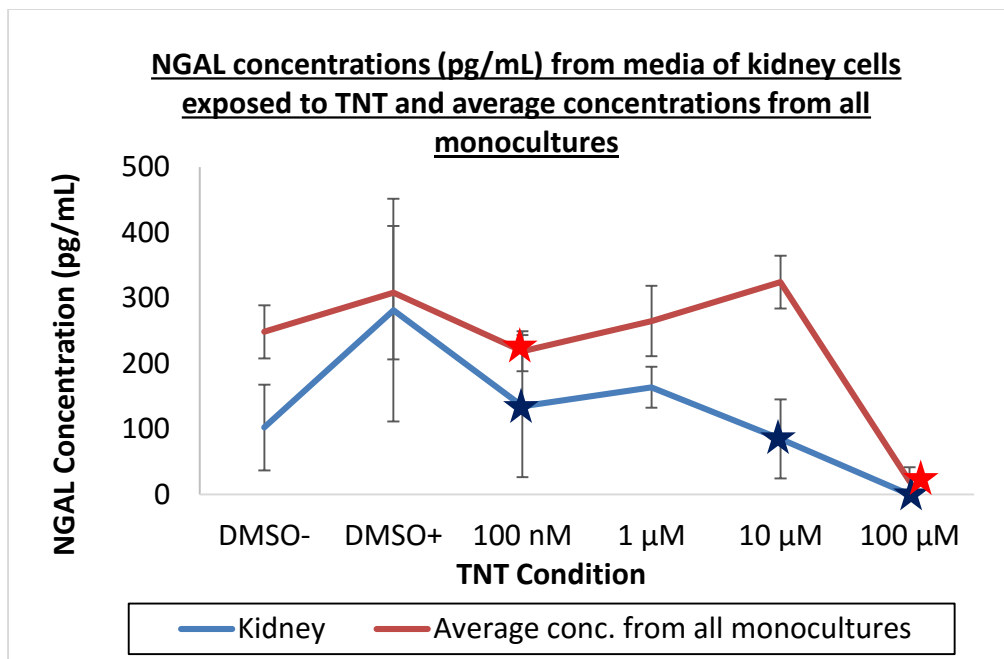

Figure B2. NGAL concentrations (pg/mL) of culture media from kidney cells exposed to TNT and average concentrations (pg/mL) of all culture media collected from the five cell lines exposed to TNT in monoculture setting. Error bars represent the 95% confidence interval. Stars represent conditions for which there was a significant change compared to positive control (DMSO+).
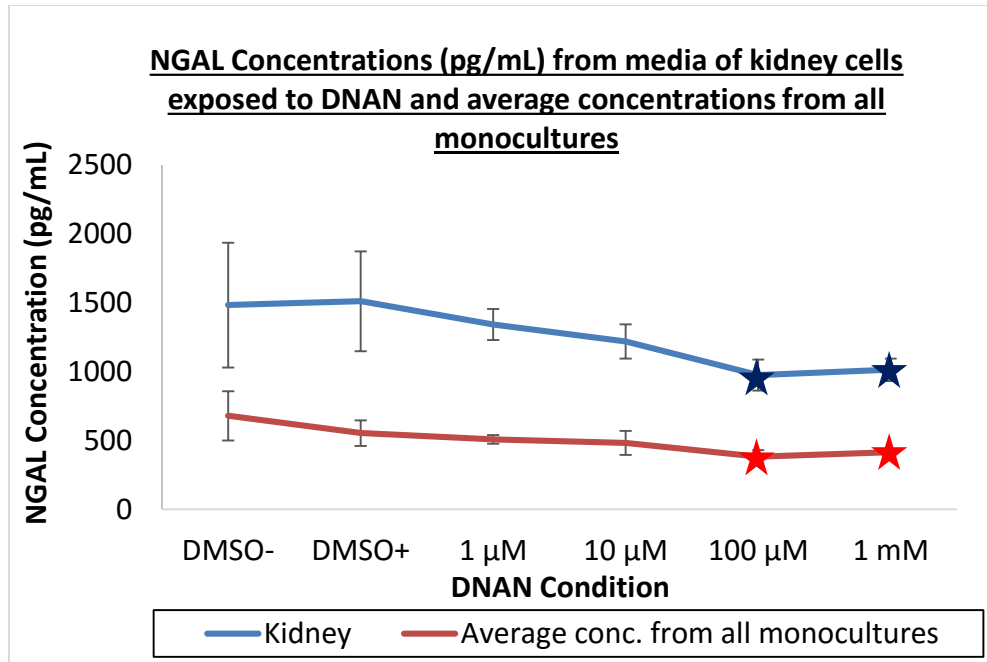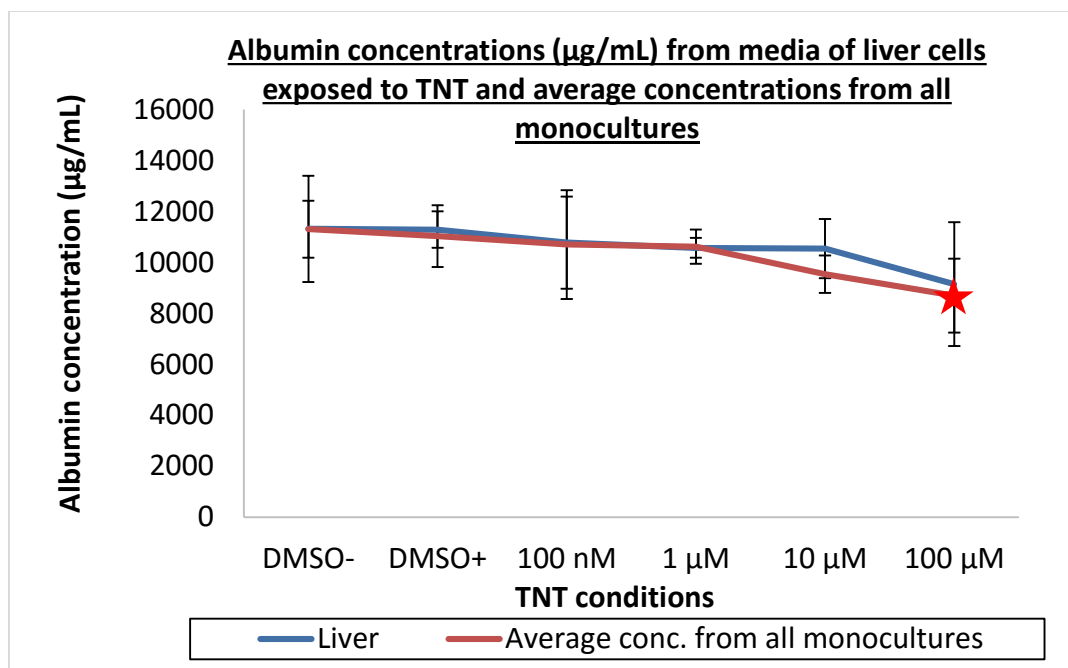
Figure B3. NGAL concentrations (pg/mL) of culture media from human cells exposed to DNAN in mono- and co-cultures. Error bars represent the 95% confidence interval. Stars represent conditions for which there was a significant change compared to positive control (DMSO+).
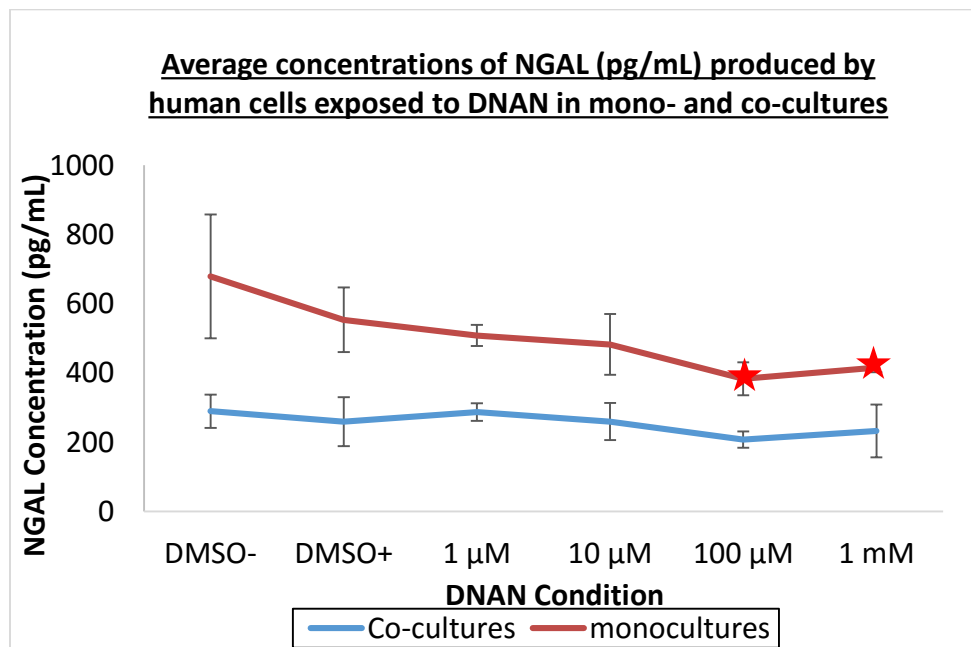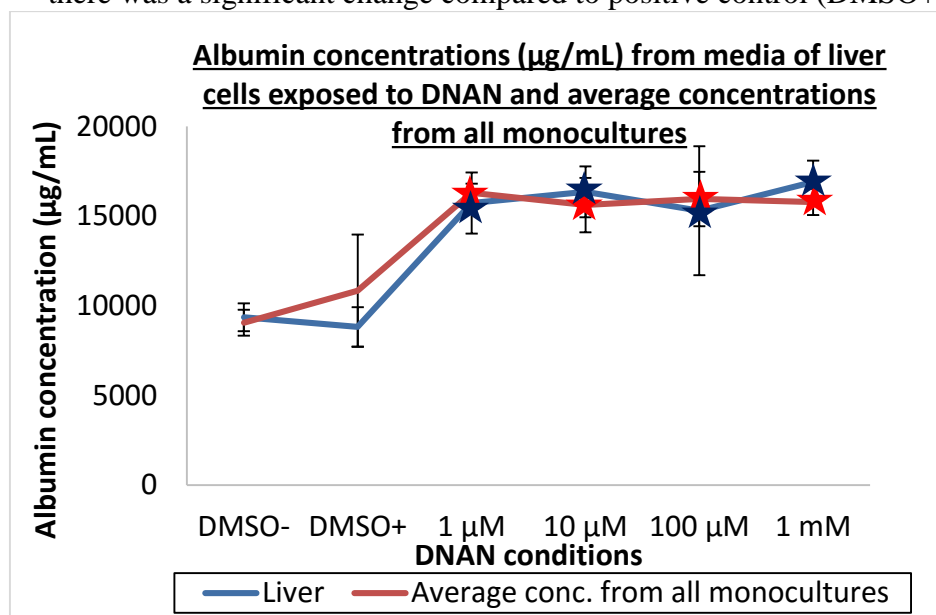

Figure B4. NGAL concentrations (pg/mL) of culture media from human cells exposed to DNAN in mono- and co-cultures. Error bars represent the 95% confidence interval. Stars represent conditions for which there was a significant change compared to positive control (DMSO+).

Figure B5. Albumin concentrations (µg/mL) of culture media from liver cells exposed to TNT and average concentrations (µg/mL) of all culture media collected from the five cell lines exposed to TNT in monoculture setting. Error bars represent the 95% confidence interval. Stars represent conditions for which there was a significant change compared to positive control (DMSO+).

Figure B6. Albumin concentrations (µg/mL) of culture media from liver cells exposed to DNAN and average concentrations (µg/mL) of all culture media collected from the five cell lines exposed to DNAN in monoculture setting. Error bars represent the 95% confidence interval. Stars represent conditions for which there was a significant change compared to positive control (DMSO+).
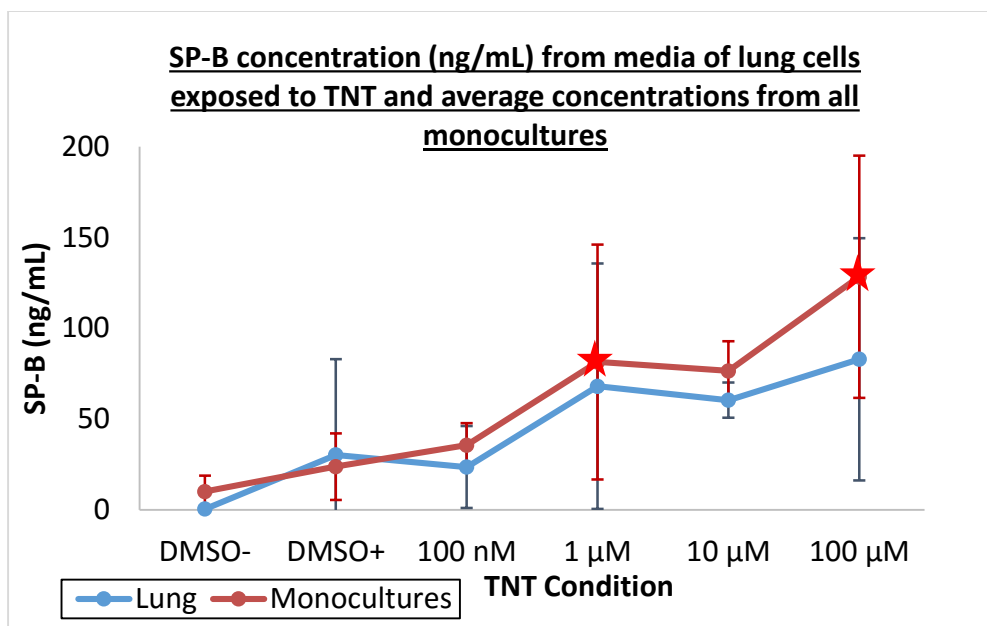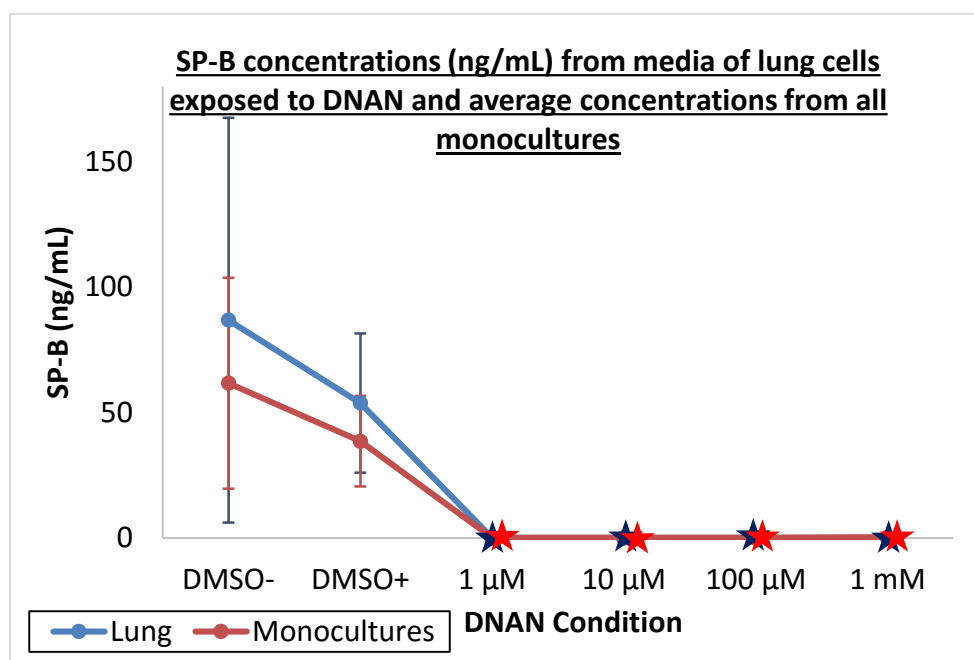
Figure B7. SP-B concentrations (ng/mL) of culture media from lung cells exposed to TNT and average concentrations (ng/mL) of all culture media collected from the five cell lines exposed to TNT in monoculture setting. Error bars represent the 95% confidence interval. Stars represent conditions for which there was a significant change compared to positive control (DMSO+).

Figure B8. SP-B concentrations (ng/mL) of culture media from lung cells exposed to DNAN and average concentrations (ng/mL) of all culture media collected from the five cell lines exposed to DNAN in monoculture setting. Error bars represent the 95% confidence interval. Stars represent conditions for which there was a significant change compared to positive control (DMSO+).
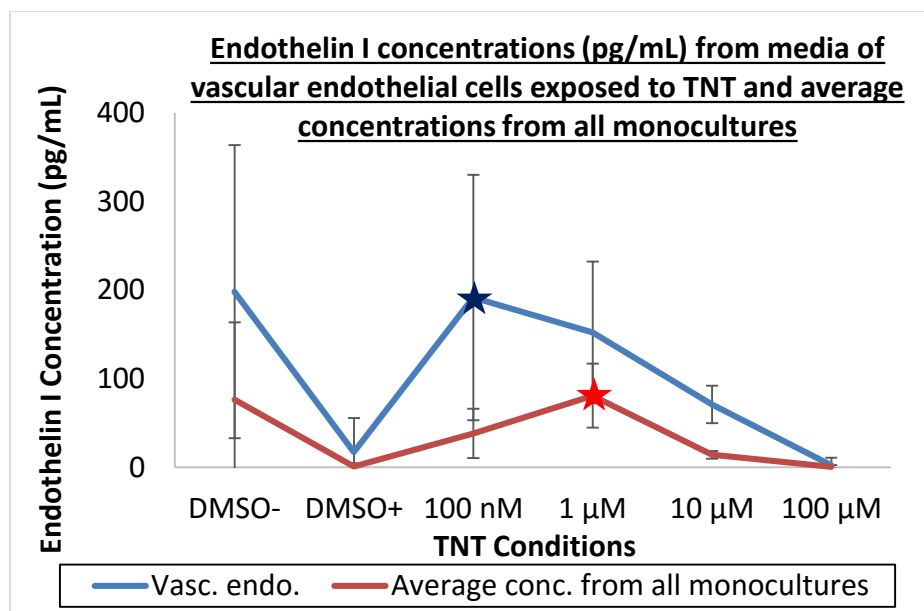
Figure B9. Endothelin I concentrations (pg/mL) of culture media from vascular endothelial cells exposed to TNT and average concentrations (pg/mL) of all culture media collected from the five cell lines exposed to TNT in monoculture setting. Error bars represent the 95% confidence interval. Stars represent conditions for which there was a significant change compared to positive control (DMSO+).
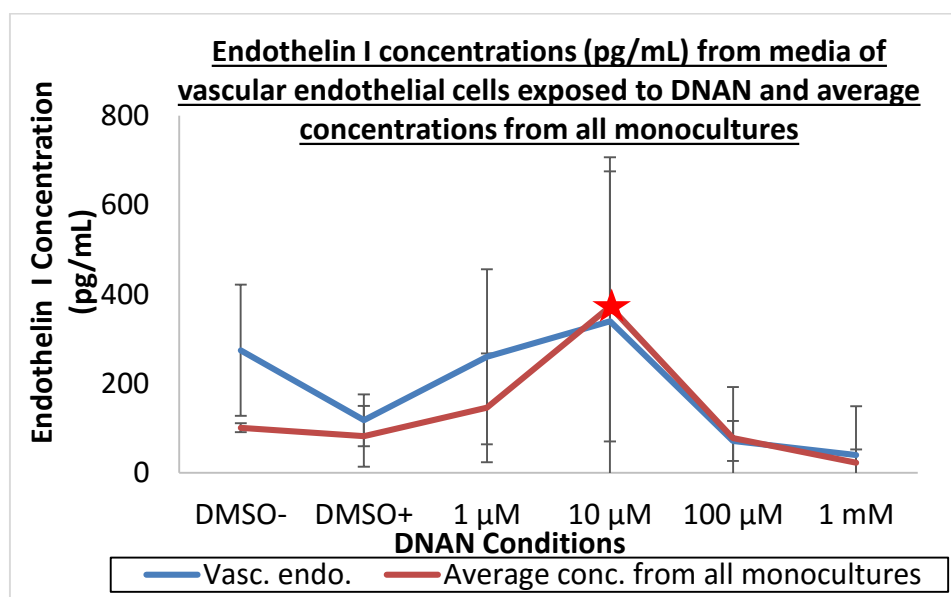

Figure B10. Endothelin I concentrations (pg/mL) of culture media from vascular endothelial cells exposed to DNAN and average concentrations (pg/mL) of all culture media collected from the five cell lines exposed to DNAN in monoculture setting. Error bars represent the 95% confidence interval. Stars represent conditions for which there was a significant change compared to positive control (DMSO+).